ΠΑΝΕΠΙΣΤΗΜΙΟ ΚΡΗΤΗΣ
ΤΜΗΜΑ ΧΗΜΕΙΑΣ

ΜΕΤΑΠΤΥΧΙΑΚΟ ΠΡΟΓΡΑΜΜΑ
ΕΠΙΣΤΗΜΕΣ ΚΑΙ ΜΗΧΑΝΙΚΗ ΠΕΡΙΒΑΛΛΟΝΤΟΣ

ΕΡΓΑΣΤΗΡΙΟ ΠΕΡΙΒΑΛΛΟΝΤΙΚΩΝ ΧΗΜΙΚΩΝ ΔΙΕΡΓΑΣΙΩΝ
(Ε.ΠΕ.ΧΗ.ΔΙ)

ΜΕΤΑΠΤΥΧΙΑΚΟ ΔΙΠΛΩΜΑ ΕΙΔΙΚΕΥΣΗΣ

ΟΞΥΤΗΤΑ ΣΩΜΑΤΙΔΙΑΚΟΥ ΝΕΡΟΥ ΣΤΗΝ ΑΤΜΟΣΦΑΙΡΑ ΤΗΣ ΑΝΑΤΟΛΙΚΗΣ ΜΕΣΟΓΕΙΟΥ

Νερολαδάκη Άννα Μαρία

ΗΡΑΚΛΕΙΟ 2021

UNIVERSITY OF CRETE
DEPARTMENT OF CHEMISTRY

POSTGRADUATE PROGRAM
ENVIRONMENTAL SCIENCES AND ENGINEERING

ENVIRONMENTAL CHEMICAL PROCESSES LABORATORY (ECPL)

Master Thesis

ATMOSPHERIC AEROSOL WATER ACIDITY IN THE EAST MEDITERRANEAN

Neroladaki Anna Maria

HERAKLION 2021

Examining Committee

Kanakidou Maria (supervisor)
Professor, Department of Chemistry, University of Crete

Mihalopoulos Nikolaos
Professor, Department of Chemistry, University of Crete

Bougiatioti Aikaterini
Senior Researcher, Institute for Environmental Research & Sustainable Development (IERSD), National Observatory of Athens (NOA)

ACKNOWLEDGEMENTS

The present work was carried out at the Environmental Chemical Processes Laboratory of the Department of Chemistry, University of Crete. This work was supported by the project "PANhellenic infrastructure for Atmospheric Composition and climatE change" (MIS 5021516) which is implemented under the Action "Reinforcement of the Research and Innovation Infrastructure", funded by the Operational Programme "Competitiveness, Entrepreneurship and Innovation" (NSRF 2014-2020) and co-financed by Greece and the European Union (European Regional Development Fund).

I would like to thank all the members of my examining committee. I would like to express my special gratitude to my supervisor Professor Maria Kanakidou for her continuous guidance, for giving me the opportunity to work with her and her team for the past years and for always being available giving me insightful comments on my work. Without the expertise of Professor Kanakidou, the completion of this work would not be possible. I would also like to express my appreciation for her not only for being such an accomplished scientist, but also an admirable professor and person willing to help her students not only on a scientific level but also on a personal one as well. I would also like to thank Dr. Aikaterini Bougiatioti for giving me insightful input on my work and last but not least Professor Nikolaos Mihalopoulos for the honor of accepting to review my thesis.

I would also like to thank Ph.D. candidate Irini Tsiodra, Dr. Pavlos Zarmpas from the Environmental Chemical Processes Laboratory and Ph.D. candidate Iasonas Stavroulas from the Institute for Environmental Research & Sustainable Development, National Observatory of Athens, for providing me with the observations of gas phase NH_3, HNO_3 and HCl, PM_1 inorganic ions including crustal species and sodium and PM_1 ions (ACSM) respectively and Professor Nikolaos Mihalopoulos for supervised these observations and the ones for Ioannina City.

I owe a great deep sense of gratitude to Professor Athanasios Nenes for providing the code of ISORROPIA-II and for his extremely useful and precious comments and input throughout this thesis. I would also like to thank Dr. Stelios Myriokefalitakis for providing the modified 1-d version of ISORROPIA-II and helping me familiarize with it.

I would also like to thank all the members of the Computational Environmental Chemical Processes Laboratory for the excellent collaboration and contribution for a pleasant and friendly environment all these years in the lad. Special thanks to Dr. Daskalakis Nikolaos whose precious computational expertise helped tremendously for the completion of this work.

I would like to thank my parents, Giorgos and Eleni, my sister Eva and brother in law Giorgos, my brother Stelios and sister in law Eirini and my friends Gogo and Murwnia, who have always been supporting me all this time. Finally, last but certainly not least a special thanks to my husband Thanasis Petsas, who is always there for me and supports me. I would never have made it through without his love and understanding.

CURICULUM VITAE

Personal Details

Full name: Neroladaki Anna Maria
Date of Birth: 24 January 1992
Work address: Department of Chemistry, University of Crete, 70013, Voutes, Heraklion, Greece
Tel.(lab): (+30)2810-545111
e-mail: amwateroil2@gmail.com

Education

2019 – currently	Master Thesis at Environmental Chemical Processes Laboratory, Department of Chemistry University of Crete. Title: ‘‘Atmospheric aerosol water acidity in the East Mediterranean’’. (supervisor: Prof. Maria Kanakidou)
2019	Diploma in Chemistry, Department of Chemistry, University of Crete.
2018-2019	Diploma Thesis at Environmental Chemical Processes Laboratory, Department of Chemistry University of Crete. Title: ‘‘Evaluation of the effect of fine particles on the formation of Cloud Condensation Nuclei at Finokalia’’. (supervisor: Prof. Maria Kanakidou)
	Greek (native language)
	English – Certificate of English Language Proficiency C2
	French – DELF A2
Language Knowledge	Operating systems: Linux, Windows
	MS Office (Word, Excel, PowerPoint
Computational Experience	Programming Languages: FORTRAN 90, Python
	Statistical programs for data analysis: Origin

Teaching Experience

Oct. 2019 – Jan. 2020	Teaching assistant in Analytical Chemistry I Laboratory
Feb. 2020 – Jun. 2020	Teaching assistant in Analytical Chemistry II Laboratory

Publications/Presentations

Neroladaki, A. M., Stavroulas, I., Tsiodra, I., Myriokefalitakis, S., Nenes, A., Mihalopoulos, N., and Kanakidou, M.: Seasonal variability of submicron aerosol acidity at a coastal site in the Eastern Mediterranean, EGU General Assembly 2020, Online, 4–8 May 2020, EGU2020-9562, https://doi.org/10.5194/egusphere-egu2020-9562, 2020

Neroladaki, Anna Maria.: Seasonal variability of submicron aerosol acidity at a coastal site in the Eastern Mediterranean, FORCeS Annual Meeting 2020, Online, 27-29 October 2020

ΠΕΡΙΛΗΨΗ

Η οξύτητα των αερολυμάτων (pH) της ατμόσφαιρας αποτελεί καθοριστικό παράγοντα καθώς επηρεάζει τη σύσταση της ατμόσφαιρας τόσο την αέρια όσο και την σωματιδιακή φάση, μεταβάλλει τις ιδιότητες των αερολυμάτων που επηρεάζουν το κλίμα, αλλά και την τοξικότητά τους με επιπτώσεις στην υγεία και τα οικοσυστήματα. Απευθείας μετρήσεις του pH των αερολυμάτων, και κυρίως του λεπτού κλάσματος των σωματιδίων (PM_1), όμως είναι δυσεύρετες καθώς είναι αρκετά περίπλοκες να εκτελεστούν. Οι πλέον αξιόπιστες εκτιμήσεις του pH των αερολυμάτων υπολογίζονται με βάση παρατηρήσεις στην αέρια και σωματιδιακή φάση που χρησιμοποιούνται ως δεδομένα εισόδου σε θερμοδυναμικά αριθμητικά μοντέλα. Τα μοντέλα αυτά αναπαράγουν την παρατηρούμενη περιεκτικότητα σε νερό των σωματιδίων και τις κατανομές ημι-πτητικών ενώσεων όπως αυτές της αμμωνίας (NH_3) και άλλων ευαίσθητων στο pH ενώσεων όπως το νιτρικό οξύ (HNO_3) και το υδροχλώριο (HCl) και υπολογίζουν την συγκέντρωση των ιόντων υδρογόνου στο σωματιδιακό νερό και από αυτό το pH.

Σε αυτή τη μελέτη, χρησιμοποιούμε μία τέτοια προσέγγιση συνδυασμού παρατηρήσεων από το ΕΠΕΧΗΔΙ και χρήσης θερμοδυναμικού μοντέλου ώστε να προσδιορίσουμε τα επίπεδα και την εποχιακή διακύμανση της οξύτητας των σωματιδίων διαμέτρου μικρότερης του 1μm (PM_1) για σχεδόν έναν ολόκληρο χρόνο στον ερευνητικό σταθμό του Φινοκαλιά χαρακτηριστικού της περιοχής της Ανατολικής Μεσογείου. Το σωματιδιακό νερό και η οξύτητα υπολογίστηκαν μέσω του θερμοδυναμικού μοντέλου ISORROPIA-II, χρησιμοποιώντας μετρήσεις της χημικής σύστασης των PM_1 και της αέρια φάσης (NH_3, HNO_3, HCl). Βρέθηκε ότι τα PM_1 στην περιοχή είναι ιδιαίτερα όξινα με μέση τιμή pH 1.16 ± 0.71, το οποίο είναι σύμφωνο και με τις μέχρι σήμερα μελέτες. Στους υπολογισμούς ελήφθη υπόψιν η συνεισφορά του σωματιδιακού νερού που σχετίζεται με τις οργανικές ενώσεις, το οποίο συνολικά είχε μικρή συνεισφορά. Το συνολικό σωματιδιακό νερό στα PM_1 βρέθηκε να είναι κατά μέσο όρο 4.01 ± 3.56 $\mu g/m^3$, με το οργανικό σωματιδιακό νερό να συνεισφέρει περίπου το 13% στο συνολικό νερό. Το σωματιδιακό pH παρουσιάζει ισχυρή εξάρτηση από τη θερμοκρασία, τη σχετική υγρασία και τα επίπεδα των θειικών, παράγοντες οι οποίοι με τη σειρά τους ωθούν στο σχηματισμό ενός έντονου εποχιακού κύκλου, με καλοκαιρινές τιμές pH να είναι περίπου 1.8 μονάδες χαμηλότερες από αυτές του χειμώνα. Επιπρόσθετα, η οξύτητα των σωματιδίων παρουσιάζει ευαισθησία στα επίπεδα των ημι-πτητικών ενώσεων και συγκεκριμένα της αμμωνίας, καθώς και στα μη-πτητικά κατιόντα που εμπεριέχονται στα PM_1, τα οποία βρέθηκε ότι αυξάνουν το σωματιδιακό pH κατά 0.73 μονάδες. Τέλος, το σωματιδιακό pH των PM_1 στην περιοχή του Φινοκαλιά βρέθηκε να είναι κατά μέσο 1.9 μονάδες πιο όξινο από το pH των λεπτών σωματιδίων ($PM_{2.5}$) στην περιοχή των Ιωαννίνων κατά τη διάρκεια του χειμώνα.

Λέξεις κλειδιά: Οξύτητα αερολυμάτων, Παράκτια απομακρυσμένη περιοχή, Σταθμός ατμοσφαιρικής παρακολούθησης Φινοκαλιά, Αστική περιοχή Ιωαννίνων, Νιτρικό οξύ, Αμμωνία, Νερό αερολυμάτων, Οργανικό αερόλυμα, Εποχιακότητα.

ABSTRACT

Aerosol acidity (pH) is a key factor since it affects the atmospheric composition of both the aerosol and the gas phase, it alters the properties of aerosols affecting the climate, and their toxicity with effects in human health and ecosystems. Direct measurements of aerosol pH, however, and especially that of submicron aerosol particles, are challenging and thus scarce. The most reliable estimates of ambient aerosol pH are inferred from observations interpreted by thermodynamic model calculations – when the latter reproduces the observed liquid water content and semi-volatile partitioning of ammonia (NH_3) and other pH-sensitive species, like nitric acid (HNO_3) and hydrochloric acid (HCl). These models can calculate the concentration of the particle hydronium concentration in the assumed aqueous solution and consequently the aerosol pH.

Here we used this thermodynamic/observation approach obtaining observations from ECPL, in order to determine the levels and seasonal variation of submicron aerosol acidity over almost an entire year at the Finokalia observatory, which is characteristic of the eastern Mediterranean region. Aerosol water content and acidity were here calculated by the thermodynamic model ISORROPIA-II using concurrent measurements of chemical composition PM_1 and gas-phase (NH_3, HNO_3, and HCl). We find that PM_1 are highly acidic with an average pH value of 1.16 ± 0.71, which is consistent with studies to date. In those calculations we took into account the contribution of the aerosol water associated with organic species, which had an overall minor effect. On average, the total aerosol water associated with all aerosol components in the PM_1 fraction was on average 4.01 ± 3.56 μg/m^3 with the organic aerosol water content contributing about 13% of the total aerosol water. Aerosol pH demonstrates a strong dependence on ambient temperature, relative humidity and sulfate levels, which in turn drive an intense seasonal cycle, with summertime pH values being about 1.8 pH units lower than wintertime values. Furthermore, aerosol acidity was also found to be sensitive to the levels of semi-volatile compounds and in particular to ammonia, as well as to the non-volatile cations in the submicron aerosol fraction, which was found to increase aerosol pH by 0.73 pH units. Finally, the aerosol pH of the PM_1 fraction at Finokalia was found to be on average 1.9 units more acidic than the $PM_{2.5}$ one at Ioannina City during the wintertime.

Keywords: Aerosol acidity, Coastal remote site, Finokalia atmospheric monitoring station, Ioannina urban environment, Nitric acid, Ammonia, Aerosol water, Organic aerosol, Seasonality.

Table of Contentss

1. Introduction

Earth's atmosphere is a complex, dynamic system consisting of a mixture of gases that surrounds our home planet. Its existence is of a great importance since it is primarily responsible of life on Earth. Apart from acting as a shield for the surface of the Earth protecting it from most of the harmful ultraviolet radiation coming from the Sun, the atmosphere warms the Earth's surface by about 33 ^{o}C via the greenhouse effect. Earth's atmosphere mainly consists of 78% nitrogen (N_2) and 21% oxygen (O_2), while argon (Ar), carbon dioxide (CO_2) and many other gases (CH_4, N_2O, CO, NO, NO_2, Volatile Organic Compounds or VOCs etc.) also exist in much lower amounts with each of them making up less than 1% of the atmosphere's mixture of gases. These trace gases are of a great importance for the Earth's radiative balance and for the chemical properties of the atmosphere. The atmosphere also includes water vapor, the next most abundant constituent, which is found in the lower atmosphere and it varies considerably reaching mixture ratios up to 3% (Seinfeld & Pandis, 2006). Its abundance is controlled by evaporation and precipitation processes. Trace constituents in the atmosphere can exist in the gas (NH_3, SO_2, HNO_3 etc.), aqueous (SO_3^{2-}, HSO_3^- etc.) or particulate phase (SO_4^{2-}, HSO_4^-, NH_4^+, NO_3^- etc.) making up the chemical composition of the atmosphere.

1.1 Atmospheric Aerosols

An atmospheric aerosol is generally defined as a suspension of liquid or solid particles in a gas. Aerosols in the atmosphere can come from direct emissions (primary aerosol) and from gas-to-particle conversion of vapor precursors (secondary aerosol). When there are in the atmosphere, particles can vary in their size and composition via several processes such as condensation of vapor or evaporation, coagulation with other particles, chemical reactions, or finally activation into cloud condensation nuclei in the presence of water supersaturation to become cloud droplets. Particles in the atmosphere are eventually removed from the atmosphere by either deposition at the Earth's surface (dry deposition) or by activating into cloud droplets or by scavenging below clouds during precipitation (wet deposition). Their lifetime in the troposphere ranges from few days to a few weeks depending on their properties (size, hygroscopicity) and the atmospheric conditions.
Aerosols' size and chemical composition are controlled by the way they are emitted and formed in the atmosphere. Atmospheric particles have diameters in the range of roughly 1nm up to 100 μm. Particles with diameter less than 2.5 μm are referred to as fine and those with greater than 2.5 μm diameter as coarse. The fine particles can further be divided into the ultrafine particles and the ones in the accumulation mode depending on their formation and size range. The ultrafine particles can further be divided into those in the nucleation mode with diameters up to 10 nm and those in the Aitken mode with sizes ranged between 10 nm to 100 nm. The accumulation mode particles have diameters from 0.1 to about 2.5 μm and they form during the coagulation of the nucleation mode particles and from condensation of vapors onto pre-existing particles resulting in their growth. The coarse mode particles are produced/released into the atmosphere by mechanical processes and have shorter lifetime due to higher sedimentation rate as they are larger and heavier than the accumulation mode particles. Generally, it has been established a broader term for the particulate matter (PM) in the atmosphere. The fine particulate matter is usually restricted to particles smaller than 2.5 μm

($PM_{2.5}$) or 1 μm (PM_1) while PM_{10} include the beforementioned and larger sizes up to 10 μm.

Atmospheric aerosol particles originate from various natural sources such as windborne dust, sea spray and volcanic eruptions, and from anthropogenic activities such as combustion of fuels, industrial processes and transport sources. The chemical composition of the tropospheric aerosols is strongly determined by the way they are formed and varies with their sources. A significant fraction of tropospheric aerosol is of anthropogenic origin. Tropospheric aerosols consist of sulfate, ammonium, nitrate, chloride, sodium, trace metals and crustal species, carbonaceous material (both elemental and organic carbon) and water. From these species sulfate, ammonium, elemental and organic carbon and some transition metals are found predominantly in the fine fraction of the particulate matter. Crustal species, i.e. calcium, magnesium, potassium, aluminum and iron, and biological organic matter like pollen are commonly found in the coarse mode. Nitrate on the other hand can exist both in the fine mode in which it is usually the product of nitric acid/ammonia reaction in order to form ammonium nitrate, and in the coarse mode which is the result of heterogeneous reactions of gaseous nitric acid or NO_2 with coarse mode particles such as dust, soil particles or sea salt (Seinfeld & Pandis, 2006). As an example, it has been shown that coarse mode nitrate is commonly existed as sodium nitrate after the reaction of nitric acid with sea salt particles which serves as a constant pathway for the removal of nitrate from the atmosphere (Pakkanen, 1996):

$$HNO_{3(g)} + NaCl_{(s)} \rightarrow NaNO_{3(s)} + HCl_{(g)}$$

Other examples of coarse nitrate formation in the atmosphere include, the reaction of nitric acid with soil particles such as calcium carbonate:

$$2HNO_{3(g)} + CaCO_{3(s)} \rightarrow Ca(NO_3)_{2(s)} + H_2O_{(aq)} + CO_{2(g)}$$

Aerosols impact on climate are crucial and they have been implicated in human morbidity and mortality in urban environments. Their effects on climate arise from their ability to scatter and absorb solar radiation back to space, which is referred to as the direct effect on climate and from their role as cloud condensation nuclei (CCN) or ice nuclei (IN), the indirect effect. The way that the atmospheric aerosols will directly affect climate depends on their size, abundance and optical properties. Their ability to either scatter or absorb radiation will result in an overall cooling or heating effect of the Earth, respectively. If the particles consist of a mixture of species that mostly scatter radiation such as ammonium sulfate, and species that tend to adsorb radiation to a limited extent such as soot, then the resulting cooling-heating effect will depend on the way the two species are mixed throughout the particle population (Seinfeld & Pandis, 2006). The so-called indirect effect refers to the impact of aerosols on optical, evaporating and precipitating properties of particles. Thus, it concerns particles that can activate and grow to cloud droplets under conditions of a supersaturation of water vapor. These particles are called cloud condensation nuclei (CCN). This phenomenon is much more complex and difficult to investigate than the direct aerosol effect on climate because it depends on the aerosol levels, CCN concentrations, atmospheric conditions and in particular the updraft velocity and relative humidity, cloud droplet number concentrations and size, which influence the cloud albedo and lifetime (Fanourgakis et al., 2019; Nenes and Seinfeld, 2003). Increases in aerosol number concentrations lead to increased cloud condensation nuclei concentrations that in return could lead to higher cloud droplet number concentrations and consequently to higher cloud albedos resulting in smaller amounts of radiation reaching the surface of the Earth. Aerosol acting as IN are responsible for freezing and thus contribute to the formation of ice and mixed phase

clouds in the atmosphere (Seinfeld & Pandis, 2006).

1.2 Atmospheric Aerosol Acidity

Aerosol acidity (pH) is defined as the degree of acidity or basicity of a solution which is quantified based on the activity of dissolved hydrogen ions (H^+). Aerosol pH is affecting the composition of the atmosphere as it controls atmospheric chemical reactions (sulfate and oligomers multiphase reactions to name a few of them) resulting thereby in implications for wet and dry deposition, the lifetime of pollutants, the climate and human health. The acidity of the atmospheric particles, clouds and droplets is involved and regulates many major processes in the atmosphere and consequently all aspects of the Earth system (Fig.1.1, (Pye et al., 2020).

As Fig.1.1 shows, aerosols' acidity spans in a wide range and can reach values of about 5 pH units, while a negative pH (-1 and sometimes even -2 pH unit) can occur depending on the composition of the aerosol and the meteorological conditions in a given area. Cloud and fog droplets on the other hand exhibit higher pH values (between 2 to 7) mainly due to the higher levels of water content compared to aerosols. However, they cover a wide range of pH levels that depends on the balance between acids and bases in solution.

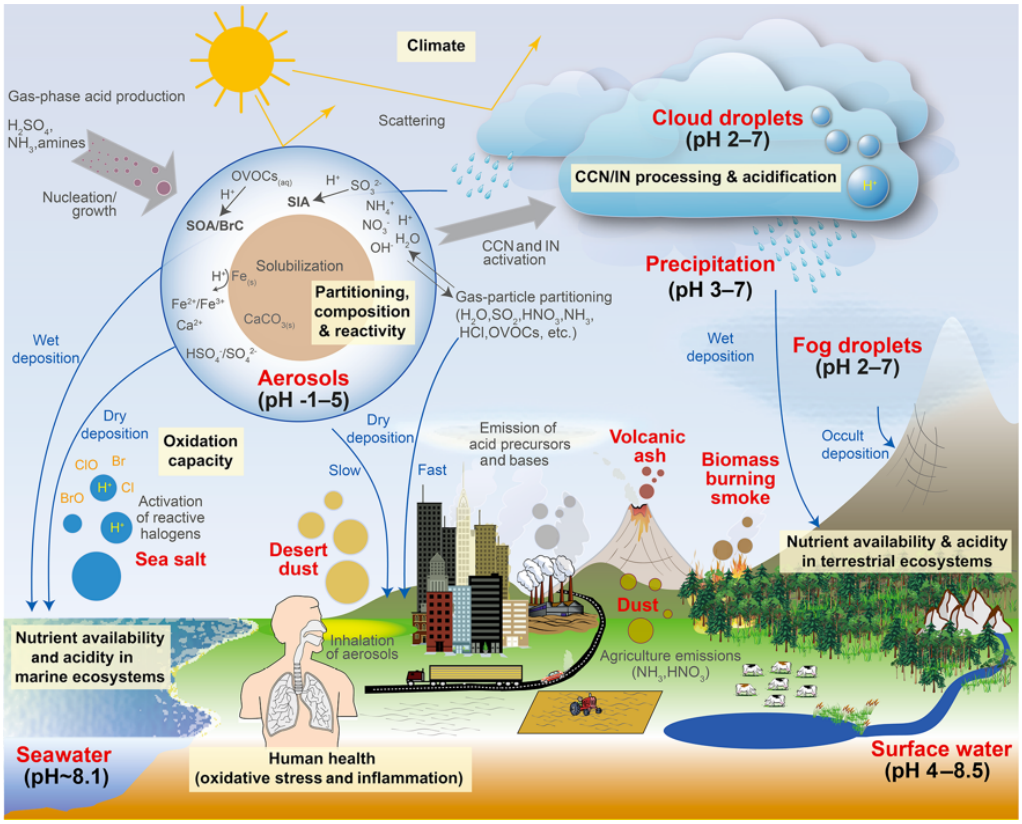

Figure 1.1: Sources and receptors of aerosol and cloud droplet acidity. Major primary sources and occurrence in the atmosphere are identified in bold red text: sea salt, dust, and biomass burning (sources); and aerosols, fog droplets, cloud droplets, and precipitation (occurrence). Key aerosol processes are indicated by arrows and grey text: nucleation/growth, light scattering, cloud condensation nuclei (CCN) and ice nuclei (IN) activation, and gas–particle partitioning. Sinks (wet, dry, and occult deposition) are indicated by blue lines and text. The effects that aerosols have in the atmosphere, and on terrestrial and marine ecosystems and human health, are highlighted in pale yellow boxes. Approximate pH ranges of aqueous aerosols and droplets, seawater, and terrestrial surface waters are also given (Pye, Nenes, Alexander, Ault, Barth, Clegg, Collett Jr., et al., 2020).

Aerosol pH affects the chemical composition of atmospheric particles and their water uptake properties; while it governs the gas-particle partitioning of semi-volatile gases such as ammonia (NH_3), nitric acid (HNO_3) and hydrochloric acid (HCl), and some organic acids with low molecular weight (formic, oxalic, acetic etc.) and bases (e.g. amines). For instance, HNO_3, because of its strong acidity and solubility, partitions more in the gas phase than in the particle phase (as nitrate, NO_3^-) at lower aerosol pH (Weber et al., 2016), while NH_3 remains in the gas phase at higher pH. On the other hand, sulfuric acid (H_2SO_4) has significantly low volatility and is assumed to exclusively reside in the aerosol phase. Moreover, metal cations including those that originate from dust and sea salt, are also nonvolatile. These constituents ultimately dictate the aerosol pH and among other parameters such as the meteorological profile, are responsible for the wide range of the pH of atmospheric particles. In addition, atmospheric acidity is controlling the uptake of sulfur dioxide (SO_2) into the aerosol- or cloud- water phase and its aqueous phase oxidation to sulfate (SO_4^{2-}, Seinfeld and Pandis, 2006) one of the main scattering components of atmospheric particles. Acid catalyzed reactions are also leading to the formation of an important contributor to absorbing aerosol (Zhang et al., 2020) brown carbon organic species in atmospheric particles (Pye et al., 2020). Atmospheric acidity also affects aerosol toxicity in the atmosphere through its effect on gas-aerosol partitioning of semi-volatile toxic organic compounds (Vierke et al., 2013) and on the solubility and concentration of toxic forms of trace metals (transition and heavy metals), which have been linked to adverse effects on human health and environmental processes (Pye, et al., 2020). Furthermore, climate is also affected by aerosol pH through changes in the water uptake property that is linked to aerosol ability to act as cloud condensation nuclei (CCN) as well as their scattering and absorption properties through the formation of scattering (i.e. sulfate, nitrate) and absorbing (i.e. brown carbon) particulate matter.

Direct measurements of particle pH are scarce due to many limitations in developing the methods and the data required for such measurements, i.e. measuring semi-volatile species and maintaining aqueous concentrations found in ambient particles is a very challenging task, making in situ measurements of particle pH exist very scarce (Pye, Nenes, Alexander, Ault, Barth, Clegg, Collett, et al., 2020). More specifically, NH_4^+, which is a very important constituent of submicron aerosol, is in chemical equilibrium with gas phase NH_3 thus collection and analysis of such species can, under circumstances, result in many biases (Pye et al., 2020). Furthermore, possible changes in aerosol liquid water content that might occur during the period from sampling to analysis can modify the particle pH itself. Therefore, many indirect methods have been developed using proxies for the approximation of aerosol acidity, some of which approximate the aerosol pH as to whether the particles are acidic or basic, and some as to whether the particulate matter is sensitive to ammonia vs. oxidized nitrogen via molar ratios of the given species (Pye et al., 2020). The most common in use are the ion balance and the molar ratio (Hennigan et al., 2015) both of which are based on the principle of solution electroneutrality. In both cases, H^+ is assumed to balance the excess of anions, and usually five cations (NH_4^+, Na^+, Ca^{2+}, Mg^{2+} and K^+) and three anions (Cl^-, NO_3^- and SO_4^{2-}) (Quinn et al., 2006; Sun et al., 1998)) are taken into account and occasionally a limited group of organic anions (Kerminen et al., 2001). Simplified versions of these proxies are also been widely used, mainly limiting the species considered to these that represent the most dominant fraction of inorganic ions, such as NH_4^+, SO_4^{2-} and NO_3^-, or even only NH_4^+ and SO_4^{2-}, in environments with low levels of crustal and marine species, and relatively low NO_3^- respectively. Other methods (gas ratio (Ansari & Pandis, 1998) and adjusted gas ratio (Pinder et al., 2008a)) have been developed to include both the particle and gas phase of the semi volatiles (ammonia and

nitric acid) whose partitioning in the two phases is sensitive to pH and address that way the non-linear response of the inorganics to changes in sulfate concentrations. All the available proxies that can be used to estimate the aerosol acidity levels are presented in Table 1.1.

However, none of the current proxies including the latter, can predict accurately the submicron aerosol acidity and even if it does, it must be verified with thermodynamic equilibrium models. As a result, currently, aerosol pH is mostly predicted using thermodynamic equilibrium models (such as ISORROPIA II; Fountoukis and Nenes, 2007, MOSAIC; (Zaveri et al., 2008), E-AIM; (Clegg et al., 2001; Wexler and Clegg, 2002)) combined with aerosol composition measurements including semi-volatile species measured both in the gas and the particulate phases. Differences on the degree of aerosol acidity estimations have been noted depending on the thermodynamic model used and its assumptions. For instance, difference of about 0.6 pH units has been found comparing the calculated aerosol pH of fine particles for Beijing winter haze derived from ISORROPIA-II and E-AIM, both run in forward mode (Song et al., 2018). This deviation for the aerosol acidity estimation was mainly due to the different way the two models estimate the activity coefficient for hydrogen ions. In particular, ISORROPIA-II assumes that the activity coefficient γ_{H^+} (and γ_{OH^-}) is equal to unity and due to the fact that γ_{H^+} and ionic strength correlate greatly to the RH, they found that ISORROPIA-II overestimates the aerosol pH at more extent at low levels of RH.

Table 1.1: Definitions of proxies that can be used to estimate the aerosol pH levels. The units are moles of chemical species per unit of air (mol/m^3) for all quantities. The [TSO_4] refers to the total particulate sulfate, or the sum of [HSO_4^-] + [SO_4^{2-}]. (Pye et al., 2020)

Cation/anion equivalent ratio	Cation/Anion = $\frac{[NH_4^+] + [Na^+] + [K^+] + 2[Ca^{2+}] + 2[Mg^{2+}]}{2[TSO_4] + [NO_3^-] + [Cl^-]}$
Degree of sulfate neutralization	DSN = $\frac{[NH_4^+] - [NO_3^-]}{2[TSO_4]}$
Degree of neutralization	DON = $\frac{[NH_4^+]}{2[TSO_4] + [NO_3^-]}$
TNH_4:TSO_4	TNH_4:TSO_4 = $\frac{[NH_4^+] + [NH_3]}{2[TSO_4]}$
Ion balance (H^+ from charge balance)	H^+_{air} = 2[TSO_4] + [NO_3^-] + [Cl^-] – ([NH_4^+] + [Na^+] + [K^+] + 2[Ca^{2+}] + 2[Mg^{2+}])
Gas ratio (GR)	GR = $\frac{[NH_4^+] + [NH_3] - 2[TSO_4}{[HNO_3] + [NO_3^-]}$
Adjusted gas ratio (adjGR)	adjGR = $\frac{[NH_3] + [NO_3^-]}{[HNO_3] + [NO_3^-]}$

In order to accurately predict the aerosol pH, the aerosol liquid water content (LWC) needs to be first calculated and for this, temperature, aerosol chemical composition and relative humidity must be known (Fountoukis & Nenes, 2007). Atmospheric particles tend to uptake water, which is in equilibrium with the water vapor in the atmosphere and is strongly dependent on the relative humidity, the temperature and the aerosol composition. Consequently, LWC is a function of the ambient meteorological conditions and the aerosol chemical composition and concentration. Liquid water exists in large quantities in the atmosphere in clouds, precipitation and aerosols. It is thought to be the most abundant atmospheric particle-phase species and thus

affecting the particle size and scattering properties. Pilinis et al. (1995) showed that LWC contributes strongly to direct radiative cooling by aerosols.

LWC shows clearly both diurnal and seasonal variability that influences that of aerosol pH (Seinfeld and Pandis, 2006), (Ansari, 1999), (Bougiatioti et al., 2016a), (Pye, Nenes, Alexander, Ault, Barth, Clegg, Collett, et al., 2020), (Tao & Murphy, 2019). However, little is currently known regarding the seasonal variability of submicron aerosol pH. The available studies worldwide show seasonal patterns of aerosol pH with summertime minimum and wintertime maximum values (Pye et al., 2020) as it can be seen in Fig. 1.2, while overall the aerosols of the fine mode are continuously acidic. Tao and Murphy (2019b), reported over a 10-year period of study (2007-2016) at 6 sites in eastern Canada that, $PM_{2.5}$ aerosol pH varies seasonally with 1 pH unit of difference between summertime minimum and wintertime maximum pH (~2 and ~3, respectively). According to their study, temperature seems to be the main driver of summer pH, while both meteorological conditions and chemical composition of the aerosol affect winter pH. In the Eastern Mediterranean, (Bougiatioti et al., 2016a) determined the LWC and predicted the fine aerosol pH at the Finokalia station during the late summer and fall months of 2012. The diurnal profile of aerosol pH and water were also thoroughly investigated. What was found is that the fine aerosol water content exhibited a significant diurnal cycle with nighttime maximum values due to elevated levels of relative humidity. The acidity levels of the submicron aerosols was significantly high throughout the studied period with aerosol pH varying from 0.5 to 2.8 pH units, while investigating the influence of the air masses origin, the highest pH values were found to occur for aerosol sources from biomass burning events.

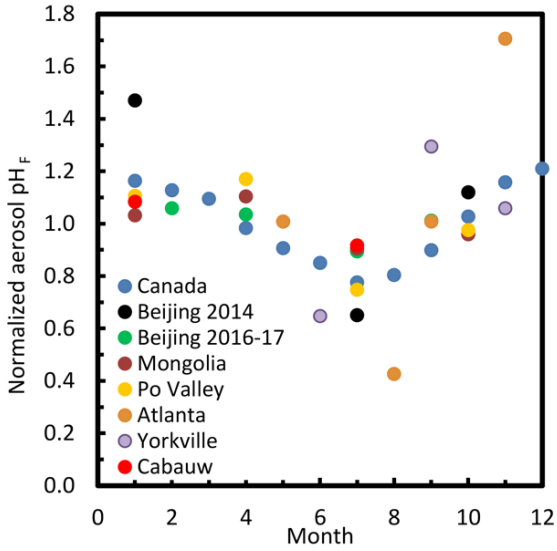

Figure 1.2: Seasonal variability of fine-aerosol acidity (pH_F divided by the annual average). The annual average pH for Canada, Beijing 2014, Beijing 2016-2017, Inner Mongolia, the Po Valley, Cabaw, Atlanta, and Yorkville is 2.5, 2.8, 4.3, 5.5, 3.1, 3.6, 1.3, and 1.7, respectively (Pye, Nenes, Alexander, Ault, Barth, Clegg, Collett Jr., et al., 2020).

1.3 Aim of the study

This study aims to investigate the seasonal and diurnal variability of submicron aerosol (PM_1) pH and associated aerosol water in the East Mediterranean atmosphere and more precisely at Finokalia atmospheric monitoring station of ECPL of the University of Crete.

The study is motivated by the fact that the Eastern Mediterranean atmosphere is a cross-road of air masses influenced by both anthropogenic and natural sources (the area is surrounded by Europe, Asia and Africa) that is also affected by intensive photochemistry. It is thus expected that various pollutant sources are affecting aerosol chemical composition, hygroscopicity and acidity, making Finokalia a suitable location for studying aerosol pH variability. Earlier studies of aerosol acidity in the area over short time periods have shown aerosol pH values that range between 0.5 and 2.8 (Bougiatioti et al., 2016) depending on the air mass origin. They have also shown a large diurnal variability in aerosol pH with minima during day and maxima during night when relative humidity is also high.

High aerosol acidity has been found to be associated with aerosols harmful for human health. Furthermore, it is well known that the East Mediterranean Sea is highly oligotrophic, a marine desert, with extremely low biological productivity, due to low availability of inorganic nutrients such as dissolved phosphate that are needed for phytoplankton to grow (Powley et al., 2017). On the other hand, the Eastern Mediterranean atmosphere is subject to many dust outbreaks from the Saharan desert which contains various minerals and metals mainly in insoluble forms. In order for such elements to be bioavailable they have to be in soluble form. The conversion of insoluble to soluble form of a given nutrient is favored under acidic conditions (Kanakidou et al., 2018). For instance, (Nenes et al., 2011b) proposed that significant amount of phosphorus which was present in Saharan dust aerosol can be solubilized by acidification in the atmosphere and upon deposition will remain in solution and thus available for phytoplankton.

Aerosol acidity is thus of a great importance in areas such as the Eastern Mediterranean which has low availability of primary P. Iron solubility and thus its bioavailability to ecosystems is also driven by acidity as it is enhanced in the presence of acidic species. Theodosi et al. (2008) found out that in the Eastern Mediterranean the Fe solubility ranged from about 28% for polluted rainwater (pH between 4 and 5) and 0.5% for Sahara dust episodes (pH=8). Bougiatioti et al. (2016) examined the pH of both PM_1 and PM_{10} fractions and its regional sources. They found that the PM_1 aerosol pH from almost all sources was highly acidic, including that of PM_1 influenced by desert dust, which is an indication for potential nutrient enrichment; even though at such small sizes the nutrient flux is lower than in the coarse mode.

Here we present the first yearlong study that investigates the levels of pH and aerosol water of PM_1 and their seasonal variability and its main drivers. For this, observed chemical composition data of PM_1 aerosol (available observations conducted using the Aerosol Chemical Speciation Monitor (ACSM)) at the Finokalia site from February to December 2014 in combination with gas phase NH_3, HNO_3 and HCl concentration measurements in the Eastern Mediterranean atmosphere are used as inputs into the ISORROPIA-II thermodynamic equilibrium model (Fountoukis and Nenes, 2007). The LWC and submicron aerosol pH in the area are thus calculated for almost one year and then the seasonality of the derived pH and the drivers of this variability are investigated.

The sensitivity of submicron aerosol pH to non-volatile cations and gas phase ammonia is also investigated and the particulate matter's sensitivity to gas phase ammonia and nitric acid emissions is also assessed. In order to examine the accuracy of our aerosol water and pH predictions, an evaluation of ISORROPIA-II was conducted looking into its ability to reproduce the partitioning of semi-volatile compounds and investigate the potential discrepancies due to meteorological conditions. Finally, the pH of fine aerosol ($PM_{2.5}$ particles with diameter less than 2.5 μm) at another location in Greece, in Ioannina City, an urban region

at the NW part of Greece, was calculated and compared with that of PM_1 at the background station of Finokalia.

.

2. Model Description and Methodology

Aerosols play a significant role in the most important processes in the atmosphere such as cloud formation, heterogeneous reactions, scattering and absorption of solar radiation. They contribute to atmospheric deposition of nutrients and/or toxic elements and affect human health. As a result, the knowledge of their chemical composition and physical state is crucial in order to assess their impact on climate, ecosystems and human health. For this, numerous thermodynamic equilibrium models have been developed, which differentiate regarding the chemical species that they examine, the solution methods used and the input data that they use and assume acceptable. In order to determine the composition and state of the aerosols, each atmospheric gas/aerosol models require knowledge of the thermodynamic equilibrium state to the aerosol components due to the fact that the driving force for mass transfer of species between gas and aerosol phases is the deviation from equilibrium.

2.1 ISORROPIA-II

The thermodynamic equilibrium model ISORROPIA (Nenes et al., 1998; Nenes et al., 1999) predicts the physical state and composition of inorganic NH_4^+ –Na^+ –SO_4^{2-} –NO_3^- –Cl^- –H_2O aerosol systems in thermodynamic equilibrium with gas phase precursors. ISORROPIA-II (Fountoukis and Nenes, 2007) which is an extension of ISORROPIA and is used in this study, uses the same principles and routines as ISORROPIA with the only difference being the addition of the crustal species K^+, Ca^{2+} and Mg^{2+} which are a major component of dust and consequently contribute substantially to the total particulate matter.

ISORROPIA-II's system contains the following possible constituents:

Gas phase: $NH_{3(g)}$, $HNO_{3(g)}$, $HCl_{(g)}$, $H_2O_{(g)}$

Liquid phase: $NH_4^+{}_{(aq)}$, $Na^+{}_{(aq)}$, $H^+{}_{(aq)}$, $Cl^-{}_{(aq)}$, $NO_3^-{}_{(aq)}$, $SO_4^{2-}{}_{(aq)}$, $HNO_{3(aq)}$, $NH_{3(aq)}$, $HCl_{(aq)}$, $HSO_4^-{}_{(aq)}$, $OH^-{}_{(aq)}$, $H_2O_{(aq)}$, $\mathbf{Ca^{2+}_{(aq)}}$, $\mathbf{Mg^{2+}_{(aq)}}$, $\mathbf{K^+_{(aq)}}$

Solid phase: $(NH_4)_2SO_{4(s)}$, $NH_4HSO_{4(s)}$, $(NH4)_3H(SO_4)_{2(s)}$, $NH_4NO_{3(s)}$, $NH_4Cl_{(s)}$, $NaCl_{(s)}$, $NaNO_{3(s)}$, $NaHSO_{4(s)}$, $Na_2SO_{4(s)}$, $\mathbf{CaSO_{4(s)}}$, $\mathbf{Ca(NO_3)_{2(s)}}$, $\mathbf{CaCl_{2(s)}}$, $\mathbf{K_2SO_{4(s)}}$, $\mathbf{KHSO_{4(s)}}$, $\mathbf{KNO_{3(s)}}$, $\mathbf{KCl_{(s)}}$, $\mathbf{MgSO_{4(s)}}$, $\mathbf{Mg(NO_3)_{2(s)}}$, $\mathbf{MgCl_{2(s)}}$

where in bold are the new species incorporated in ISORROPIA-II. All the equilibrium reactions with the corresponding values of the equilibrium constants used in the model are presented in Table 2.1.

Table 2.1: Equilibrium reactions and their equilibrium constants used in ISORROPIA-II (Nenes et al., 1998; Fountoukis and Nenes, 2007).

Equilibrium reactions	**Expression of equilibrium constants**
$Ca(NO_3)_{2(s)} \leftrightarrow Ca^{2+}_{(aq)} + 2NO_3^-{}_{(aq)}$	$[Ca^{2+}]\,[NO_3^-]^2\,\gamma Ca^{2+}\;\gamma^2 NO_3^-$
$CaCl_{2(s)} \leftrightarrow Ca^{2+}_{(aq)} + 2Cl^-_{(aq)}$	$[Ca^{2+}]\,[Cl^-]^2\,\gamma Ca^{2+}\;\gamma^2 Cl^-$
$CaSO_4.2H_2O_{(s)} \leftrightarrow Ca^{2+}_{(aq)} + SO_4^{2-}{}_{(aq)} + 2H_2O$	$[Ca^{2+}]\,[SO_4^{2-}]\,\gamma Ca^{2+}\;\gamma SO_4^{2-}$
$K_2SO_{4(s)} \leftrightarrow 2K^+_{(aq)} + SO_4^{2-}{}_{(aq)}$	$[K^+]^2\,[SO_4^{2-}]\,\gamma^2 K^+\;\gamma SO_4^{2-}$
$KHSO_{4(s)} \leftrightarrow K^+_{(aq)} + HSO_4^-{}_{(aq)}$	$[K^+]\,[HSO_4^-]\,\gamma K^+\;\gamma HSO_4^-$
$KNO_{3(s)} \leftrightarrow K^+_{(aq)} + NO_3^-{}_{(aq)}$	$[K^+]\,[NO_3^-]\,\gamma K^+\;\gamma NO_3^-$
$KCl_{(s)} \leftrightarrow K^+_{(aq)} + Cl^-_{(aq)}$	$[K^+]\,[Cl^-]\,\gamma K^+\;\gamma Cl^-$
$MgSO_{4(s)} \leftrightarrow Mg^{2+}_{(aq)} + SO_4^{2-}{}_{(aq)}$	$[Mg^{2+}]\,[SO_4^{2-}]\,\gamma Mg^{2+}\;\gamma SO_4^{2-}$
$Mg(NO_3)_{2(s)} \leftrightarrow Mg^{2+}_{(aq)} + 2NO_3^-{}_{(aq)}$	$[Mg^{2+}]\,[NO_3^-]^2\,\gamma Mg^{2+}\;\gamma^2 NO_3^-$
$MgCl_{2(s)} \leftrightarrow Mg^{2+}_{(aq)} + 2Cl^-_{(aq)}$	$[Mg^{2+}]\,[Cl^-]^2\,\gamma Mg^{2+}\;\gamma^2 Cl^-$
$HSO^-{}_{4(s)} \leftrightarrow H^+_{(aq)} + H^{+2-}{}_{(aq)}$	$\dfrac{[H^+][SO_4^{2-}]\,\gamma H^+\gamma SO_4^{2-}}{[HSO_4^-]\gamma HSO_4^-}$
$NH_{3(g)} \leftrightarrow NH_{3(aq)}$	$\dfrac{[NH_{3(aq)}]\,\gamma NH_{3(aq)}}{P_{NH_{3(g)}}}$
$NH_{3(aq)} + H_2O_{(aq)} \leftrightarrow NH_4^+{}_{(aq)} + OH^-_{(aq)}$	$\dfrac{[NH_4^+]\,[OH^-]\,\gamma OH^-\gamma NH_4^+}{[NH_{3(aq)}]a_w\;\gamma NH_{3(aq)}}$
$HNO_{3(g)} \leftrightarrow H^+_{(aq)} + NO_3^-{}_{(aq)}$	$\dfrac{[H^+][NO_3^-]\,\gamma H^+\gamma NO_3^-}{P_{HNO_{3(g)}}}$
$HNO_{3(g)} \leftrightarrow HNO_{3(aq)}$	$\dfrac{[HNO_{3(aq)}]\,\gamma HNO_{3(aq)}}{P_{HNO_{3(g)}}}$
$HCl_{(g)} \leftrightarrow H^+_{(aq)} + Cl^-_{(aq)}$	$\dfrac{[H^+][Cl^-]\,\gamma H^+\gamma Cl^-}{P_{HCl(g)}}$
$HCl_{(g)} \leftrightarrow HCl_{(aq)}$	$\dfrac{[HCl_{(aq)}]\,\gamma HCl_{(aq)}}{P_{HCl_{(g)}}}$
$H_2O_{(aq)} \leftrightarrow H^+_{(aq)} + OH^-_{(aq)}$	$\dfrac{[H^+][OH^-]\,\gamma H^+\gamma OH^-}{a_w}$
$Na_2SO_{4(s)} \leftrightarrow 2Na^+_{(aq)} + SO_4^{2-}{}_{(aq)}$	$[Na^+]^2\,[SO_4^{2-}]\,\gamma^2 Na^+\;\gamma SO_4^{2-}$
$(NH_4)_2SO_{4(s)} \leftrightarrow 2NH_4^+{}_{(aq)} + SO_4^{2-}{}_{(aq)}$	$[NH_4^+]^2\,[SO_4^{2-}]\,\gamma^2 NH_4^+\;\gamma SO_4^{2-}$
$NH_4Cl_{(s)} \leftrightarrow NH_{3(g)} + HCl_{(g)}$	$P_{NH3}P_{HCl}$
$NaNO_{3(s)} \leftrightarrow Na^+_{(aq)} + NO_3^-{}_{(aq)}$	$[Na^+]\,[NO_3^-]\,\gamma Na^+\;\gamma NO_3^-$
$NaCl_{(s)} \leftrightarrow Na^+_{(aq)} + Cl^-_{(aq)}$	$[Na^+]\,[Cl^-]\,\gamma Na^+\;\gamma Cl^-$
$NaHSO_{4(s)} \leftrightarrow Na^+_{(aq)} + HSO^-{}_{4(aq)}$	$[Na^+]\,[HSO_4^-]\,\gamma Na^+\;\gamma HSO_4^-$
$NH_4NO_{3(s)} \leftrightarrow NH_{3(g)} + HNO_{3(g)}$	$P_{NH3}P_{HNO3}$
$NH_4HSO_{4(s)} \leftrightarrow NH_4^+{}_{(aq)} + HSO_4^-{}_{(aq)}$	$[NH_4^+]\,[HSO_4^-]\,\gamma NH_4^+\;\gamma HSO_4^-$
$(NH_4)_3H(SO_4)_{2(s)} \leftrightarrow 3NH_4^+{}_{(aq)} + SO_4^{2-}{}_{(aq)} + HSO_4^-{}_{(aq)}$	$[NH_4^+]^3\,[SO_4^{2-}]\,[HSO_4^-]\,\gamma^2 NH_4^+\;\gamma SO_4^{2-}\;\gamma HSO_4^-$

The model can be run in two ways:

- Forward problems (or ‘‘closed’’) in which the temperature, relative humidity and the total concentrations (aerosol + gas) of aerosol precursors (NH_3, H_2SO_4, Na, HCl, HNO_3, Ca, K and Mg) are known.

- Reverse problems (or ‘‘open’’) in which known quantities are the temperature, relative humidity and the concentrations of only the aerosol phase of NH_3, H_2SO_4, Na, HCl, HNO_3, Ca, K and Mg i.e. NH_4^+, SO_4^{2-}, Na^+, Cl^-, NO_3^-, Ca^{2+}, K^+ and Mg^{2+}.

In both cases the output is the concentration of species in the aerosol (solid, liquid) and gas phase, liquid water content and the particle hydronium ion concentration per volume air, and thus the particle pH. The number of the equilibrium reactions that can take place in the system and the possible species are determined in both cases by the relative abundance of each of the aerosol precursor and the meteorology (ambient temperature and relative humidity). The following ratios are used to determine the major species that could be present in the aerosol phase:

$$R_1 = \frac{[NH_4^+]+[Ca^{2+}]+[K^+]+[Mg^{2+}]+[Na^+]}{[SO_4^{-2}]}$$
$$R_2 = \frac{[Ca^{2+}]+[K^+]+[Mg^{2+}]+[Na^+]}{[SO_4^{-2}]}$$
$$R_3 = \frac{[Ca^{2+}]+[K^+]+[Mg^{2+}]}{[SO_4^{-2}]}$$

where the concentrations of each aerosol precursor are in mol/m^3 of air. The terms are the R_1 ‘‘sulfate ratio’’, R_2 ‘‘crustal species and sodium ratio’’ and R_3 ‘‘crustal species ratio’’. According to these ratios there are five possible aerosol types and corresponding possible species in each type are listed in Table 2.2.

The water activity (a_w) in an atmospheric aerosol solution is equal to the relative humidity (given that RH is expressed in 0-1 scale) (Seinfeld & Pandis, 2006). This is due to the fact that water vapor in the atmosphere exists in large amounts while its concentration in the aerosol phase is less than 1 mg/m^3 of air. Consequently, transport of water to and from the aerosol phase does not affect the ambient vapor pressure of water in the atmosphere. In combination with the assumption that the curvature effect is negligible, phase equilibrium between gas and aerosols gives the water activity to be equal to the ambient RH. The curvature effect is determined by the Kelvin equation according to which, the vapor pressure over a curved surface is always higher than that of the same substance over a flat surface (Seinfeld & Pandis, 2006). This can be explained by the fact that comparing to a flat surface, in the occurrence of a curved surface, the molecules are closer to one another and fewer molecules are adjacent to a molecule on the surface. As a consequence, the surface’s molecules are transferred into the vapor phase more easily and thus the vapor pressure over a curved interface is greater than that over a flat surface.

Table 2.2: Possible species for the five different aerosol types **(**Fountoukis and Nenes, 2007**).**

R_1	R_2	R_3	Aerosol type	Solid phase	Major species Aqueous phase	Gas phase	Minor species
$R_1<1$	Any value	Any value	Sulfate rich (free acid)	$NaHSO_4$, NH_4HSO_4, $KHSO_4$, $CaSO_4$	Na^+, NH_4^+, H^+, HSO_4^-, SO_4^{2-}, NO_3^-, Cl^-, Ca^{2+}, K^+, H_2O	H_2O	$NH_{3(g)}$, $NO_3^-{}_{(aq)}$, $Cl^-{}_{(aq)}$, $NH_{3(aq)}$, $HCl_{(aq)}$, $HNO_{3(aq)}$
$1\leq R_1<2$	Any value	Any value	Sulfate rich	$NaHSO_4$, NH_4HSO_4, $(NH_4)_2SO_4$, Na_2SO_4, $(NH_4)_3H(SO_4)_2$, $CaSO_4$, $KHSO_4$, K_2SO_4, $MgSO_4$	Na^+, NH_4^+, H^+, HSO_4^-, SO_4^{2-}, NO_3^-, Cl^-, Ca^{2+}, K^+, Mg^{2+}, H_2O	H_2O	$NH_{3(g)}$, $NO_3^-{}_{(aq)}$, $Cl^-{}_{(aq)}$, $NH_{3(aq)}$, $HCl_{(aq)}$, $HNO_{3(aq)}$
$R_1\geq 2$	$R_2<2$	Any value	Sulfate poor, Crustal and Sodium poor	Na_2SO_4, $(NH_4)_2SO_4$, NH_4NO_3, NH_4Cl, $CaSO_4$, K_2SO_4, $MgSO_4$	Na^+, NH_4^+, H^+, SO_4^{2-}, NO_3^-, Cl^-, Ca^{2+}, K^+, Mg^{2+}, H_2O, $NH_{3(aq)}$, $HCl_{(aq)}$, $HNO_{3(aq)}$	H_2O, NH_3, HCl, HNO_3	$HSO^-_{4(aq)}$
$R_1\geq 2$	$R_2\geq 2$	$R_3<2$	Sulfate poor, Crustal and Sodium rich, Crustal poor	Na_2SO_4, $NaNO_3$, NH_4NO_3, NH_4Cl, $NaCl$, $CaSO_4$, K_2SO_4, $MgSO_4$	Na^+, NH_4^+, H^+, SO_4^{2-}, NO_3^-, Cl^-, Ca^{2+}, K^+, Mg^{2+}, H_2O, $NH_{3(aq)}$, $HCl_{(aq)}$, $HNO_{3(aq)}$	H_2O, NH_3, HCl, HNO_3	$HSO^-_{4(aq)}$
$R_1\geq 2$	$R_2\geq 2$	$R_3>2$	Sulfate poor, Crustal and Sodium rich, Crustal rich	$NaNO_3$, $NaCl$, NH_4NO_3, NH_4Cl, $CaSO_4$, K_2SO_4, $MgSO_4$, $Ca(NO_3)_2$, $CaCl_2$, $Mg(NO_3)_2$, $MgCl_2$, KNO_3, KCl	Na^+, NH_4^+, H^+, SO_4^{2-}, NO_3^-, Cl^-, Ca^{2+}, K^+, Mg^{2+}, H_2O, $NH_{3(aq)}$, $HCl_{(aq)}$, $HNO_{3(aq)}$	H_2O, NH_3, HCl, HNO_3	$HSO^-_{4(aq)}$

ISORROPIA determines the aerosol water content using the Zbanovskii-Stokes-Robinson (ZSR) correlation in which it is assumed that water uptake by a mixture of materials is additive of the water content retained by each chemical species (Stokes & Robinson, 1966):

$$W = \sum_i \frac{M_i}{m_{oi}(a_w)} \quad (1)$$

where W is the mass concentration of aerosol water (kg/m^3 air), M_i is the molar concentration of species i (mol/m^3 air), and m_{oi} (a_w) is the molality (mol/kg) of an aqueous binary solution of i-th electrolyte with the same a_w (i.e. relative humidity) as in the multicomponent solution.

At very low relative humidity, atmospheric aerosol particles that contain inorganic salts are solid. As the ambient RH increases, the particles remain in solid phase until relative humidity reaches a threshold value, characteristic to the particle composition (Seinfeld & Pandis, 2006). At this RH, the solid phase particle spontaneously absorbs water resulting in the production of a saturated aqueous solution. This relative humidity level at which this transition occurs is the deliquescence relative humidity (DRH). If the relative humidity increases beyond this level, further water condensation onto the salt solution will occur in order to maintain thermodynamic equilibrium. On the contrary, evaporation of water occurs as the RH over a wet particle decreases. The solution however does not generally crystallize at the DRH, but rather remains supersaturated until RH decreases much further until the crystallization occurs. For each relative humidity, a single salt can exist in either a solid state or an aqueous solution. For RH lower than the DRH, the Gibbs free energy of the solid salt is lower than the energy of the corresponding solution, as a result the salt remains in the solid state (Fig. 2.1, (Seinfeld & Pandis, 2006)). Increasing the RH, the Gibbs free energy of the corresponding solution decreases, and at the DRH it becomes the same as the energy of the solid. As RH increases further the particle absorbs water spontaneously and a saturated salt solution is formed.

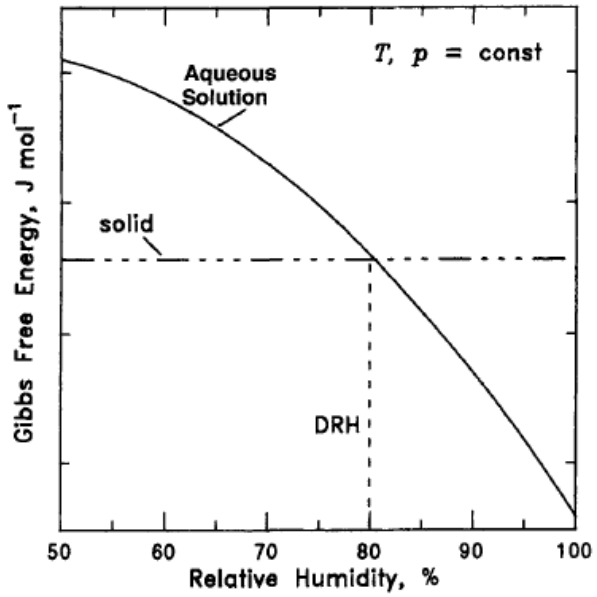

Figure 2.1: Gibbs free energy of a solid salt and its aqueous solution as a function of Relative Humidity. At the DRH (deliquescence relative humidity) these energies become equal (Seinfeld & Pandis, 2006).

Similarly, to the single-component salts, in multicomponent mixtures there is a characteristic relative humidity below which, a solid phase is thermodynamically favored, and is termed mutual deliquescence relative humidity (MDRH). MDRH point corresponds to the mixture with a composition that minimizes water activity (Gibbs Free energy of the solution), which means the aerosol with multiple components will deliquesce at a lower RH than the minimum DRH of each individual component. Estimating the aerosol composition in a mutual deliquescence region (MDR) is a computationally demanding task and a different approach is used in ISORROPIA-II. The MDRH means that when MDRH is lower than the DRH of the

salt with the lowest DRH in a given mixture, the solution is said to be in the mutual deliquescence region, MDR. The aerosol composition in the model is assumed as a weighted mean of two states, one in which there is no water (dry state) and one in which the most hygroscopic salt (meaning the one with the lowest DRH) is completely dissolved (wet state). Below the MDRH of an aerosol mixture, the particle is a solid. However, when the RH over a wet particle decreases, the wet aerosol may not crystallize below the MDRH and may remain in a metastable state, where it is an aqueous supersaturated solution (Fountoukis and Nenes, 2007; Nenes et al., 1998). ISORROPIA-II can address both states, the stable one, where salts precipitate if saturation is exceeded, and the metastable one, where salts do not precipitate under supersaturated conditions. The aerosol in the first case can be solid, liquid or both, while the second case is always an aqueous solution.

Summarizing the basic procedure and steps followed by ISORROPIA-II, depending on the three ratios (R_1, R_2, R_3) as described earlier, the meteorology (ambient temperature and relative humidity), the model solves a number of equilibrium equations needed and along with calculations for mass conservation, electroneutrality, water activity, and activity coefficient, the resulting concentrations at thermodynamic equilibrium are outputted. Figure 2.2 (Fountoukis and Nenes, 2007) shows the general description of the typical procedure followed by the model.

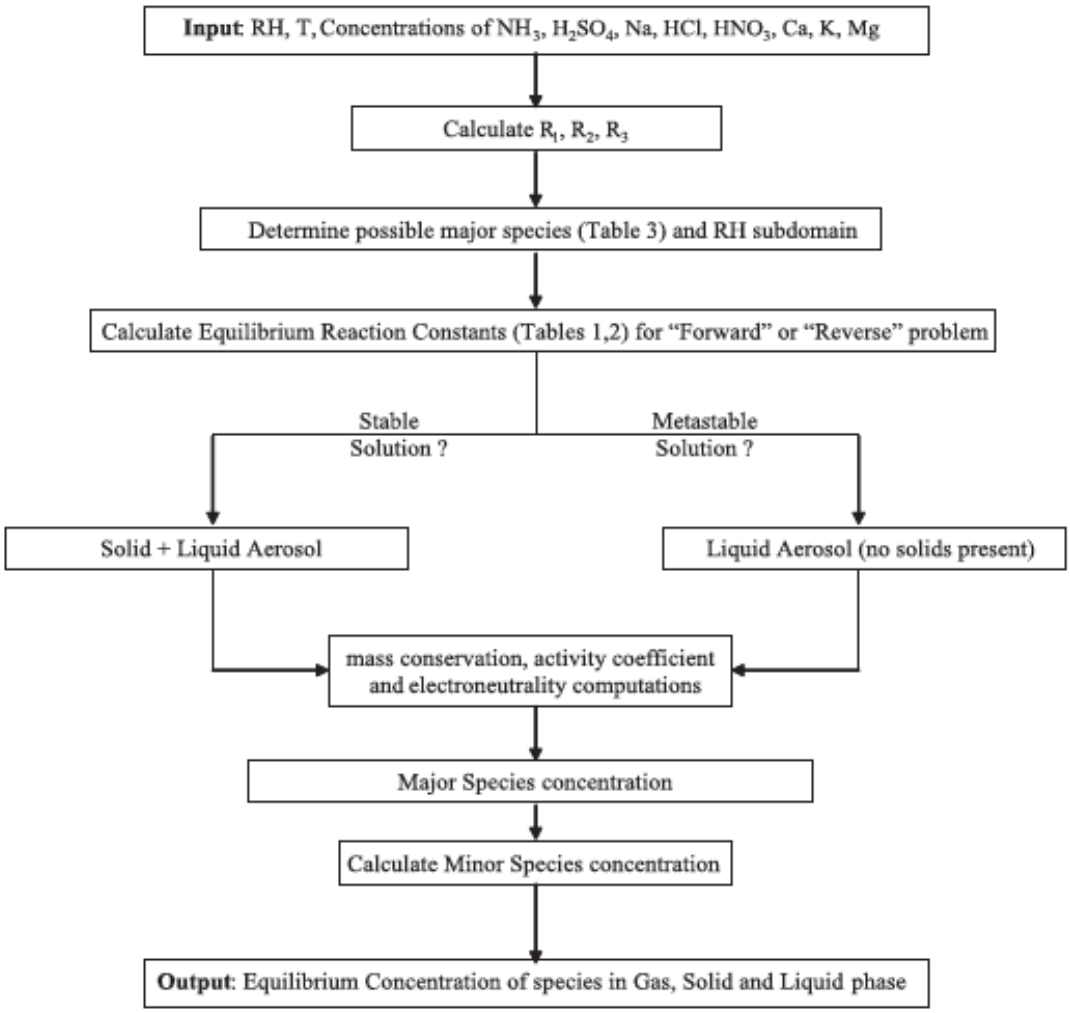

Figure 2.2: General solution procedure of ISORROPIA-II (Fountoukis and Nenes 2007).

Some important conceptual issues and assumptions of ISORROPIA-II include the fact that

1. when calculating the concentration of species, the stable state solution algorithm of the model begins assuming a completely dry aerosol and when the relative humidity gradually increases or decreases, the model dissolves each salt (according to their DRH) and determines solid and ion concentrations and water uptake.
2. Also, in order to determine the aerosol composition at low relative humidity levels (meaning the aerosol is solid) and when aerosol contains volatile anions, sulfate and non-volatile species such as sodium and potassium, the following concept is applied. When this is the case, $Na^{+}_{(aq)}$ and $K^{+}_{(aq)}$ preferentially associate with $SO_4^{2-}{}_{(aq)}$ to form $Na_2SO_{4(s)}$ and $K_2SO_{4(s)}$ before they are bound with $NO_3^{-}{}_{(aq)}$ and $Cl^{-}_{(aq)}$ to form the corresponding salts.
3. An important assumption made in the model is that H_2SO_4, sodium and crustal species are assumed to utterly reside in the aerosol phase due to their extremely low vapor pressure.
4. The first dissociation of H_2SO_4 in which $H_2SO_{4(aq)} \rightarrow H^{+} + HSO_4^{-}$, is assumed to be complete and it is not considered in the calculations.
5. Furthermore, when crustal species are dominating the aerosol system that it is examined compared to all the ions, the model assumes the solution to be close to neutral (pH≈7). This is consistent when excess carbonate is present in the aerosol phase, which has a $pK_a \approx 6.4$ (Meng et al., 1995).
6. ISORROPIA-II does not take into account the organic anions in the thermodynamic calculations and the non-volatiles (crustal species and sodium) that may be associated with organic acids are assumed excess and they are not considered in the model.
7. The activity coefficients γ_{OH^-} and γ_{H^+} are considered equal to unity since the activity coefficient routines present cannot explicitly calculate them. For sulfate poor ratios ($R_1 > 2$) the HSO_4^{-} ion is considered a minor species from its reaction $HSO_4^{-}{}_{(aq)} \leftrightarrow H^{+}_{(aq)} + SO_4^{2-}{}_{(aq)}$.

2.2 Methodology and observational data

2.2.1 Measurements

Observations of submicron aerosol particles (organic, sulfate, ammonium, nitrate and chloride) and gas phase ammonia, nitric acid and hydrochloride were performed at the Finokalia atmospheric observatory of the University of Crete in Crete, Greece (35°20´N, 25°40´E; 250 m a.s.l.) from February to December 2014. The Finokalia station (Fig. 2.3) (http://finokalia.chemistry.uoc.gr/) is located at a coastal remote background site (50 m from the shore and 230 m above sea level) in the northeastern part of the island of Crete, far from any significant local anthropogenic emissions, and is facing the Mediterranean Sea within the sector of 90° - 270°. Depending on the prevailing wind direction, the site is receiving air masses of various origins, predominantly from the north/northwest sector (coming from Balkans, mainland Greece and Central Europe), but also from the south with dust events from the Sahara desert occurring frequently through the year and more often close to the equinox conditions in spring and fall (Mihalopoulos et al., 1997). Overall, Finokalia station is a representative background site for the eastern Mediterranean.

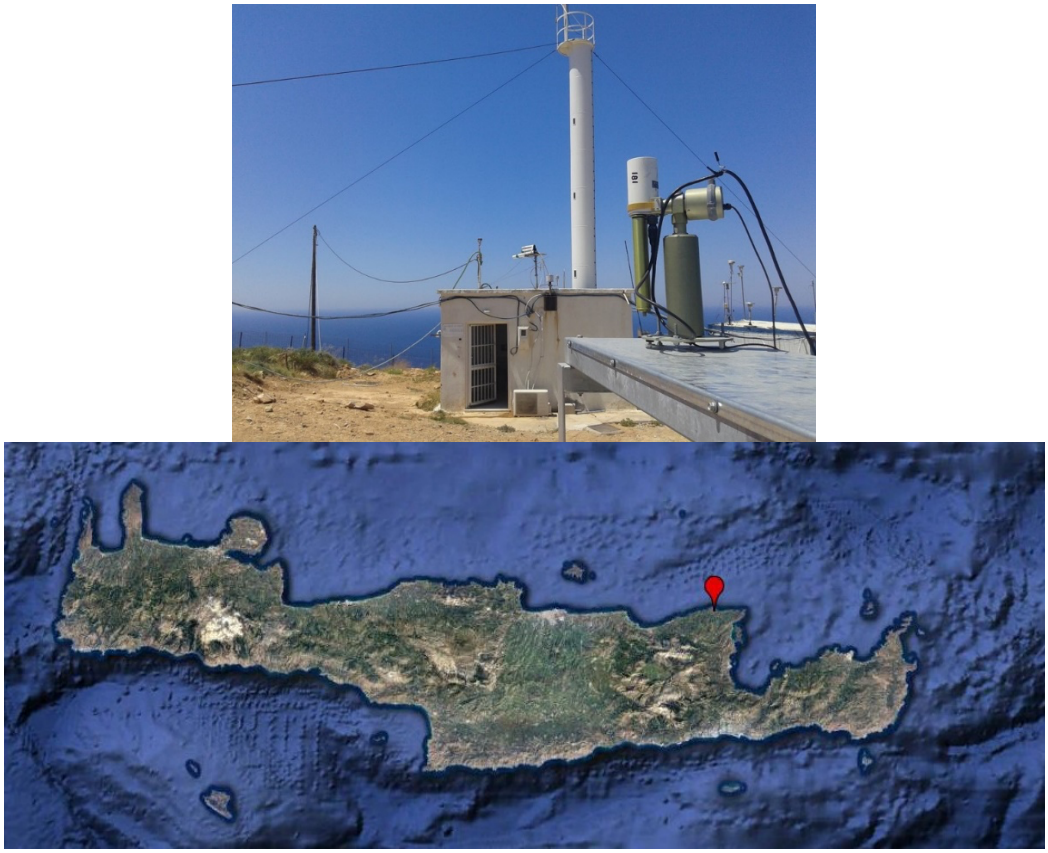

Figure 2.3: Finokalia atmospheric observatory of the University of Crete in Crete, Greece (35°20´N, 25°40´E; 250 m a.s.l.). (http://finokalia.chemistry.uoc.gr/)

The chemical composition and mass of non-refractory submicron aerosol particles at Finokalia were measured online with an Aerosol Chemical Speciation Monitor (ACSM) from February

to December 2014 (Stavroulas et al. 2020 in preparation). The ACSM provides real time measurements of ammonium, sulfate, chloride, nitrate and organic mass in non-refractory submicron atmospheric particles (Ng et al., 2011). ACSM data were recorded every 30 minutes and analyzed using hourly averaged values in ISORROPIA-II following the procedure described by (Bougiatioti et al., 2016), together with meteorological data recorded at Finokalia every 5 minutes and averaged to hourly values. Further details and information about the mass concentration measured at Finokalia with the ACSM during this 11-months period can be found in Stavroulas et al. (2020 in preparation).

Using the thermodynamic model ISORROPIA-II aerosol pH can be accurately predicted as shown in past studies when gas-particle partitioning observations are interpreted by thermodynamic model calculations. Multiple studies (Guo et al., 2015, Weber et al., 2016) have shown that neglecting gas phase NH_3 in the thermodynamic equilibrium calculation of pH results in an underestimation of at most one unit. Bougiatioti et al. (2016) estimated that at Finokalia neglecting gas phase NH_3 levels of about 0.1 to 0.7 $\mu g/m^3$ could lead to an underestimation in the fine particle pH of around 0.5 units.

Gas phase measurements were also conducted at the Finokalia station for NH_3 from January 2013 to January 2015 and for HNO_3 and HCl from April 2013 to January 2015. For this, filter samples were collected every 3days by two different glass fiber filters positioned the one after the other, one coated with Na_2CO_3 for the acidic gas phase compounds and one coated with phosphoric acid for the basic gases. The analysis was performed in the laboratory by ion chromatography. Gas phase measurements were linearly interpolated in order to fit the timing of ACSM data series and these particulate and gas phase measurements for the period of our study together with the corresponding meteorology (temperature and relative humidity in hourly values) were used as input to the thermodynamic equilibrium model ISORROPIA-II that was run in the forward mode assuming a metastable aerosol state (which is the state in which the aerosol is constituted by solely an aqueous phase which can be supersaturated concerning the dissolved salts) in order to predict the aerosol pH.

From February to December 2014 (70 days in total), PM_1 filter measurements including sodium, ammonium, potassium, magnesium, calcium, chloride, bromine, nitrate, sulfate and oxalate were also conducted at Finokalia. The average and median values of the measured ions, which also were used in this study, are shown in Table 2.3. These measurements were used to investigate the dependence of aerosol pH on crustal species and sodium. Further sensitivity tests to gas phase ammonia levels were performed (see section 3.4 *Sensitivity of aerosol pH and nitrate partitioning*).

Table 2.3: PM_1 measurements conducted at the Finokalia station for 70 days (from 06/02/2014 to 13/12/2014) used in the sensitivity tests for the three simulations performed with ISORROPIA-II.

$\mu g/m^3$	**Sulfate**	**Nitrate**	**Ammonium**	**Chloride**	**Calcium**	**Potassium**	**Magnesium**	**Sodium**
mean	7.33	0.21	2.28	0.40	0.41	0.32	0.04	0.34
stdev	7.70	0.57	2.12	0.74	1.17	0.34	0.11	0.60
median	4.95	0.08	1.75	0.19	0.13	0.21	0.01	0.17

2.2.2 Methodology

Aerosol pH calculations

ISORROPIA-II calculates the equilibrium particle hydronium ion concentration per volume air (H_{air}^{+}), along with the particle water associated with the inorganic species (W_{inorg}) in order to predict the aerosol pH. Since organics contribute substantially to the fine fraction mass (Bougiatioti et al., 2009; Koulouri et al., 2008), the particle water associated with the organic species (W_{org}) should be considered in the aerosol pH prediction. For this, the W_{org} was calculated according to the following equation (Guo et al., 2015) using the organic hygroscopicity parameter (κ_{org}) as derived in Cellury et al. (2015):

$$W_{org} = \frac{m_{org}\rho_w}{\rho_{org}} \frac{k_{org}}{\left(\left(\frac{1}{RH}\right)-1\right)} \quad (2)$$

where m_{org} is the organic mass concentration measured by ACSM (in μg/m^3), ρ_{org} is a typical organic density of 1350 kg/m^3 (Lee et al., 2010), ρ_w is the density of water, k_{org} is the organic hygroscopicity parameter with a value of 0.16 and RH the relative humidity measured at Finokalia for the studied period.

As ISORROPIA-II does not calculate the particle water associated with the organic species (W_{org}), but only that associated with the inorganic species (W_{inorg}), pH was recalculated using the total LWC as the sum of W_{inorg} from the model and W_{org} derived from eq. (2), and the H_{air}^{+} as derived from the model, using the following equation (Guo et al., 2015):

$$\text{pH} = -log_{10}H_{aq}^{+} = -log\frac{1000H_{air}^{+}}{W_{org}+W_{inorg}} \quad (3)$$

where H^{+}_{aq} is the hydronium concentration in an aqueous solution (mol/L), H^{+}_{air} is the equilibrium particle hydronium ion concentration per volume air (μg/m^3) as derived from the model, W_{org} is the liquid water content associated with the organic species and W_{inorg} the particle water associated with the inorganics derived from the model (both W_{org} and W_{inorg} are in μg/m^3).

3. Results and Discussion

3.1 PM_1 chemical composition and gas phase

For the studied period (27 February to 31 December 2014) the average values of the submicron aerosol components were 2.04 ± 1.38, 2.44 ± 1.37, 0.43 ± 0.24, 0.66 ± 0.41 and 0.015 ± 0.027 μg/m^3 for the organics, sulfate, nitrate, ammonium and chloride, respectively. Figure 3.1a shows the contribution of each component to the total PM_1 mass concentration. Past studies have shown that sulfate contributes more than 50% to the submicron aerosol mass in the Eastern Mediterranean atmosphere, which is not the case for the Western Europe and North America (Mihalopoulos et al., 2007; Bardouki et al., 2003a,b; Sciare et al., 2005). Indeed, throughout the year sulfate and organics were the dominant constituents contributing up to 44% and 37% respectively to the PM_1 mass while nitrate and ammonium contributed 8% and 12% respectively and chloride mass contribution was negligible. The contribution of each species on a seasonal basis is shown in Fig. 3.1b with sulfate being the most abundant aerosol component during spring, summer and autumn (41% to 49% of total PM_1). The contribution of organics to PM_1 maximizes in winter when organics dominate (45% of total PM_1) while their contribution is minimum during autumn (33%) when sulfate contribution is maximum.

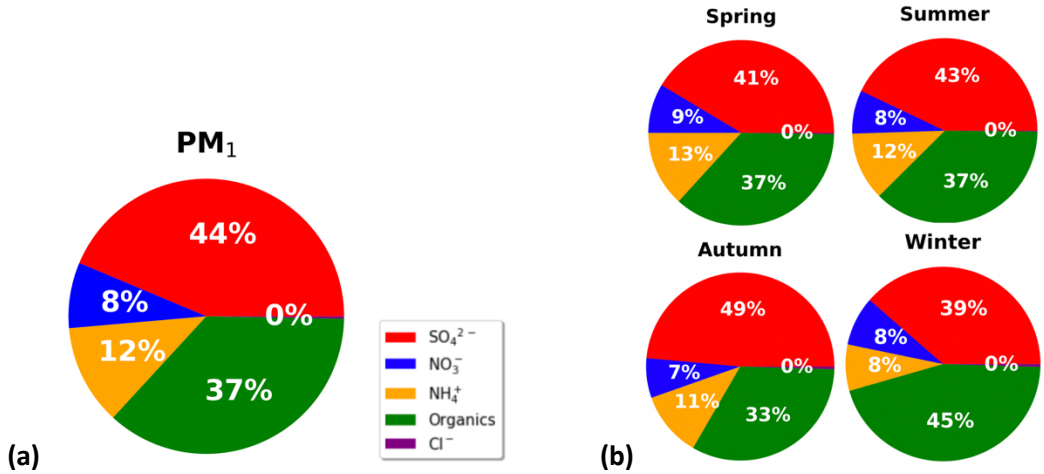

Figure 3.1: a) contribution of each component to the total PM1 mass concentration, ASCM data (27/02/2014 to 31/12/2014), b) Seasonally contribution to the PM_1 mass of each species.

As it can be seen also in Fig. 3.2 sulfate concentration at Finokalia exhibits higher values during summer as it arises from the homogeneous (photochemical) oxidation of sulfur dioxide (SO_2) in the gas phase resulting in the formation of H_2SO_4, which due to its extremely low vapor pressure resides in the aerosol phase as SO_4^{2-}.

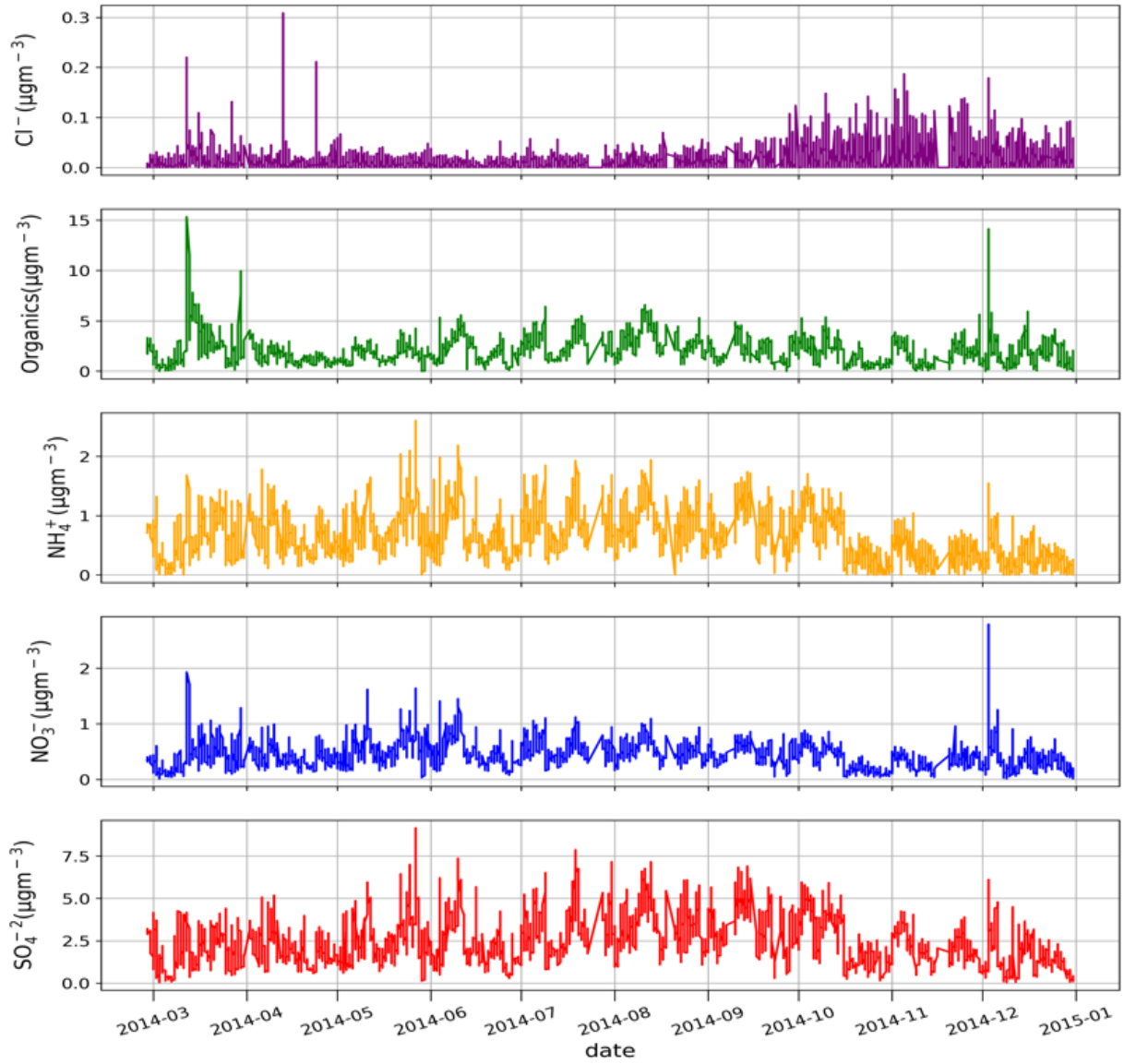

Figure 3.2: Timeseries of the species as measured by the ACSM in μg/m^3 from February to December 2014 at the Finokalia station.

The dominant oxidising agent during the day is the hydroxyl radical OH, which exhibits high concentrations in the aera during summer (mostly in regions with low cloud coverage and intensive photochemistry) (Mihalopoulos et al., 2007). During winter the chemical reactions for the production of sulfate (which are pH dependent) in the aqueous phase are also important. Multiple reactions of SO_2 with several reactants can occur for its transformation to sulfate, with some of them being with O_3, H_2O_2, O_2 (which are catalyzed by transition metal ion e.g. Mn(II) and Fe(III)), CH_3OOH, PAN, NO_2, OH (Seinfeld & Pandis, 2006). As for the dependence on aerosol pH, Chen et al (2016) suggested that during severe haze events in China, depending on the aerosol acidity levels, the dominant multiphase reaction pathways can change at pH values higher than 4.5 from reactions of NO_2 and O_3 to O_2 and to H_2O_2 at pH less than 4.5. On the contrary, despite nitric acid being a pollutant which is produced photochemically, the elevated nitrate concentrations during winter can be attributed to the formation of ammonium nitrate (NH_4NO_3) aerosol. The dissociation constant of ammonium nitrate strongly depends on

temperature and relative humidity levels. Low temperatures correspond to low values of the dissociation constant and therefore low equilibrium concentrations of ammonia and nitric acid in the gas phase, increasing the aerosol mass of ammonium nitrate. Depending on the ambient relative humidity, NH_4NO_3 may exist as an aqueous solution of NO_3^- and NH_4^+, or as a solid (typically at low levels of RH).

During summer due to high temperature, gaseous nitric acid is present rather than nitrate in the particle phase. The high concentrations of organics in winter are quite clear in Fig. 3.2. Usually during winter there are additional sources of organics due to high heating needs and aerosol concentrations additionally increase due to low mixing heights during that period. In summer, the photochemical production of secondary organic aerosol (SOA) contributes as well to the organic aerosol matter. Chloride is an overall negligible part of the submicron particulate matter. However, it shows the highest concentrations during winter that can be most probably attributed to strong wintertime winds resulting in transport of sea salt to the area. As for ammonium, generally ammonia is transferred to the aerosol phase in order to neutralize the acidic constituents and form ammonium sulfates (ammonium bisulfate, NH_4HSO_4 and ammonium sulfate, $(NH_4)_2SO_4$) and ammonium nitrate. Usually the ammonium concentration profile follows that of the sum of sulfate and nitrate. Looking into the entire timeseries of ammonium (Fig. 3.2) it can be seen that in general during the studied period ammonium follows the concentration pattern of sulfate and in particular during wintertime there are similarities with that of nitrate.

Average concentrations of gas phase ammonia, nitric acid and hydrochloric acid for the period of the study were 0.77 ± 0.44 μg/m^3 (median 0.75), 0.30 ± 0.31 μg/m^3 (median 0.17) and 2.40 ± 0.93 μg/m^3 (median 2.36), respectively (Tsiodra I., Diploma Thesis, ECPL, UOC, 2015). Past studies at the Finokalia station have reported similar concentration levels of gas phase ammonia and nitric acid, i.e., Mihalopoulos et al. (1997) in their preliminary data reported a range of 0.2 – 1.2 ppbv (0.14 – 0.83 μg/m^3) and a range of 0.7 – 1.2 μg/m^3 for HNO_3. Kouvarakis et al (2001) measured at Finokalia 13.36 ± 5.75 nmol/m^3 (0.23 ± 0.1 μg/m^3) for NH_3 (March to 1997 to June 1998) and 19.07 ± 12.23 nmol/m^3 (1.2 ± 0.77 μg/m^3) for HNO_3 (November 1996 to September 1999). Pikridas et al (2010) reported a value of 178 ± 100 ppt (0.46 ± 0.26 μg/m^3) of HNO_3 at Finokalia. For NH_3 levels around the Mediterranean and Greece a wide range has been reported depending on the characteristics of each area and location. An average NH_3 concentration of 2 μg/m^3 from November 1995 to August 1996 has been reported in Patras, Greece (Danalatos and Gravas 1999), while in Thessaloniki, NH_3 was on average 2.33 ± 1.46 μg/m^3 from April 2002 to March 2003 (Anatolaki & Tsitouridou, 2007) with values in both Patras and Thessaloniki being higher than that of Finokalia as expected for urban areas like those. Apart from the different meteorological and topographical characteristics in urban and rural areas the anthropogenic sources of NH_3 are mostly due to agricultural practices. However, in urban areas fossil fuel combustion and vehicle catalytic converters play a central role in NH_3 emissions (Perrino et al., 2002), while in dense populated areas, NH_3 emissions from urban wastes and sewage can also be important (Galán Madruga et al., 2018). As for the Mediterranean basin, satellite observations have reported 5.7 ± 0.1 10^6 molecules/cm^2 of NH_3 (which is 4.02 ± 0.07 μg/m^3 within an atmospheric column from surface to about 4km) (Nair & Yu, 2020), while in some major sites in Mediterranean NH_3 concentration levels were found to be 2.2 ± 1.0 μg/m^3 in an urban background site in Barcelona (May to September 2011) (Pandolfi et al., 2012), while measurements from May 2001 to March 2002 at a rural station in Montelibretti Italy, showed that ammonia ranged from 1.2 to 3.9 μg/m^3

and from 2.9 to 4.9 μg/m^3 at an urban background site (Villa Ada Park) (Perrino et al., 2002). These measurements of gas phase NH_3 and HNO_3 at the different locations are summarized in Table 3.1.

Table 3.1: Observations of gas phase NH_3 and HNO_3 at different sites in the Mediterranean.

Location	NH_3 (μg/m^3)	HNO_3 (μg/m^3)	Reference
Finokalia station	0.14 – 0.83	0.7 – 1.2	Mihalopoulos et al., 1997
Finokalia station	0.23 ± 0.1	1.2 ± 0.77	Kouvarakis et al., 2001
Finokalia station	--	0.46 ± 0.26	Pikridas et al., 2010
Patras, Greece	2	--	Danalatos & Gravas, 1999
Thessaloniki, Greece	2.33 ± 1.46	--	Anatolaki & Tsitouridou, 2007
Barcelona, Spain	2.2 ± 1.0	--	Pandolfi et al., 2012
Montelibretti, Italy	1.2 – 3.9	--	Perrino et al., 2002
Villa Ada Park, Italy	2.9 – 4.9	--	Perrino et al., 2002

3.2 Aerosol Water

The aerosol water associated with the inorganic components of the aerosol (W_{inorg}) derived from ISORROPIA-II was on average 3.40 ± 2.97 μg/m^3 (median 2.67), which is quite high compared to the 1.77 ± 1.45 μg/m^3 calculated by Bougiatioti et. al. (2016) for a shorter summer/autumn period in 2012 (from June to November 2012) than the here studied 11-months period in 2014. In the present study, W_{org} calculated from equation (2) was on average 0.60 ± 0.59 (median 0.43) μg/m^3, which is slightly higher than the 0.56 ± 0.37 μg/m^3 in that earlier study, most probably due to the wintertime contribution of organics to the aerosol water. The mean aerosol concentrations (both the inorganics and organics) used in this study are summarized in Table 3.2 and compared with those used in Bougiatioti et al. (2016).

Table 3.2: Observations of submicron aerosol species in the Mediterranean used in this work (February to December 2014) and compared to those used in Bougiatioti et al. (2016) (June to November 2012).

Organics	2.04 ± 1.38	1.85 ± 0.94
SO_4^{2-}	2.44 ± 1.37	2.31 ± 1.61
NH_4^+	0.66 ± 0.41	0.81 ± 0.58
Contribution to PM_1 mass concentration	**This work**	**Bougiatioti et al. (2016)**
Organics	37 %	34 %
SO_4^{2-}	44 %	40 %
NH_4^+	12 %	15 %
NO_3^-	8 %	2 %

Figure 3.3 shows the time series of the aerosol water associated with the inorganic and organic components of the aerosol. W_{inorg} ranged from 0.03 to about 50 μg/m^3, while W_{org} from 0 to 7.35 μg/m^3. The highest values in both time series occurring in September were associated with high levels of relative humidity. Here is important mentioning that we used a value of 0.16

hygroscopicity for the calculation of the organic water as proposed in numerous studies for Finokalia (Bougiatioti et al., 2009, 2011; Kalkavouras et al., 2019), while a value of 0.1 was proposed by Schmale et al. (2018) as a more representative value. This lower value would result in a slightly lower W_{org} and consequently slightly higher aerosol pH.

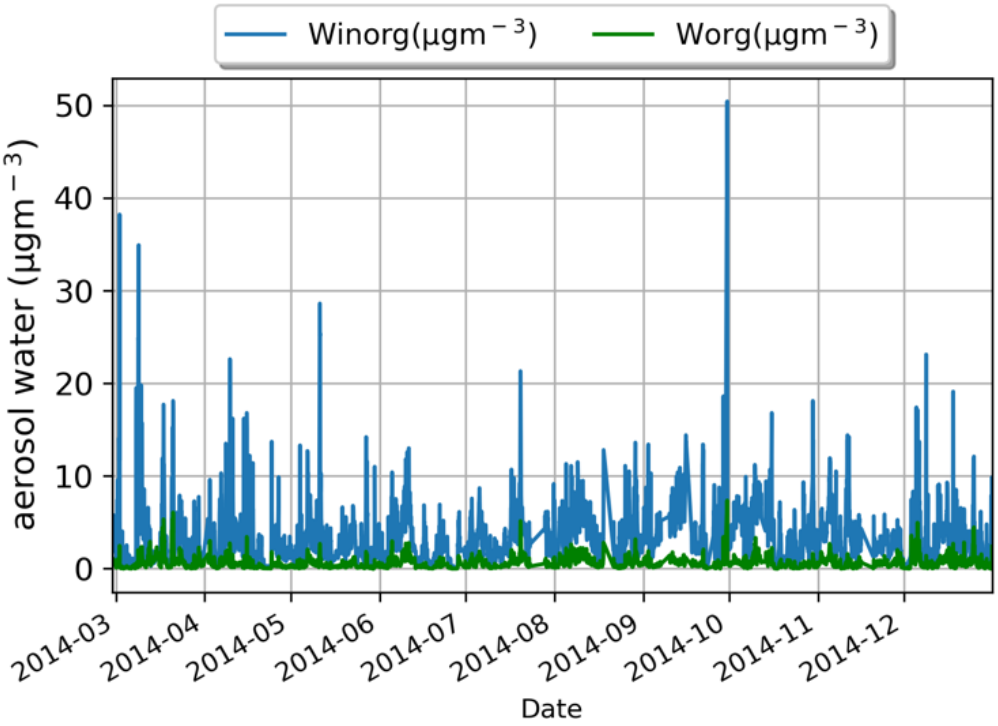

Figure 3.3: Time series of the aerosol water associated with the inorganic components (W_{inorg}) as derived from ISORROPIA-II and the aerosol associated with the organics (W_{org}), as calculated from equation 2.

Seasonally, the W_{inorg} varied as shown in Fig. 3.4 with the highest values occurring during autumn and the lowest during summer with a difference of about 1.5 μg/m^3 due to relative humidity levels, temperature and inorganic species. Looking into the seasonality of the total water it can be seen that organic water follows on average the variability of inorganic water. Overall the organic water contributed about 13% of the total aerosol water with the highest contribution occurring during March (16%) due to higher organic mass concentration.

3.3 Submicron aerosol pH

Submicron aerosol pH associated only with inorganics ($pH_{\_Wi}$) as derived from ISORROPIA-II, was found to be highly acidic ranging from -1.42 to 3.21 (Fig. 3.5), with an average value of 1.10 ± 0.70 throughout the studied period (median 1.12), which is consistent with earlier studies (Bougiatioti et al., 2016b; Nenes et al., 2011a) in the area. Bougiatioti et al. (2016) found that the submicron aerosol pH associated with the inorganics was on average 1.25 ± 1.14 at Finokalia. Aerosol pH accounting both for organic and inorganic water ($pH_{\_Wi+Wo}$) as calculated by equation (3) ranged from -1.37 to 3.30 with a mean value of 1.16 ± 0.71 (median 1.19) and was on average 0.07 units higher than pH_{Wi}. This small contribution of organic water in aerosol pH prediction has been also shown in Bougiatioti et al (2016) in which the average

increase in aerosol pH when organic water is taken into account was 0.14 units, while overall the organic water was 27.5% of the total water.

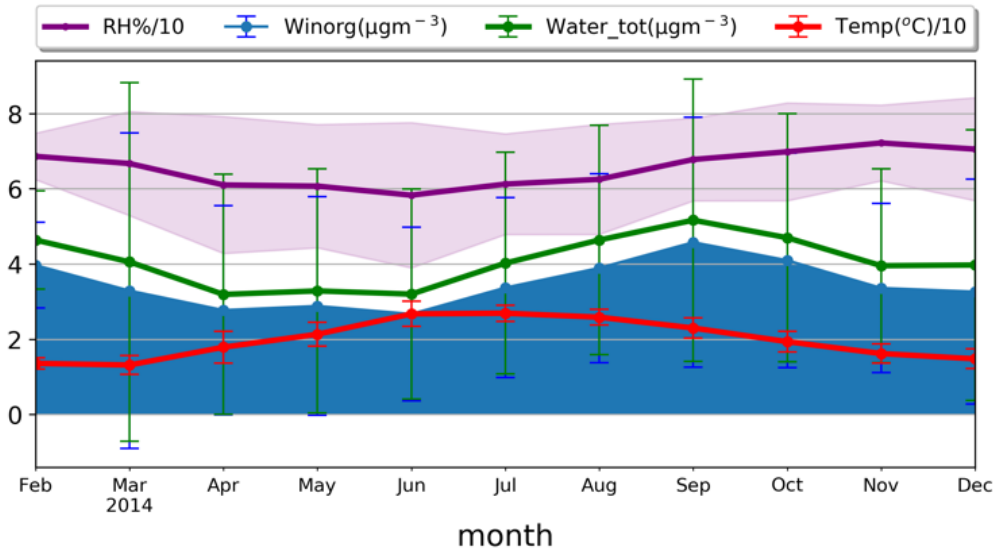

Figure 3.4: Seasonal variability of aerosol water associated with inorganics (W_{inorg}) and total liquid water content (Water_tot = W_{inorg} + W_{org}) along with temperature (Temp) and relative humidity (RH).

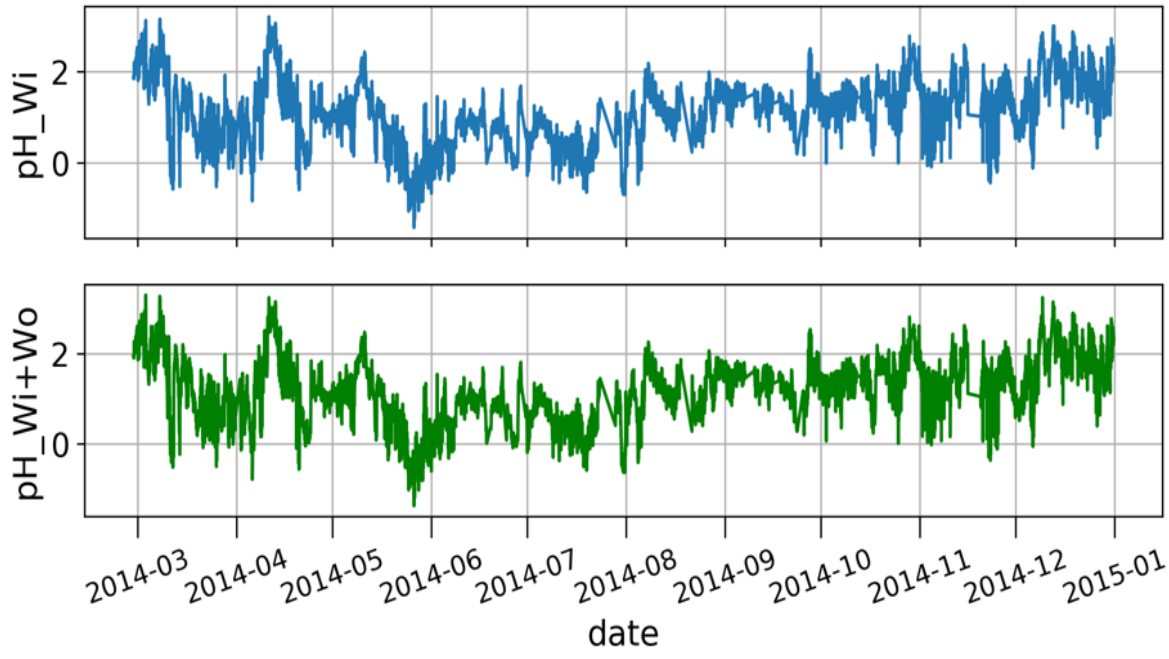

Figure 3.5: Time series of the aerosol pH associated with the inorganic components (pH_Wi) as derived from ISORROPIA-II and the aerosol pH associated with the total liquid water content (pH_Wi+Wo), as calculated from equation 2.

Seasonal variability

Figure 3.6 shows the seasonal variability of aerosol pH along with that of temperature and relative humidity. Aerosol pH associated with inorganic species (pH_Wi) varied considerably with a summertime minimum (0.40 ± 0.45 in July) and a wintertime maximum (2.16 ± 0.20 in February) and an amplitude of 1.8 units. The strong aerosol acidity (low pH) occurring in summer can be attributed to both meteorological conditions (high ambient temperatures and low relative humidity and thus low aerosol water content) and to the inorganic chemical composition (high H^+_{air} concentration). As for the wintertime, even though the available data were mostly of December (and only two days of February), the aerosol pH was higher in February due to higher relative humidity and lower temperature and H^+_{air}. In order to investigate the contribution of each main driver of pH's seasonal variability separately, a sensitivity test was conducted. Thee simulations were done, using the wintertime chemical concentrations and conditions and changing each time the temperature (simulation S_1), relative humidity level (S_2) and sulfate concentration (S_3) with the summertime ones. Focusing on the changes in calculated pH (ΔpH) induced by the three drivers tested ($\Delta pH = pH_{winter} - pH_{winter(summerX)}$, where summerX is the summer mean temperature, RH and sulfate concentration), shown in Fig. 3.6b and Table 3.3, it can be clearly seen that sulfate is the main contributor to this seasonal profile of aerosol pH in the area (mean ΔpH = 1.11) followed by the temperature (0.66) and relative humidity (0.25). As for the contribution of organics on aerosol pH calculations, when accounting for the organic water the monthly mean pH increased slightly, by 0.05 to 0.1 pH unit with the highest increase occurring during March.

Table 3.3: Sensitivity test for the determination of the major contributors for the seasonal variability of aerosol pH. Simulations S_1, S_2, S_3 were done, running the model using the wintertime data and for each simulation the summer mean temperature, relative humidity and sulfate levels were used respectively.

Initial pH (wintertime pH)	Simulations	Description of the simulation	Aerosol pH	ΔpH
1.74 ± 0.58	S_1	winter data with summer mean temperature	1.08 ± 0.38	0.66
	S_2	winter data with summer mean relative humidity	1.50 ± 0.42	0.25
	S_3	winter data with summer mean sulfate	0.63 ± 0.79	1.11

This difference was further investigated by looking into the influence of air masses origin on aerosol pH and chemical composition as well as NH_3 observations in the gas phase during March (Fig. 3.7a). The air masses back-trajectories originating only from the south and north were calculated by the HYSPLIT model (https://www.ready.noaa.gov, (Rolph et al., 2017), (Stein et al., 2015)).

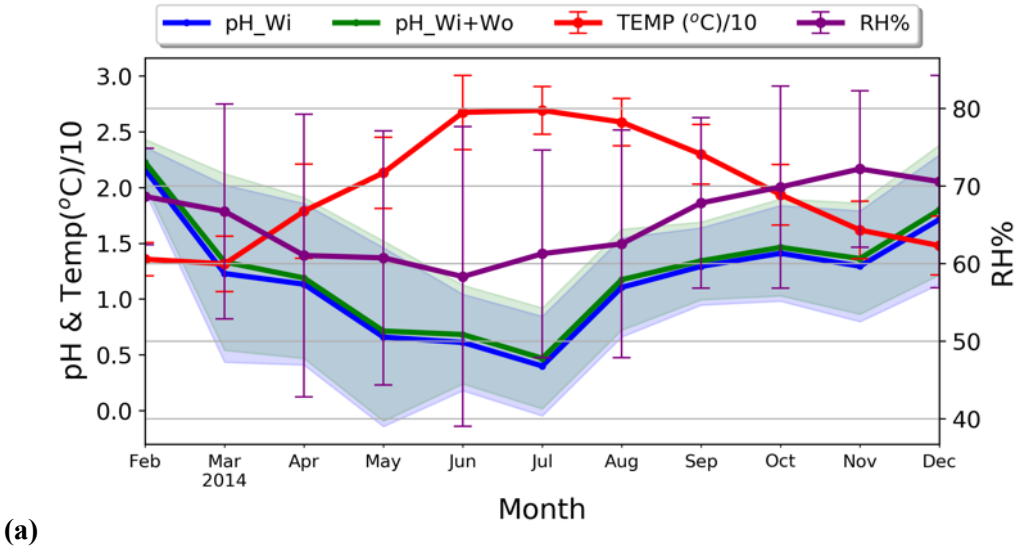

(a)

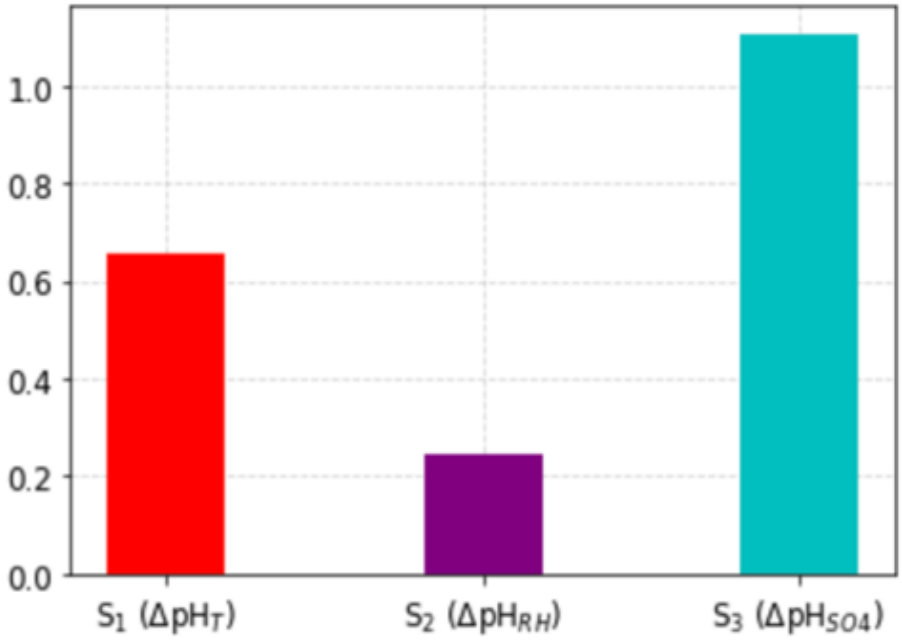

(b)

Figure 3.6: a) Monthly mean (and standard deviation) of aerosol pH associated with the inorganic components (pH_Wi) and aerosol pH associated with the total liquid water content (pH_Wi+Wo), along with temperature (in °C divided by 10) and relative humidity (in %). b) Sensitivity test for the seasonal variability of aerosol pH. ΔpH = $pH_{winter} - pH_{winter(summerX)}$, where summerX is the mean summer temperature (first simulation, S_1), relative humidity (S_2) and sulfate concentration (S_3) used to calculate the wintertime conditioned aerosol pH.

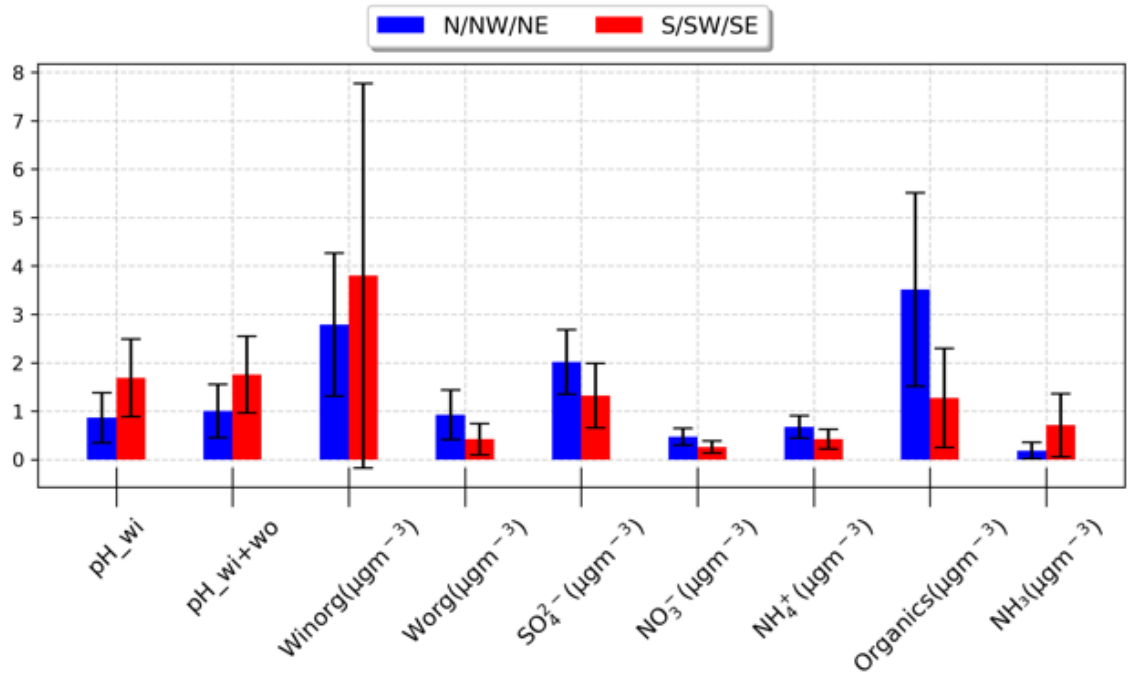

(a)

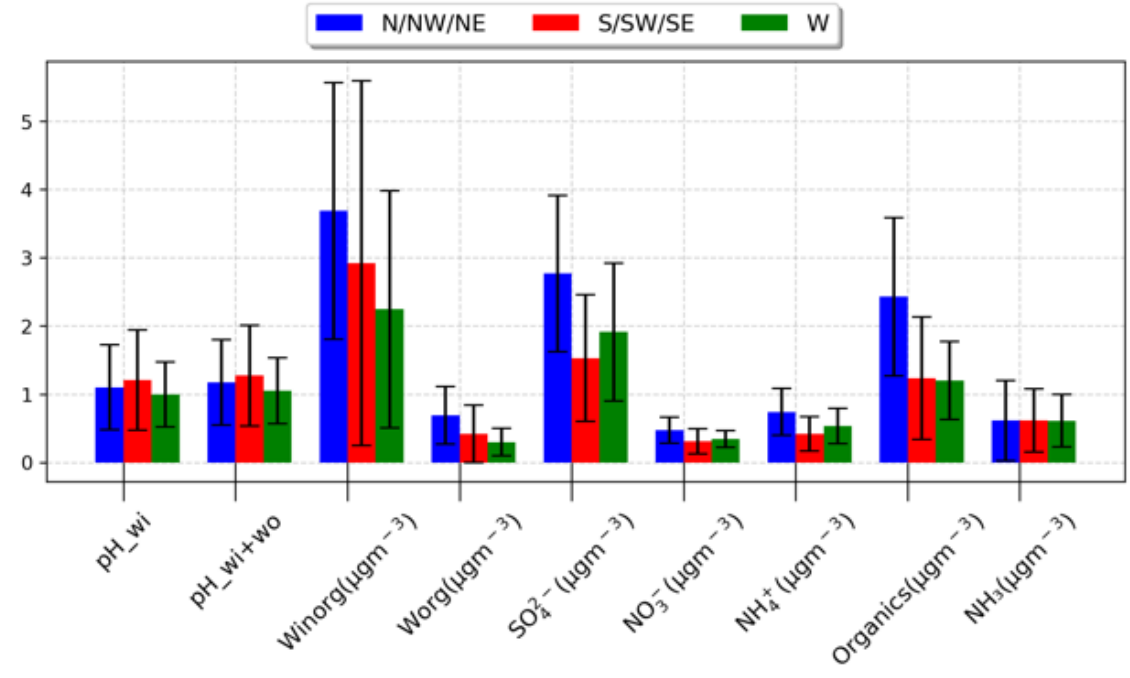

(b)

Figure 3.7: Influence of air masses origin on aerosol pH and air pollutants for a) March 2014, and b) the whole period pf this study (February to December 2014), based on back-trajectories calculated by the HYSPLIT model and using only air masses of south and north origin for a) and north. South and west in b). For aerosol pH and all species daily averages and standard deviation are given.

In March, aerosol pH was found to be lower for air masses originating from the north (Europe and the Greek mainland) as well as the aerosol water associated with the inorganic components of the aerosol while sulfate was higher for the northern origin. Therefore, during that period the inorganic aerosol water and the inorganic chemical composition were the main drivers of aerosol pH. The air masses back-trajectories for the period of the study originating from the south (south, southwest and southeast, 49 points), north (north, northwest and northeast, 186

points) and west (36 points) were calculated again by the HYSPLIT model with similar analysis as done for Fig. 3.7a. Similar results with those for March were expected but this was not the case. The results for the entire study period are summarized in figure 3.7b where it can be seen that aerosol pH does not differentiate significantly for the different air masses origin. Figure 3.8 shows the influence of air masses origin on aerosol pH for the period of the study in seasons for the three sectors at air masses origin sectors as in Fig. 3.7b. Overall, the submicron aerosol pH was as expected highly acidic in summer compared to the other seasons, while for winter higher pH values were calculated. Looking into the three air masses sectors separately, only for the west origin the seasonal difference in aerosol pH can be attributed to sulfate concentration in which there is a statistically significant difference in winter compared to the other seasons. For the other two air mass origins there is no significant difference in the main drivers of aerosol pH, similar to the annual pattern shown in Fig. 3.7b.

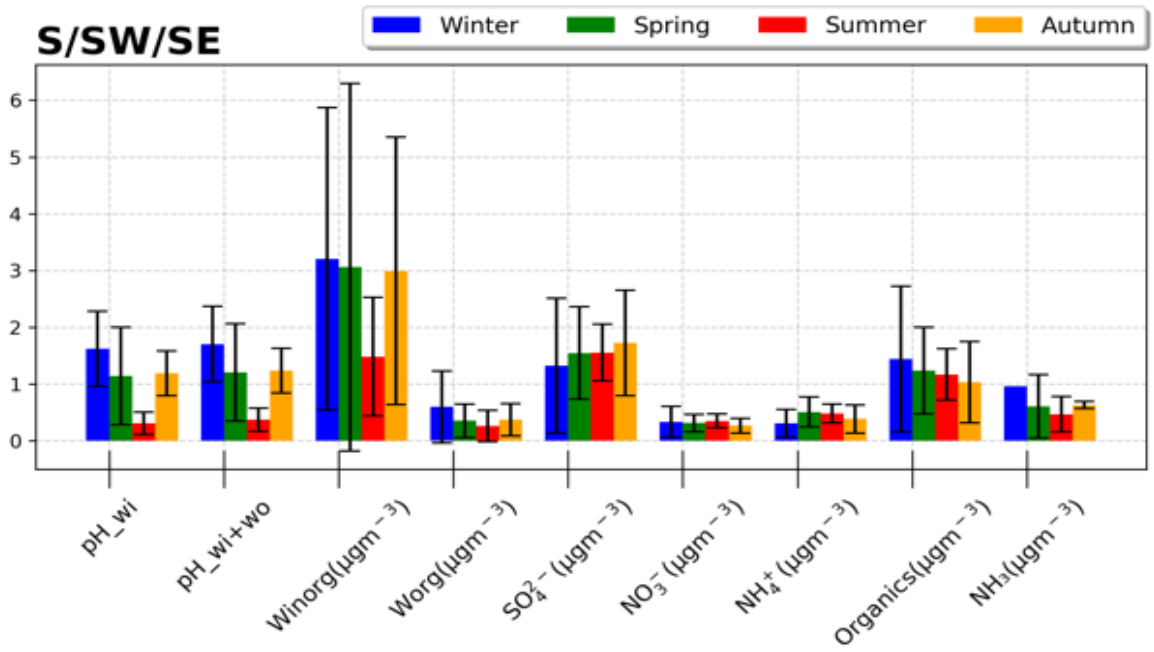

(a)

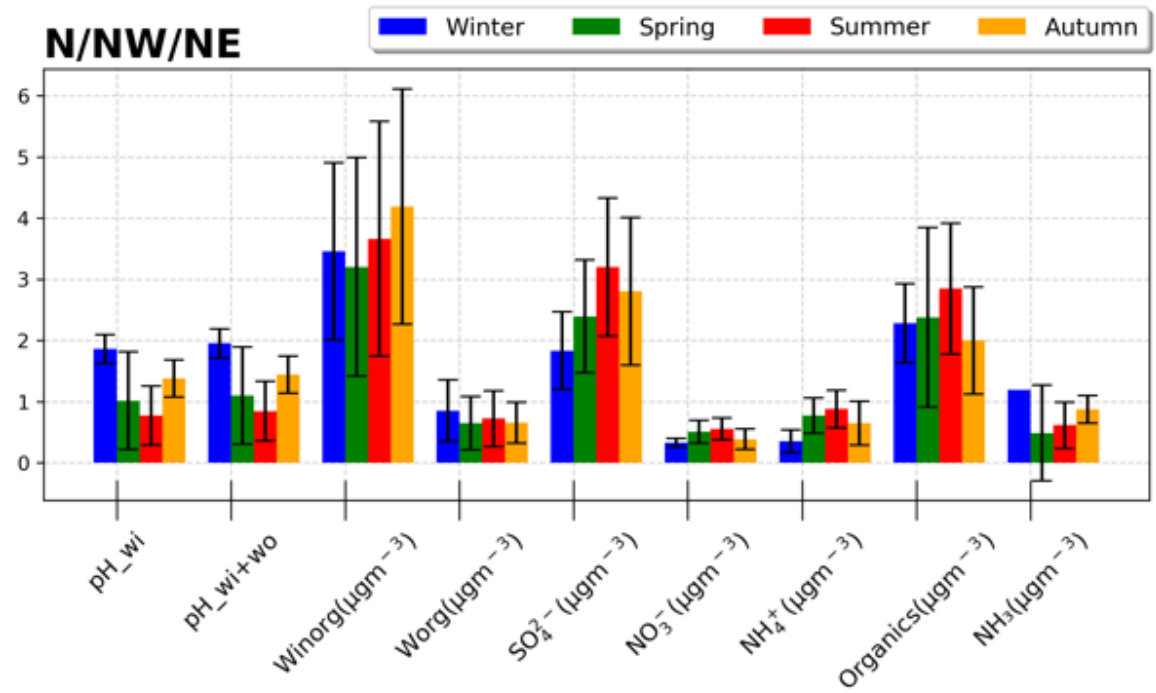

(b)

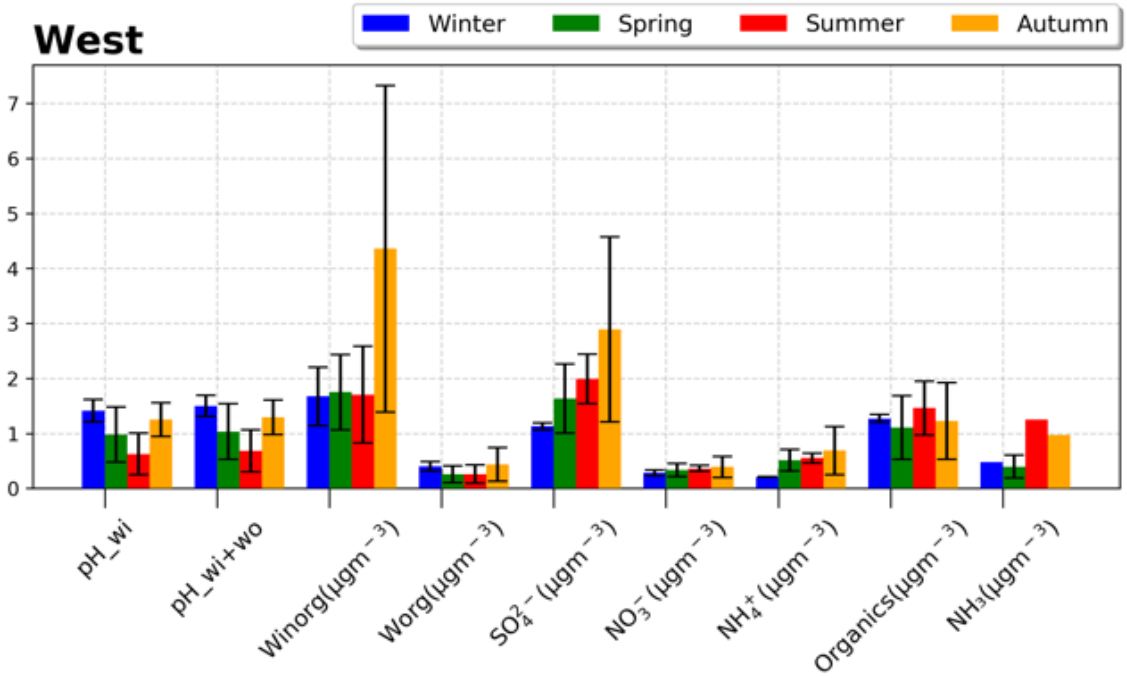

(c)

Figure 3.8: Influence of air masses origin on aerosol pH and air pollutants for the period of the study divided by seasons, based on back-trajectories calculated by the HYSPLIT model a) for south, southwest and southeast origin b) for north, northwest and northeast origin, c) for west origin. For aerosol pH and all species daily averages and standard deviation are given.

Diurnal variability

In order to examine the diurnal variability of pH, we investigated its behavior in two months in summer and winter, respectively (July and December). As shown in Fig. 3.9a in July in general aerosol pH was highly acidic throughout the day (0.40 ± 0.08 and 0.47 ± 0.08 for pH_{Wi} and pH_{Wi+Wo} respectively) with an early afternoon minimum (0.23 ± 0.40) and an early morning maximum (0.56 ± 0.42) with 0.33 for pH_{Wi} and 0.31 for pH_{Wi+Wo} pH unit difference. This behavior can be attributed to afternoon maximum and morning minimum values of temperature (Fig. 3.10a) and sulfate levels (Fig 3.10a).

On the other hand, in December (Fig. 3.9b) aerosol pH has a slightly different diurnal profile with midday minimum and nighttime maximum (with 0.38 and 0.35 pH unit difference for pH_{Wi} and pH_{Wi+Wo} respectively), which is concurrent with the variability of both meteorological conditions and sulfate (Fig. 3.10b). In general, in December aerosol pH was on average by 1.31 pH_{Wi} and 1.33 for pH_{Wi+Wo} units higher than in July.

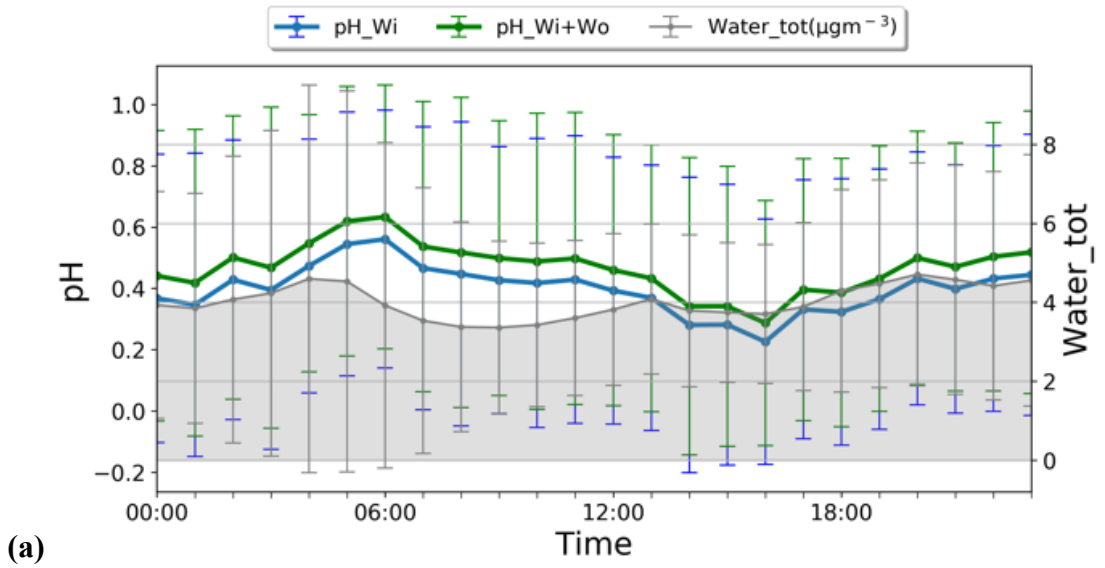

(a)

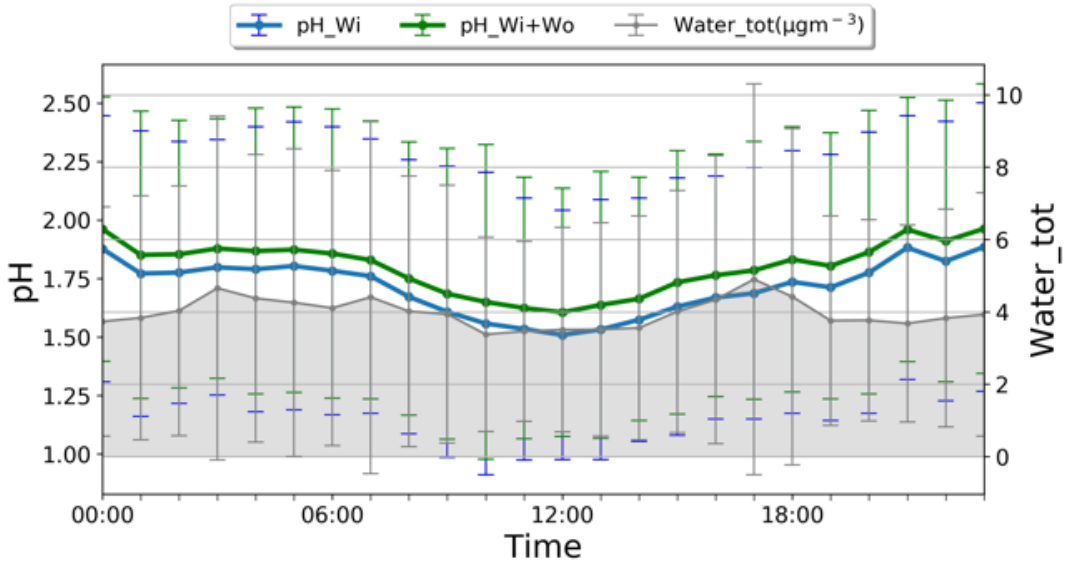

(b)

Figure 3.9: Diurnal profile of aerosol pH (pH_Wi and pH_Wi+Wo) along with the total water content in a) July 2014 and b) December 2014.

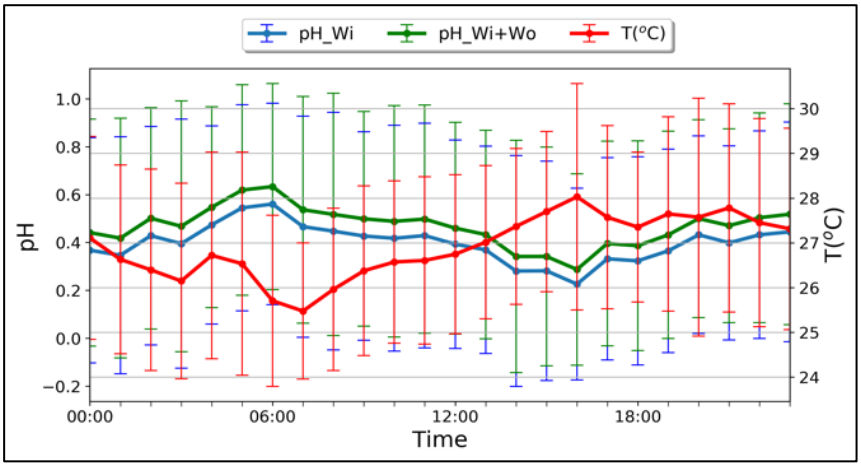

(a)

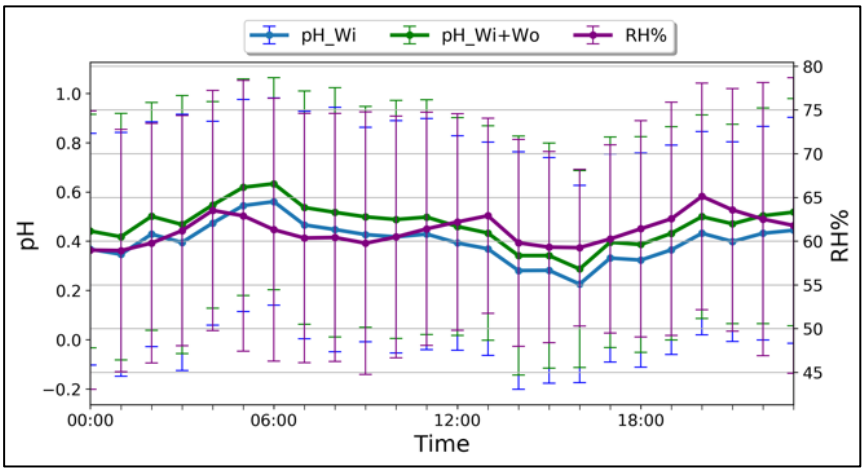
pH_Wi
pH_Wi+Wo
RH%
pH
RH%
Time
00:00
06:00
12:00
18:00

(b)

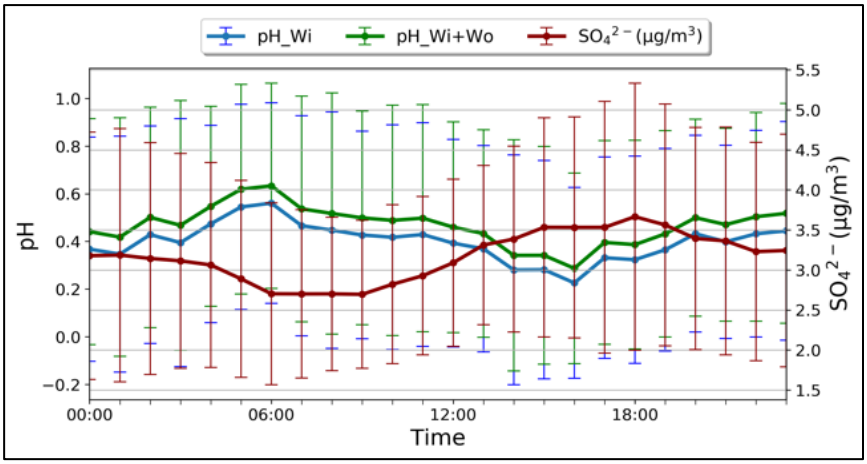
pH_Wi
pH_Wi+Wo
SO_4^{2-} (μg/m³)
pH
SO_4^{2-} (μg/m³)
Time
00:00
06:00
12:00
18:00

(c)

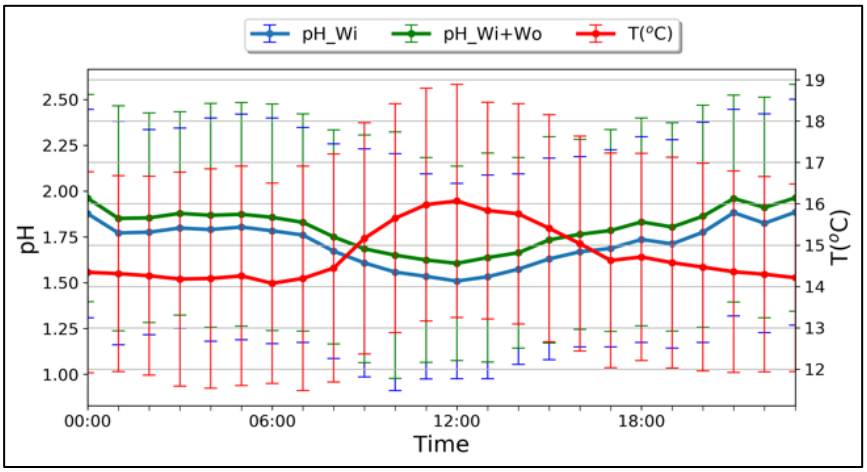
pH_Wi
pH_Wi+Wo
T(°C)
pH
T(°C)
Time
00:00
06:00
12:00
18:00

(d)

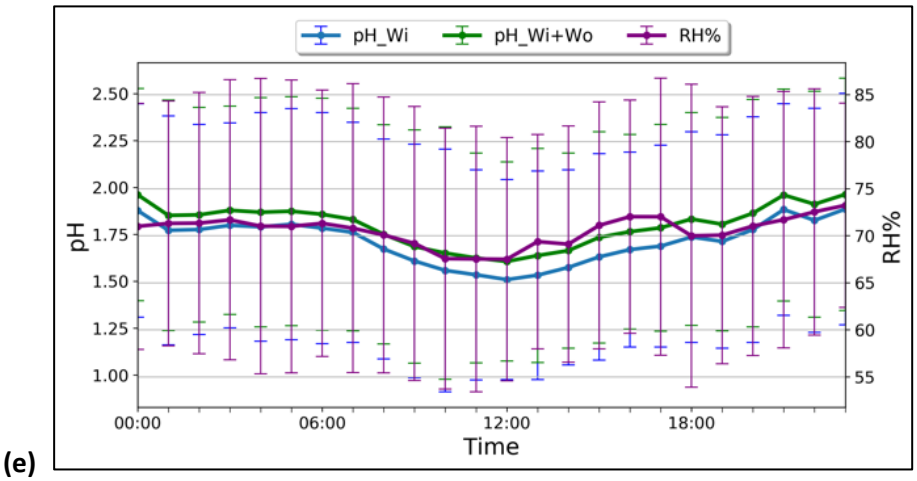

(e)

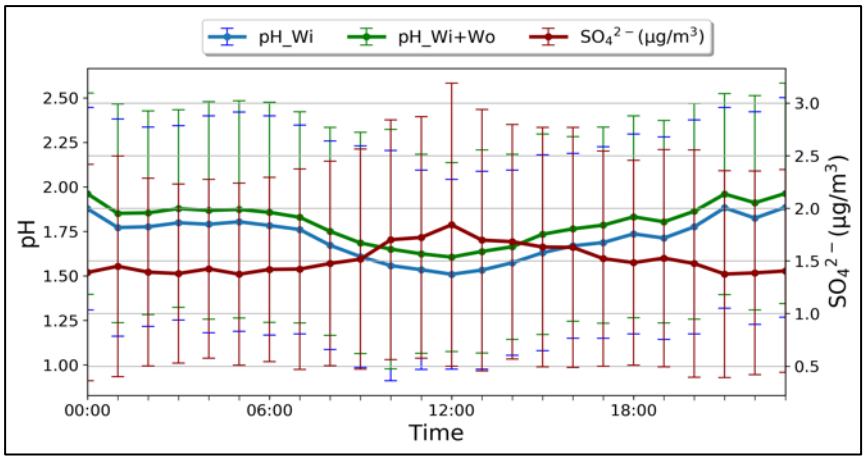

(f)

Figure 3.10: Diurnal profile of aerosol pH along with temperature (a,d), relative humidity (b,e) and sulfate (c,f) in a), b), c) July and d), e), f) December.

3.4 Sensitivity of aerosol pH and nitrate partitioning

Crustals and excess ammonia

As above mentioned, ISORROPIA-II examines the thermodynamics of inorganic K^+ –Ca^{2+} –Mg^{2+} –NH_4^+ –Na^+ –SO_4^{2-} –NO_3^- –Cl^- –H_2O aerosol systems. Crustal species and sodium measurements weren't available for the whole period of the study. However, PM_1 measurements of these species as mentioned in section 2.2.1 were conducted at Finokalia for 70 days of the same year. In order to investigate the sensitivity of aerosol pH to crustal species (Ca^{2+}, Mg^{2+} and K^+), sodium (Na^+) and to gas-phase ammonia levels, three additional simulations of ISORROPIA-II were performed (in forward mode, assuming metastable aerosol). The first (simulation 1, Sim1) was similar to the one performed using the ACSM data and already presented, since the sulfate, ammonium, nitrate and chloride along with the previous mentioned gas-phase measurements were used as inputs. For the second simulation

(Sim2) the crustal ions and sodium were used as input to the model, while in the third simulation (Sim3) the crustal ions and sodium were neglected but excess gas-phase ammonia was added. These three simulations were used to predict the aerosol pH (Table 3.4). On average pH without the addition of crustals, sodium and ammonia (Sim1) was 0.68 ± 0.82 pH units. Considering the crustal species and sodium increased the pH by 0.73 units, while adding excess amount of gas phase ammonia increased pH by 1.46 units. These results were used to calculate and compare the partitioning coefficient of nitrate and plotted as a function of aerosol pH as shown in Fig. 3.11.

The partitioning coefficient of nitric acid (ε) between the particle (NO_3^-) and the gas phase (HNO_3) is given by the ratio of $NO_3^-/(NO_3^- + HNO_3)$. In the first sensitivity test, the partitioning of nitrate was found to be 0.07 ± 0.12 for a mean aerosol pH of 0.68 while it increased by 0.08 units with the addition of the crustals and sodium and by 0.31 with the excess addition of gas phase ammonia. Equal amounts of particle phase nitrate and gas phase nitric acid to be present (ε = 0.5), the aerosol pH should be around 1.6 (Sim1), while with the crustal species and sodium present the aerosol pH is calculated to be one unit higher. When excess amount of gas phase ammonia is added to the system the equal formation of particle and gas phase nitrate is taking place when the aerosol pH is slightly above 3.

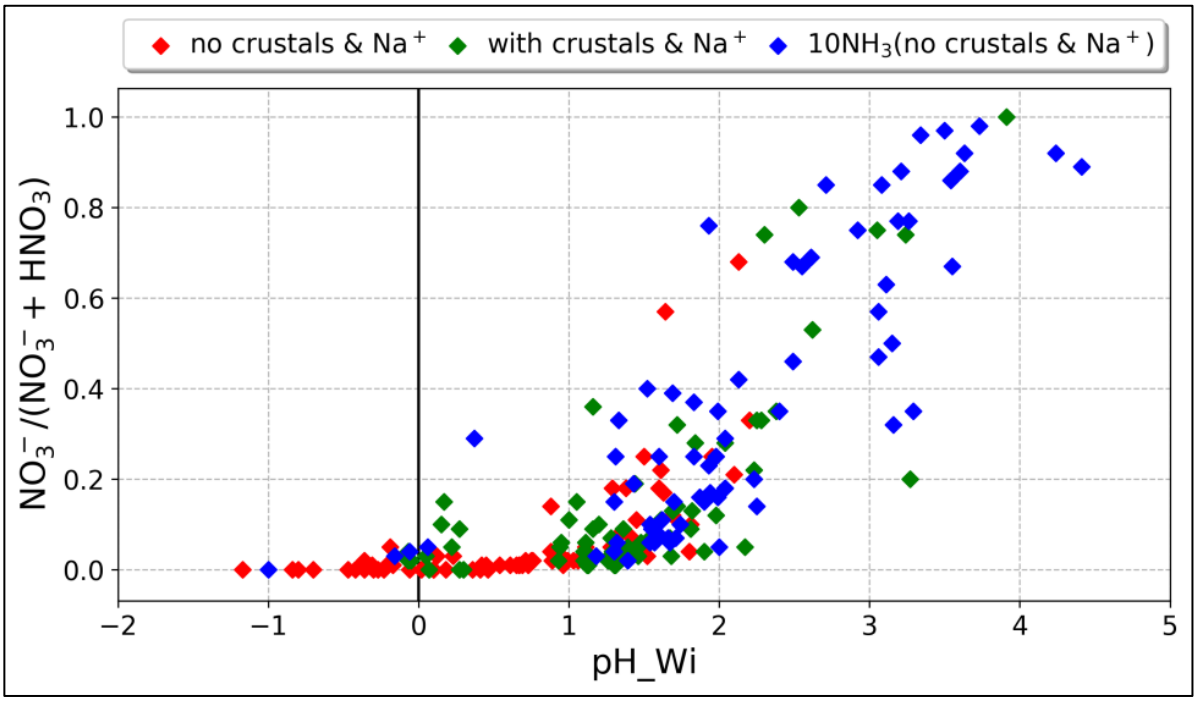

Figure 3.11: Partitioning of nitric acid between gas and particulate phase as a function of aerosol pH associated with inorganics for the three runs of ISORROPIA-II, red) with no crustal species and sodium included (only species present were sulfate, nitrate, chloride and ammonium along with gas phase ammonia, nitric acid and hydrochloride, Sim1), green) with the addition of crustal species and sodium (Sim2) and blue) with no crustals and sodium but with excess amount of ammonia added (Sim3).

Table 3.4: Sensitivity test of aerosol pH to crustal species and sodium and to NH_3. The aerosol pH and the partitioning coefficient of nitrate values are the averages for each simulation.

Simulations	Description of the simulation (species used in ISORROPIA-II)	Aerosol pH	Partitioning coefficient of nitrate
Sim1	NH_3, HNO_3, HCl, SO_4^{2-}, NH_4^+, NO_3^-, Cl^-	0.68 ± 0.82	0.07 ± 0.12
Sim2	NH_3, HNO_3, HCl, SO_4^{2-}, NH_4^+, NO_3^-, Cl^-, **Ca^{2+}, Mg^{2+}, K^+, Na^+**	1.41 ± 0.82	0.15 ± 0.22
Sim3	**10xNH_3**, HNO_3, HCl, SO_4^{2-}, NH_4^+, NO_3^-, Cl^-	2.14 ± 1.04	0.38 ± 0.31

In order to look into the influence of air masses origin on aerosol pH for the period that crustal species and sodium measurements were available, similar analysis was done as in section 3 and the results are presented in Fig. 3.12. As it can be seen, the decreasing acidity occurring for air masses that originated from the south, was due to elevated concentration of crustals, mainly calcium, while generally the anthropogenic influence is quite distinct, although for the pH's drivers such as the sulfate levels, the air mass origin does not differ significantly.

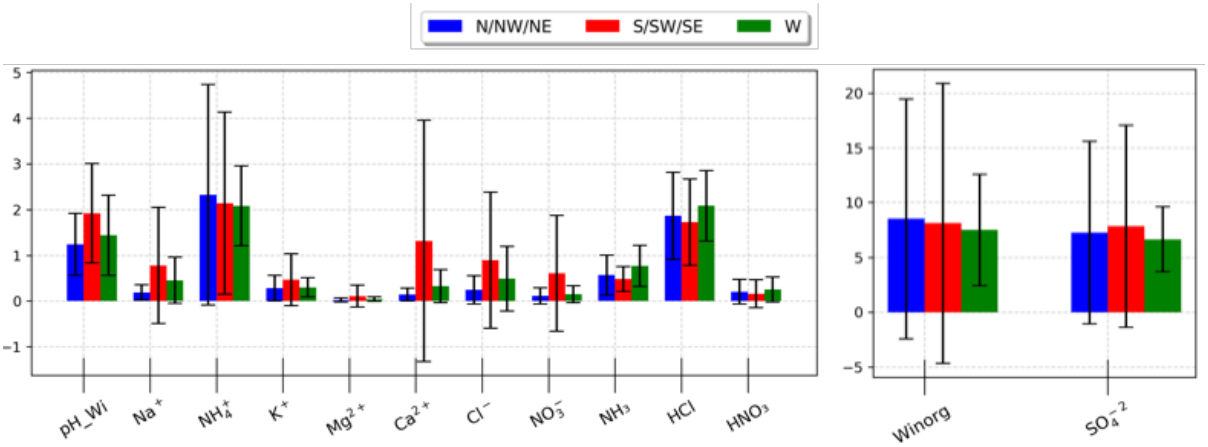

Figure 3.12: Influence of air masses origin on aerosol pH and air pollutants for the 70 days in 2014 that crustal species and sodium were available (See section 4) based on back-trajectories calculated by the HYSPLIT model and using only air masses of south and north and west origin. For aerosol pH and all species daily averages and standard deviation are given. All aerosol species and gas phase in μg/m^3.

Gas phase

The system's sensitivity to either gas phase ammonia, nitric acid or both was further investigated using a newly developed framework by (Nenes et al., 2020). This framework was developed based on the levels of aerosol pH required to exist in order for aerosol nitrate (and ammonium) to form. These levels of aerosol pH range between 1.5 to 3.5 (Guo et al., 2016; Guo, Liu, et al., 2017; Meskhidze et al., 2003) (also shown in this study, see section 3.4), depending on temperature and liquid water content. As described previously (section 3.4), if aerosol pH is high enough, nitrate mostly resides in the aerosol phase and if the aerosol is quite low (usually below 1.5 to 2), nitrate resides almost entirely in the gas phase as HNO_3, regardless of the amount present. Between these pH values there is a ''sensitivity window'', in which the

partitioning of nitrate shifts from nitrate being predominantly gaseous to mostly in the aerosol phase. When acidity is below this ‘‘pH window’’, particulate nitrate is almost non-existent and consequently aerosol levels are insensitive to HNO_3 availability, so policies aimed only on nitric acid reductions are not effective since there is no nitrate in the aerosol phase. When acidity is above this window, most of the nitrate resides in the aerosol phase and aerosol levels are sensitive to HNO_3 availability. Similarly, ammonium exhibits these sensitivity patterns between aerosol-gas partitioning and aerosol pH but in the opposite way (at high aerosol pH values ammonia resides mostly in the gas phase). Based on these criteria this framework defines characteristic levels of aerosol acidity, where aerosol becomes insensitive to NH_3 (or HNO_3) amounts and vice versa. According to this framework, required quantities are the aerosol pH, liquid water content and temperature for the determination of the four possible regimes of PM sensitivity, i) neither NH_3 nor HNO_3 are important for PM formation, ii) HNO_3 dominated, iii) both NH_3 and HNO_3, and iv) NH_3 dominated. To interpret our data (derived as described in section 3 and used here as daily values) based on this framework (Fig. 3.13) we used activity coefficients derived from ISORROPIA-II ($\gamma_{H^+}\gamma_{NO_3^-}$=0.262, $\gamma_{NH_4^+}\gamma_{NO_3^-}$=0.225, where both are median values). We found that PM at Finokalia is mostly in the “NH_3 sensitive” region (Regime 4) as expected, where the acidity is considerably high and there is no NH_4NO_3 present. It can also be seen that, as mentioned above and pointed out in the study by Nenes et al., (2020), the transition point between NH_3-dominated and HNO_3-dominated sensitivity occurs at a pH value around 2. On the contrary, this transition point exists around 6-7 μg/m^3 of liquid water content but not at a fixed value or range of the liquid water content. This result indicates the importance of the knowledge of both aerosol pH and aerosol water in order to determine the type of aerosol sensitivity.

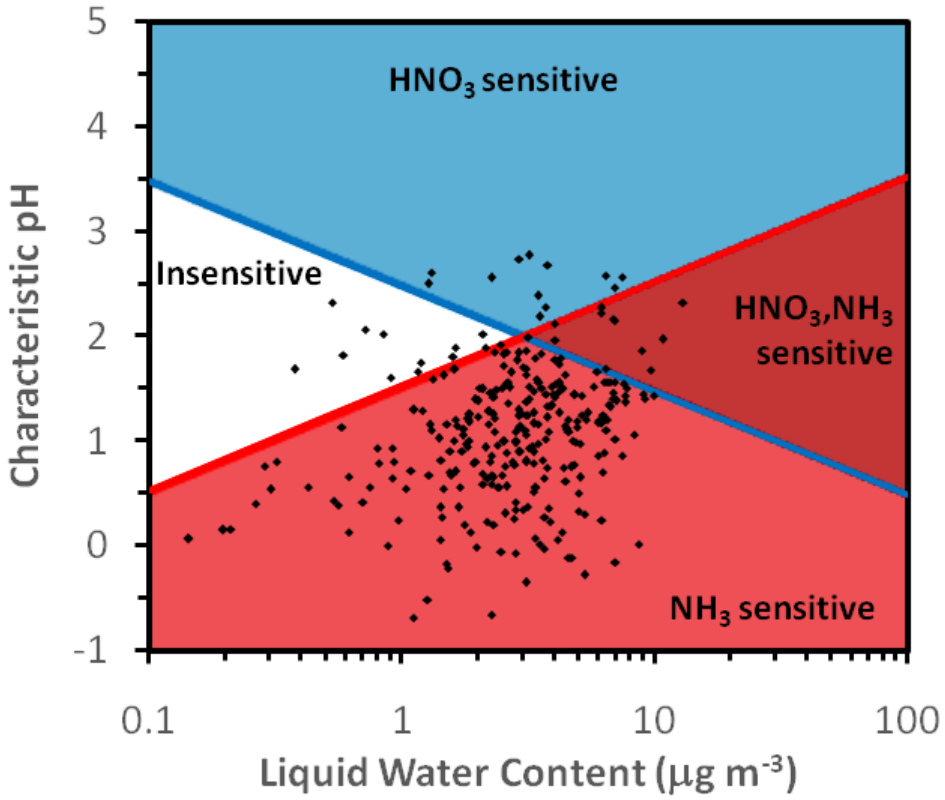

Figure 3.13. Chemical domains of sensitivity of aerosol to NH_3 and NO_x emissions for the studied period and region as derived from the framework developed in (Nenes et al., 2020). The average temperature used here is the measured one for the study period at the site, 293.25 K. Daily averaged values for aerosol pH and liquid water content were used.

Furthermore, in order to investigate the seasonal variability of the sensitivity of PM at Finokalia, we used activity coefficients, aerosol pH and water derived from the model for each season and interpreted them based on this framework. The seasonally median values of the activity coefficients used are presented in table 3.5 along with the mean values of temperature, aerosol pH and water for each season. During summer, the PM at Finokalia reside exclusively in the ammonia sensitive regime (Fig. 3.14), where acidity is significantly higher than during the rest of the year and liquid water content is lower. On the contrary, during less acidic conditions in winter, the PM is beginning to deviate from the ammonia sensitive region and somewhat reside also in the HNO_3 region, even though the wintertime data used were only for the months of February and December. This was the case for spring where, probably due to low temperatures, there could be NH_4NO_3 present and the PM might be sensitive to HNO_3, but still the system is mostly sensitive to NH_3. During autumn, similarly to summer the aerosol system is sensitive to NH_3. Since during the entire year the submicron aerosols are acidic, it is expected to be more or less sensitive to NH_3 emissions as shown in Fig. 3.13, while the deviation from this regime (NH_3 sensitive) seems to occur during spring and winter. It is clear however that, during summer the PM at Finokalia is entirely influenced by NH_3 (and consequently SO_4^{2-}) emissions, so NH_3-reduction policies are more efficient for the area.

Table 3.5: Seasonally median values of the activity coefficients ($\gamma_{H^+}\gamma_{NO_3^-}$ and $\gamma_{NH_4^+}\gamma_{NO_3^-}$) that were derived for ISORROPIA-II and used in the Nenes et al. (2020) framework. The temperature, aerosol pH and water used in the framework are presented here as mean values for each season.

Season	Temperature (°C)	$\gamma_{H^+}\gamma_{NO_3^-}$	$\gamma_{NH_4^+}\gamma_{NO_3^-}$	Aerosol pH	Aerosol water (μg/m^3)
Winter	14.72 ± 2.60	0.306	0.240	1.75 ± 0.49	3.35 ± 2.24
Spring	17.48 ± 4.78	0.260	0.220	1.02 ± 0.76	2.07 ± 2.23
Summer	26.48 ± 2.62	0.250	0.220	0.69 ± 0.51	3.26 ± 1.94
Autumn	19.36 ± 3.78	0.270	0.230	1.35 ± 0.32	4.00 ± 2.13

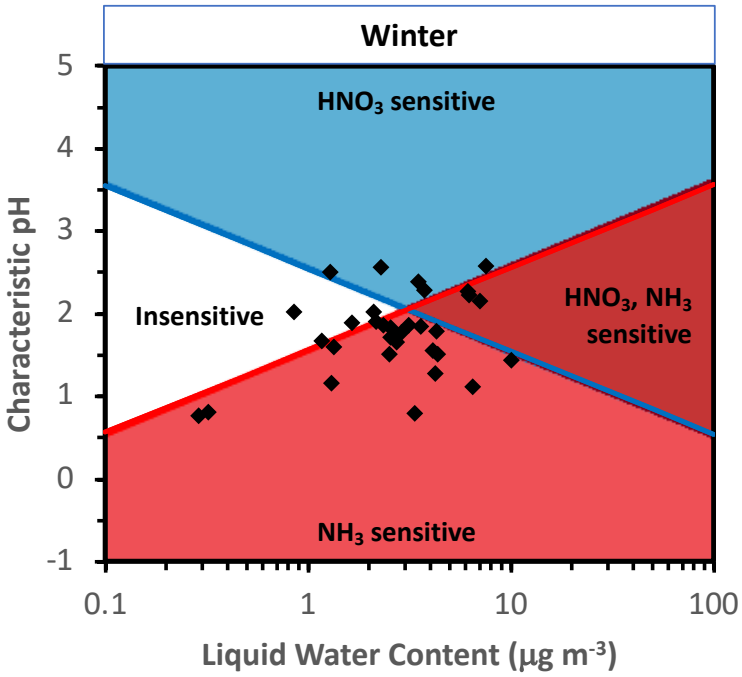
Winter
HNO3 sensitive
Insensitive
HNO3, NH3 sensitive
NH3 sensitive
Characteristic pH
5
4
3
2
1
0
-1
0.1
1
10
100
Liquid Water Content (µg m-3)

(a)

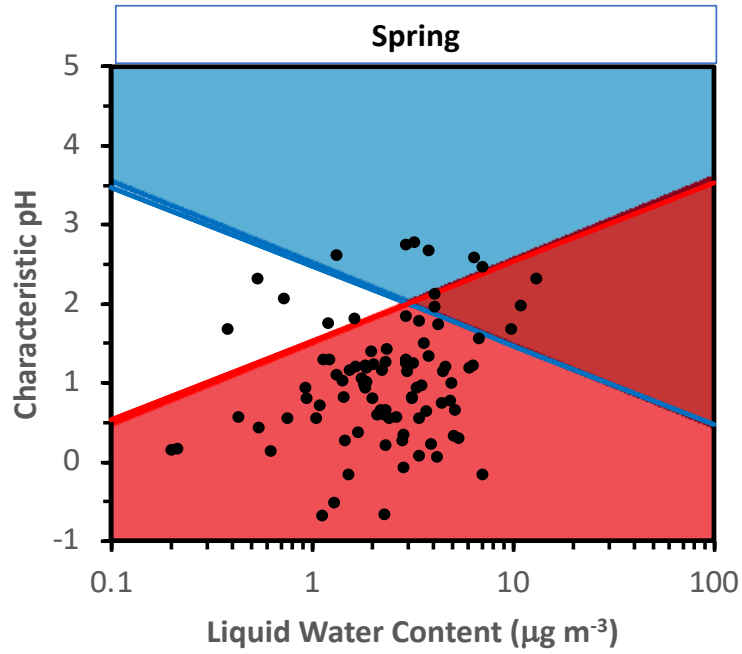
Spring
Characteristic pH
5
4
3
2
1
0
-1
0.1
1
10
100
Liquid Water Content (µg m-3)

(b)

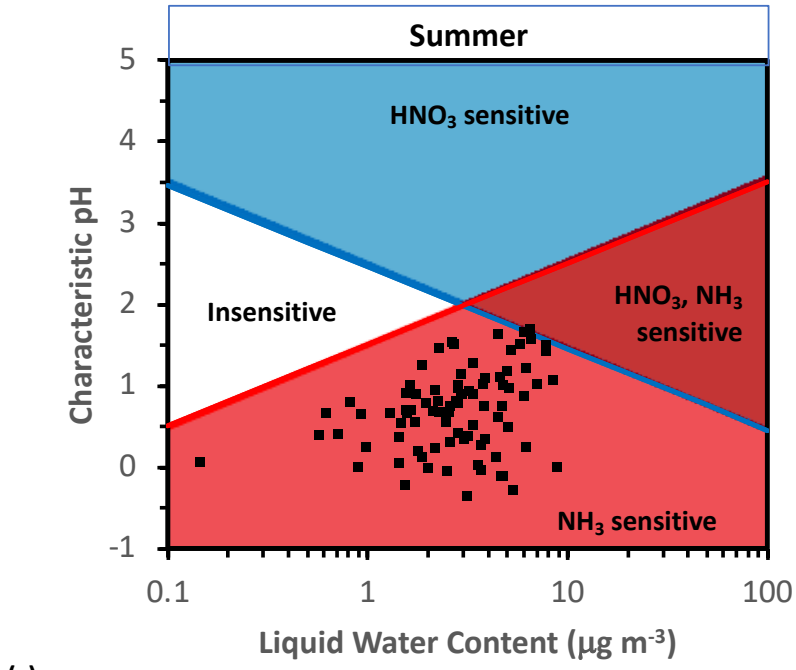

(c)

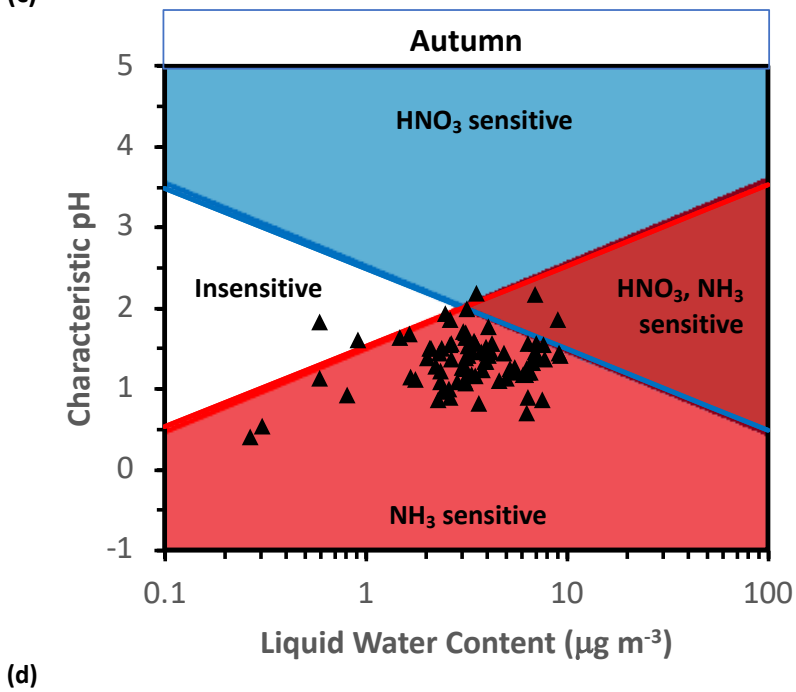

(d)

Figure 3.14. Chemical domains of sensitivity of aerosol to NH_3 and NO_x emissions for the studied period and region for each season (a) in winter, (b) spring, (c) summer, (d) autumn, as derived from the framework developed in Nenes et al. (2020). The average temperature used here is the measured one for the study period at the site, for each season. Daily averaged values in each season for aerosol pH and liquid water content were used.

3.5 Evaluation of ISORROPIA-II

In order to determine the accuracy and potential uncertainties in the aerosol pH predictions, the predicted concentrations of the species used in the model were compared with the measurements conducted by the ACSM. Figure 3.15a shows these comparisons for SO_4^{2-} and NH_4^+. Sulfate predictions agreed extremely well with the measurements (R^2=1); predicted ammonium levels also agreed quite well with the measurements (R^2=79), as well as gas phase ammonia (Fig.3.15b) (R^2=75), while ammonium was generally overpredicted throughout the dataset (slope=1.11) and gas phase ammonia was underpredicted (slope=0.73). For lower and moderate temperature levels (Fig.3.16) ammonium seems to deviate from the 1:1 line resulting in even higher overprediction of ammonium in the aerosol phase. In order to examine the potential deviation from the 1:1 line of aerosol ammonium due to relative humidity levels, we divided the dataset in two (Fig.3.16). The one with relative humidity below its mean value (mean RH=65% so RH<65%) and the other above it (RH>65%).

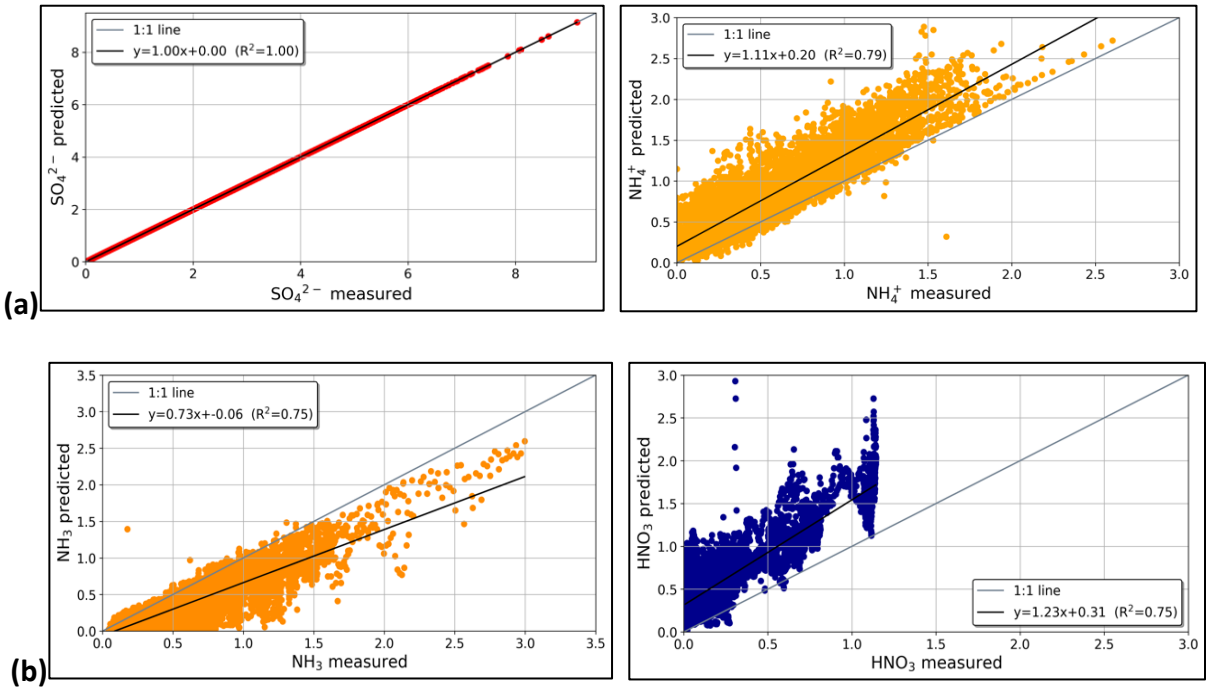

Figure 3.15: (a) Comparison of species in the aerosol phase (SO_4^{2-}, NH_4^+) predicted by ISORROPIA-II with measurements. (b) Comparison of species in the gas phase (NH_3, HNO_3) predicted by ISORROPIA-II with measurements. Both aerosol species and gases in μg/m^3.

For lower relative humidity levels the model seems to overpredict more than when RH is high while the correlation between measurements and predictions is better when RH<65%. This can also be seen in Fig. 3.17b in which the partitioning coefficient increases when temperature is at low and moderate levels and relative humidity is relatively high, making ammonium reside more towards the particle phase. Moreover, the model reproduces very well the nitric acid with correlation coefficient R^2=0.75 when compared to the observations (Fig. 3.15b).

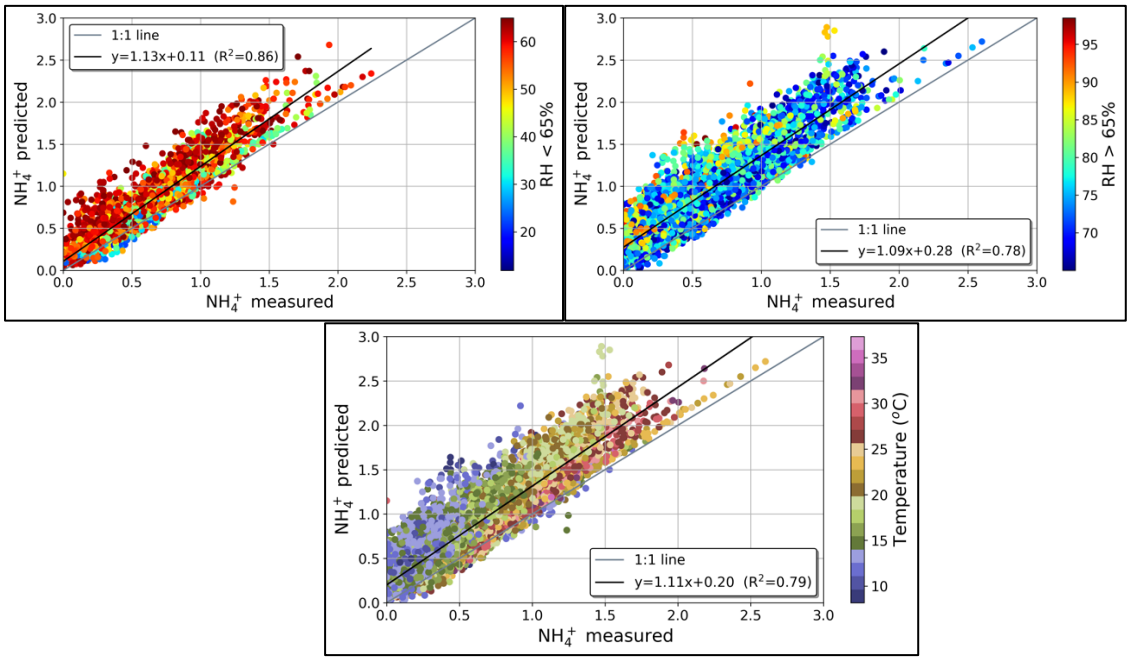

Figure 3.16: Comparison of aerosol NH_4^+, predicted by ISORROPIA-II with measurements, colored by relative humidity below 65% (left), above 65% (right) and temperature (center). Both predicted and measured NH_4^+ in $\mu g/m^3$.

The model, also captures the partitioning of NH_4^+/NH_3 with R^2=0.54 at some extent (Fig. 3.17) which makes the aerosol pH and liquid water content predictions reasonable given the fact that, as shown previously, non-volatile species are an important parameter in the aerosol pH predictions. This is further supported, when the comparison between predictions and observations is investigated when the non - volatile cations are included in the system (Fig. 3.18) and the correlation for the NH_4^+ improved with correlation coefficient being equal to R^2 = 0.87.

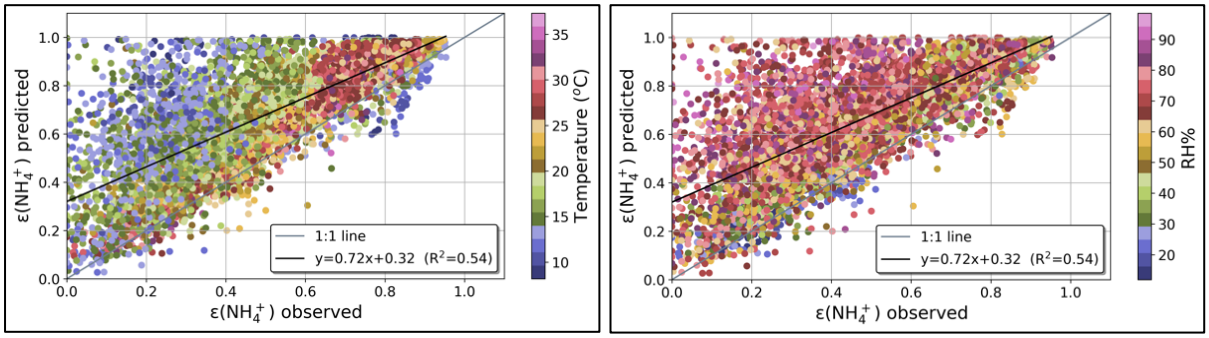

Figure 3.17: Partitioning coefficient ammonium ($\varepsilon(NH_4^+)$) calculated with the corresponding predicted species ($NH_4^+/(NH_4^+ + NH_3)$), compared with the measured ones, along with temperature (left) and relative humidity (right).

Here we focused on the correlation between predictions and measurements in order to investigate the accuracy of our aerosol pH predictions since generally, assessing predicted and

measured comparison of gas-particle partitioning fractions of the semi volatile species is a more useful way to validate these model's predictions. Semi volatile species however are dependent on the aerosol pH levels on a given aerosol system. As Guo et al. (2016) pointed out that semi volatile species that reside in both phases (aerosol and gas) more evenly, are more suitable parameters to use in order to evaluate the model and not those that reside mostly in one or the other phase. This was the case in Guo et al. (2016) where NH_3 was estimated to reside mainly in the particle phase, while HNO_3 was more evenly distributed between the two phases, making it thus a more suitable parameter for the evaluation. On the contrary, in Guo et al. (2015) the conditions were such that HNO_3 was almost exclusively in the gas phase, as in this study, while NH_3 was evenly distributed between gas and aerosol phase, making it more useful parameter to test the model.

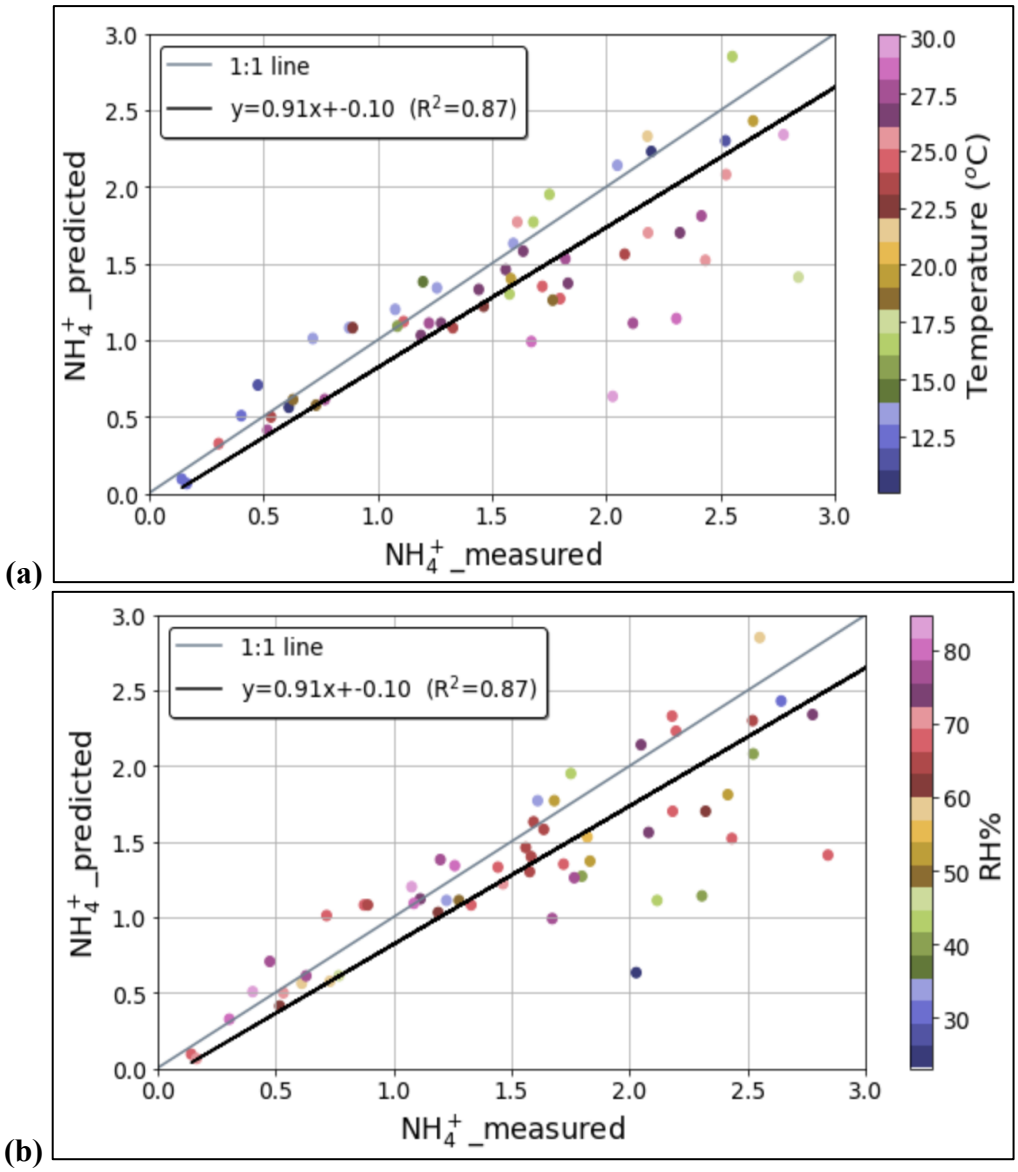

Figure 3.18: Comparison of aerosol NH_4^+ between predictions and observations when crustal species (Ca^{2+}, Mg^{2+}, K^+) and sodium (Na^+) are added to the system (PM_1 data including the crustals and sodium as described in section 2.2.1). the two panels show in color the corresponding (a) Temperature (°C) and (b) RH (%)

4. $PM_{2.5}$ aerosol pH in Ioannina City

From December 2019 to February 2020 (58 days in total), $PM_{2.5}$ filter measurements of inorganic species (sodium, ammonium, potassium, magnesium, calcium, chloride, nitrate, sulfate) and water-soluble organic carbon were conducted in Ioannina City, Greece (Fig. 4.1), along with temperature and relative humidity measurements. Ioannina is located in Epirus Region in northwestern Greece, which is separated from the rest of the country, by the Pindus mountain range (which is orientated from NW to SE and exceeds 2000 m in height), located to its east edge. As a result, during the wet period of the year, depressions, which mostly form in the cyclogenesis regions through the northern Mediterranean coasts and move towards east over the relatively warm Mediterranean waters (Nissen et al., 2010; Sindosi et al., 2012; Trigo et al., 2002), facilitate the development of severe precipitation events over the windward NW Greece. Ioannina is city with a population of 120,000 lying in a plateau of about 500 m altitude and surrounded by mountains. The city is next to the Pamvotis lake and is characterized by frequent fog events during the winter, due to increased relative humidity levels, weak winds and basin-like attributes and winter-time biomass burning events (Kaskaoutis et al., 2020).

Figure 4.1: Ioannina City in Epirus, Greece. (https://maps.google.com)

The average and median values of the measured inorganic ions in Ioannina are shown in Table 4.1 (Mihalopoulos and co-workers unpublished data), while the average meteorological conditions were for temperature 7.32 ± 2.48 ºC (typical for winter-time temperatures in the area, Kaskaoutis et al., 2020) and for relative humidity 66.88 ± 19.67%.

Table 4.1: $PM_{2.5}$ measurements conducted at Ioannina City for 58 days (from 13/12/2019 to 16/02/2020).

	Sulfate μg/m^3	Nitrate μg/m^3	Ammonium μg/m^3	Chloride μg/m^3	Calcium μg/m^3	Potassium μg/m^3	Magnesium μg/m^3	Sodium μg/m^3	POM μg/m^3
mean	2.55	3.34	1.03	0.56	0.53	1.34	0.03	0.17	46.88
stdev	1.31	2.49	0.75	0.34	0.40	0.91	0.02	0.10	31.75
median	2.33	2.97	0.89	0.50	0.38	1.20	0.03	0.15	41.13

To predict the fine aerosol pH in Ioannina City in wintertime we used the same approach as for Finokalia data. For the calculations of the aerosol water content associated with the organic species, the total organic particulate matter is used (POM in μg/m^3) calculated by multiply the measured organic carbon with 1.8. As mentioned in section 2.2.2, a value of 0.16 for the hygroscopicity of the organics at Finokalia for the calculation of the organic water from eq. (2) was used, while for Ioannina we used a value of 0.12 as derived from CCN activity in wintertime in Athens (Psichoudaki et al., 2018) since Ioannina often experiences biomass burning events during winter similarly to Athens.

It has been observed that globally fine atmospheric particles ($PM_{2.5}$), exhibit a bimodal acidity pattern with a population of particles that has an average pH between 1 and 3 pH units and another one having a mean pH close to 4 and 5, which is due to dust and sea spray influence (Sindosi et al., 2012; Pye, et al., 2020). Figure 4.2 shows both the fine aerosol pH associated with the inorganic liquid water content and that calculated when particle water derived as the sum of aerosol water associated with inorganic and organic species in Ioannina City. On average pH_{Wi} was found to be 3.91 ± 0.65, while the addition of the organic water content resulted in a moderate acidic aerosol pH with a mean value of 4.32 ± 0.74. This pH increase throughout the wintertime period was partially expected due to the elevated levels of organics in the area (mean organic wintertime value 46.88 ± 31.75 μg/m^3) and ranged from 0.09 to 0.89 pH units. Comparing the effect of interpreting the organic fraction of the aerosol to the calculations of aerosol pH at the two areas studied here (Ioannina and Finokalia), it was seen a larger increase in aerosol pH when organics were included as expected, due to the significantly higher concentration of the organic species in Ioannina than at Finokalia. Consequently, in areas like Ioannina where the contribution of the organics to the total particulate matter is substantial, it is important for the aerosol pH predictions to include them in order to estimate more accurately the aerosol acidity levels.

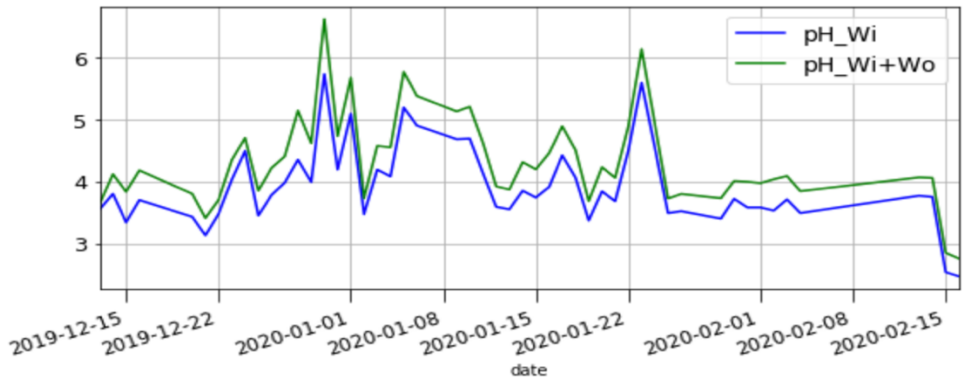

Figure 4.2: Timeseries (from 13/12/2019 to 16/02/2020) of fine aerosol pH in Ioannina City associated with the inorganic components of the aerosol (pH_Wi) as predicted by ISORROPIA-II and the one associated with both the inorganic and organic components (pH_Wi+Wo) as calculated according to Guo et al.,2015.

Comparing the pH_{wi} for the Ioannina City with other studies that investigate the acidity of fine atmospheric particles, comparable slightly and in some cases quite lower levels of acidity can be found. For instance, multiple studies in Beijing indicate a mean wintertime $PM_{2.5}$ aerosol pH of 4.2 units (Liu et al., 2017), 4.5 (Guo, Liu, et al., 2017), 4.9 in a study conducted close to Beijing, in Tianjin (Shi et al., 2017) and 4.5 (Ding et al., 2019). Additionally, Tao and Murphy (2019b) reported that the fine aerosol pH in winter at all 6 sites studied in Canada was around 3 and was greatly influenced by temperature, relative humidity and chemical composition levels. According to the sensitivity test conducted in that work, wintertime low temperatures resulting in significant sensitivity of pH to variations of NH_x, sulfate and total nitrate concentrations. The higher picks in Fig. 4.2 for both calculated pHs (with and without the contribution of organics to aerosol water) where acidity is above 5 units, are due to relatively low levels of sulfate and significantly low nitrate and chloride concentrations in combination with

1) relatively high calcium concentration on the 30th of December,

2) high calcium and significantly high potassium levels on the 1st and on the 5th of January, and

3) relatively high calcium and markedly higher calcium, potassium and ammonium on the 23rd of January.

Due to the lack of gas phase ammonia and nitric acid measurements in the area, we here used mean values reported in Patras almost two decades ago since measurements of these species in the gas phase are quite rare. Danalatos & Glavas (1999) measured an average gas phase ammonia of 2 μg/m^3 in Patras Greece, between November 1995 and August 1996. An average wintertime value of 0.53 ± 0.12 μg/m^3 was used for the nitric acid, which is derived from measurements of this gas in Athens between December of 2014 and March 2016 (Liakakou et al., in preparation). A sensitivity test to gas phase nitric acid was also conducted with two additional runs of ISORROPIA-II, one with 4 times the amount of HNO_3 (x4 HNO_3) used in the main run and one dividing the HNO_3 by 4 (/4 HNO_3). These results are shown in Fig. 4.3,

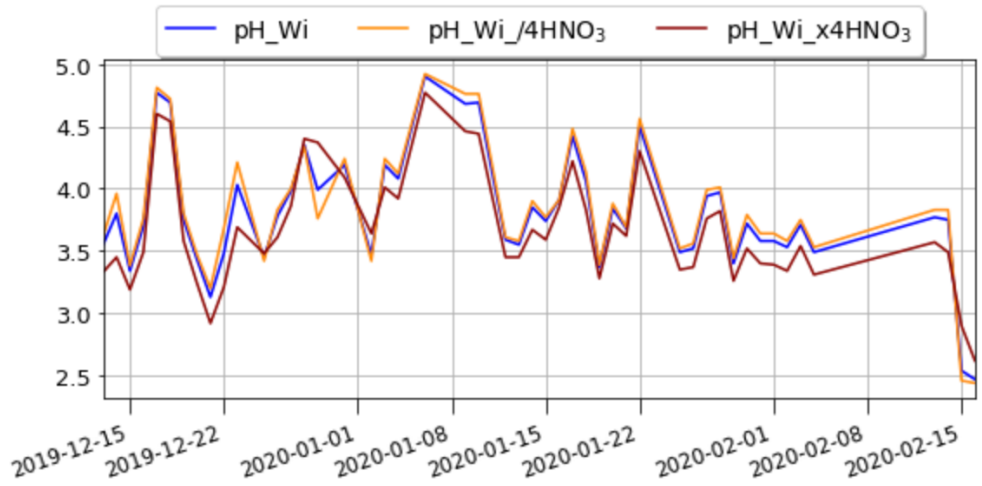

Figure 4.3: Timeseries of fine aerosol pH associated with the inorganics along with the results from the sensitivity test to nitric acid, pH_Wi/4HNO_3 is the pH predicted with reducing the amount of nitric acid by 4 and pH_Wi_x4HNO_3 is the one calculated with 4 times the nitric acid. All predictions of this sensitivity tests was conducted using ISORROPIA-II.

where it can be seen the influence and impact on aerosol pH calculation of using different levels of HNO_3. As expected, the aerosol pH increased throughout the period when lower levels of HNO_3 were used and the opposite effect occurred when the nitric acid was higher, with a negligible deviation from this behavior on 28th and 29th of December 2019 and on 2nd of January 2020. More specifically, the aerosol pH increased by 0.04 units on average when only 0.13 μg/m^3 of HNO_3 were used and decreased by 0.13 pH units when 2.12 μg/m^3 of HNO_3 were considered.

Focusing on the difference between submicron (PM_1) and fine ($PM_{2.5}$) aerosol acidity levels, a comparison of the aerosol pH at Finokalia and Ioannina was conducted. Generally, it has been shown that atmospheric aerosol pH is size dependent and coarse-mode particles tend to be much less acidic than fine particles (differences as large as 4 pH units have been reported, (Fang et al., 2017; Pye et al., 2020; Young et al., 2013)) due to variations in inorganic composition with particle size. Comparing the fine aerosol pH with that of submicron particles, a more subtle difference is found (1-2 pH units ,Pye et al., 2020). This difference in $PM_{2.5}$ aerosol acidity levels and that of PM_1 is due to the stronger presence of non-volatile cations attributed to dust and sea salt at the larger sizes. This was also the case here, Fig. 4.4, where we compared the aerosol pH calculated for the submicron particles at Finokalia and the fine particles in Ioannina City for the same season (e.g. winter). The winter average submicron pH (from 13/12/2014 to 31/12/2014) was 1.89 ± 0.30, while the $PM_{2.5}$ pH (from 13/12/2019 to 31/12/2019) was on average 1.9 units higher, while it reached almost 2.5 pH units of difference. This overall increase going from PM_1 to $PM_{2.5}$ acidity levels can mainly be attributed to crustal species and sodium levels present in the fine aerosol.

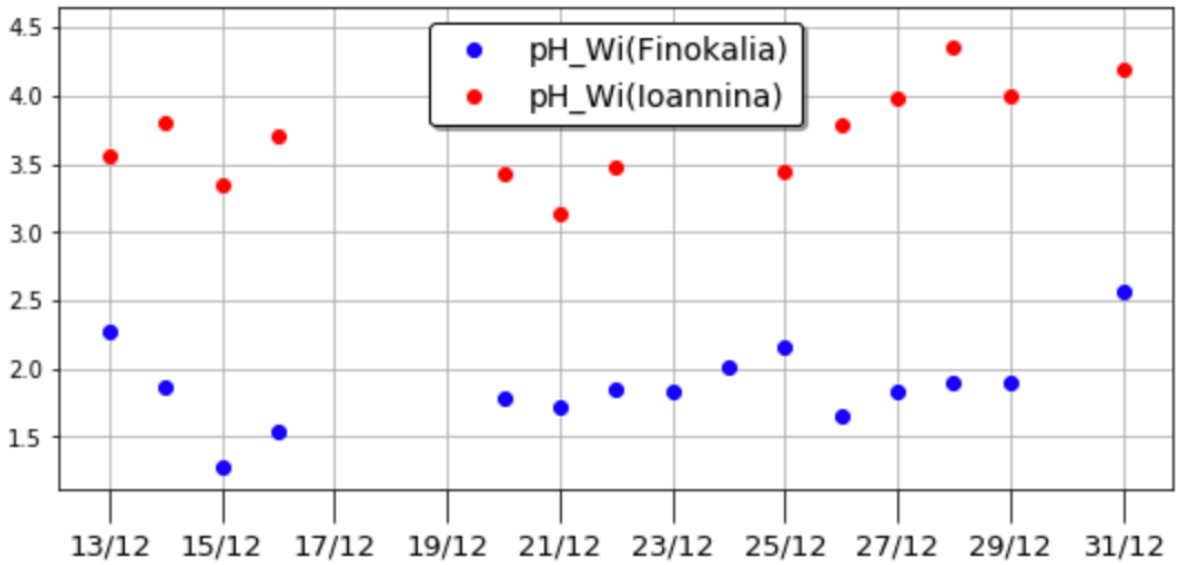

Figure 4.4: December (2019) fine aerosol pH in Ioannina in comparison with the submicron aerosol pH at the Finokalia station also in December (2014) as (both) predicted by ISORROPIA-II.

Furthermore, the same method as in section 3.4 was used, in order to examine the sensitivity of the studied fine aerosol system in Ioannina City to the gas phase NH_3 and HNO_3, mainly due to the fact that the differences in aerosol acidity that we found between the two aerosol systems can result in different responses of aerosols to the gas phase and consequently differentiate the potential policy measures needed to be established in regulating the aerosol activity at a given area. For this, we interpreted our aerosol pH and water predictions derived from ISORROPIA-II using the framework described in section 3.4, with activity coefficients also derived from the model ($\gamma_{H^+}\gamma_{NO_3^-}$=0.6, $\gamma_{NH_4^+}\gamma_{NO_3^-}$=0.2, where both are median values). We found that, the $PM_{2.5}$ system in Ioannina City is mostly in the "HNO_3 sensitive" region (Regime 2) (Fig. 4.5). This means that the $PM_{2.5}$ levels in this area are almost exclusively sensitive to changes in the total nitrate's precursors emissions. If we compare the sensitivity of the fine aerosol system in the urban region of Ioannina to the gas phase, with that of the submicron one at Finokalia remote coastal site (Fig. 3.13), it is obvious that the more acidic aerosol system (PM_1 system at Finokalia) is more sensitive to ammonia than to nitric acid, as expected.

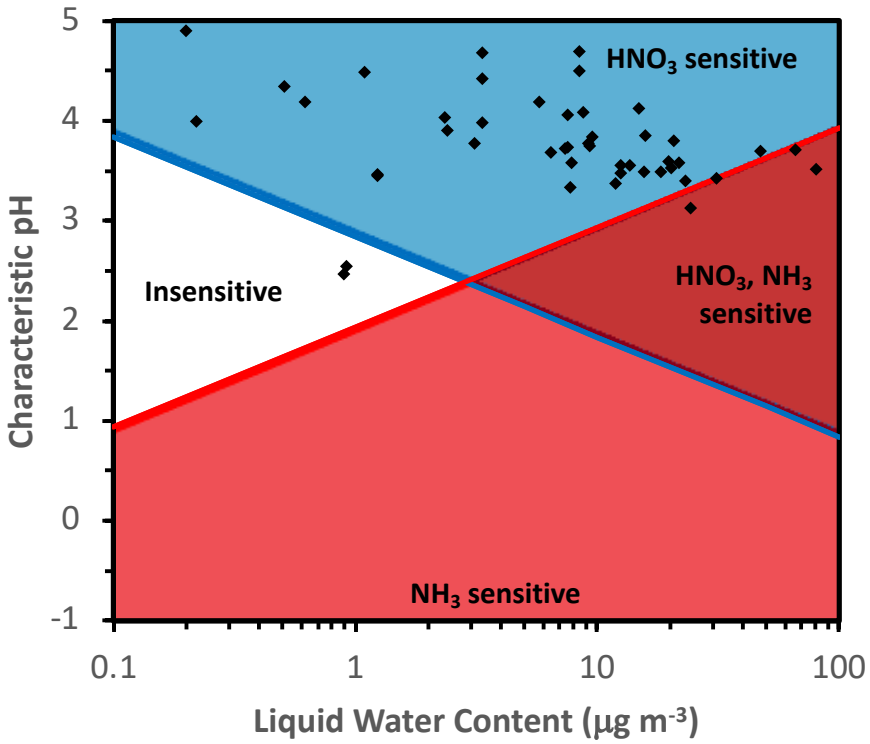

Figure 4.5: Chemical domains of sensitivity of aerosol to NH3 and NOx emissions for the studied period in Ioannina City as derived from the framework developed in (Nenes et al., 2020). The average temperature used here (as in Fig. 3.13) is the measured one for the study period at the site, 280.4 K. Daily values for aerosol pH and liquid water content were used

5. Conclusions

Submicron aerosol chemical composition data along with NH_3 and HNO_3 gas phase concentrations measured at Finokalia for almost one year (from February to December 2014) are here used in the thermodynamic model ISORROPIA-II in order to predict the aerosol pH (associated with the inorganics). Using the approach proposed in (Guo et al., 2015) the aerosol water associated with the organics and the aerosol pH with the total liquid water content were also calculated. Aerosol water associated with the inorganic components as derived from the model was on average 3.40 ± 2.97 μg/m^3, while aerosol water attributed to the organics was on average 0.60 ± 0.59 μg/m^3, i.e. about 13% of the total aerosol water. Aerosol water associated with inorganics and that associated with the organics presented similar seasonality with a small difference occurring in March due to higher organic mass concentration relative to the other months.

The submicron aerosol pH was found to be highly acidic (1.10 ± 0.70 on average when accounting only for inorganic water), while it was found that accounting for the organic water in pH calculation has a minor effect (an average increase by 0.07 pH units). Aerosol pH shows clear seasonality with the highest values during winter reaching values slightly above 2 and the lowest during summer (0.40 pH units for pH_Wi and 0.47 for pH_{Wi+Wo}), with the major contributors to this seasonal cycle being sulfate levels, temperature and at a smaller extent relative humidity levels. As expected aerosol pH overall showed clear dependence on ambient temperature and relative humidity. The diurnal cycle of aerosol pH was investigated in two months (July and December) and the two diurnal profiles were found to be quite different. During daytime in July (summer) aerosol pH was on average 0.40 ± 0.08 for pH_{Wi} (0.47 ± 0.08 for pH_{Wi+Wo}), with an early afternoon minimum and early morning maximum value. On the contrary, in December aerosol pH shows midday minimum and nighttime maximum values, which follow temperature, relative humidity and sulfate levels and is on average by 1.31 units higher than that in July.

The effect of crustal species and sodium in the calculations of submicron aerosol pH has been also investigated based on PM_1 aerosol samples from 70 days with concurrent measurements of these ions during the study period. Using these PM_1 data in ISORROPIA-II it was found that consideration of these cations increases aerosol pH by 0.729 ± 0.002 units. It also affects the partitioning coefficient of nitric acid to the aerosol phase (ε_{NO3}) by 0.08 ± 0.07 units. Adding excess amount of gas phase ammonia increased the aerosol pH by 1.46 ± 0.15 units with an increase of 0.31 ± 0.14 units of nitrate partitioning coefficient. Particularly, when the system's sensitivity to gas phase ammonia and nitric acid was investigated with the newly developed framework by Nenes et al., (2020), it was found that this study's PM system at Finokalia coastal remote site is mostly sensitive to gas phase ammonia levels.

$PM_{2.5}$ aerosol pH in another somewhat large city of Greece, Ioannina, was also investigated during wintertime and compared with the acidity of the submicron aerosols at Finokalia. When investigating the contribution of organics in the aerosol pH predictions as done for the submicron pH, an increase of 0.09 to 0.89 pH units was found, which was due to the fact that organics are a major component of aerosols in the area especially during winter. The fine aerosol pH in Ioannina was found to be on average 1.9 less acidic when compared with the pH at Finokalia; an outcome which was expected since the contribution of non-volatile species to the fine fraction of the aerosol is much higher than to the submicron fraction. Finally,

interpreting our estimates of aerosol pH and water for the $PM_{2.5}$ system examined in Ioannina in order to investigate PM sensitivity to the gas phase, we found that this system is sensitive to HNO_3 and thus policies for the reduction of the pollution caused by aerosols in the area can be more targeted to NO_x emissions and not for example to NH_3 regulations as found for the PM_1 system at Finokalia. Therefore, accurately predicting the atmospheric aerosol acidity and investigating its major drivers and temporal patterns, can give valuable insight, to both understand and regulate the aerosol activity in the atmosphere.

Similar studies will be performed in other cities of Greece and during other seasons of the year to provide a more comprehensive view of aerosol pH over Greece.

6. References

Anatolaki, Ch., & Tsitouridou, R. (2007). Atmospheric deposition of nitrogen, sulfur and chloride in Thessaloniki, Greece. *Atmospheric Research*, *85*(3–4), 413–428. https://doi.org/10.1016/j.atmosres.2007.02.010

Ansari, A. S., & Pandis, S. N. (1998). Response of Inorganic PM to Precursor Concentrations. *Environmental Science & Technology*, *32*(18), 2706–2714. https://doi.org/10.1021/es971130j

Bougiatioti, A., Fountoukis, C., Kalivitis, N., Pandis, S. N., Nenes, A., & Mihalopoulos, N. (2009). Cloud condensation nuclei measurements in the marine boundary layer of the Eastern Mediterranean: CCN closure and droplet growth kinetics. *Atmospheric Chemistry and Physics*, *9*(18), 7053–7066. https://doi.org/10.5194/acp-9-7053-2009

Bougiatioti, A., Nenes, A., Fountoukis, C., Kalivitis, N., Pandis, S. N., & Mihalopoulos, N. (2011). Size-resolved CCN distributions and activation kinetics of aged continental and marine aerosol. *Atmospheric Chemistry and Physics*, *11*(16), 8791–8808. https://doi.org/10.5194/acp-11-8791-2011

Bougiatioti, A., Nikolaou, P., Stavroulas, I., Kouvarakis, G., Weber, R., Nenes, A., Kanakidou, M., & Mihalopoulos, N. (2016a). Particle water and pH in the eastern Mediterranean: Source variability and implications for nutrient availability. *Atmospheric Chemistry and Physics*, *16*(7), 4579–4591. https://doi.org/10.5194/acp-16-4579-2016

Bougiatioti, A., Nikolaou, P., Stavroulas, I., Kouvarakis, G., Weber, R., Nenes, A., Kanakidou, M., & Mihalopoulos, N. (2016b). Particle water and pH in the eastern Mediterranean: Source variability and implications for nutrient availability. *Atmospheric Chemistry and Physics*, *16*(7), 4579–4591. https://doi.org/10.5194/acp-16-4579-2016

Bougiatioti, A., Nikolaou, P., Stavroulas, I., Kouvarakis, G., Weber, R., Nenes, A., Kanakidou, M., & Mihalopoulos, N. (2016c). Particle water and pH in the eastern Mediterranean: Source variability and implications for nutrient availability. *Atmospheric Chemistry and Physics*, *16*(7), 4579–4591. https://doi.org/10.5194/acp-16-4579-2016

Chen, D., Liu, Z., Fast, J., & Ban, J. (2016). Simulations of sulfate–nitrate–ammonium (SNA) aerosols during the extremehaze events over northern China in October 2014. *Atmospheric Chemistry and Physics*, *16*(16), 10707–10724. https://doi.org/10.5194/acp-16-10707-2016

Clegg, S. L., Seinfeld, J. H., & Brimblecombe, P. (2001). Thermodynamic modelling of aqueous aerosols containing electrolytes and dissolved organic compounds. *Journal of Aerosol Science*, *32*(6), 713–738. https://doi.org/10.1016/S0021-8502(00)00105-1

Danalatos, D., & Glavas, S. (1999). Gas phase nitric acid, ammonia and related particulate matter at a Mediterranean coastal site, Patras, Greece. *Atmospheric Environment*, *33*(20), 3417–3425. https://doi.org/10.1016/S1352-2310(98)00342-2

Ding, J., Zhao, P., Su, J., Dong, Q., Du, X., & Zhang, Y. (2019). Aerosol pH and its driving factors in Beijing. *Atmospheric Chemistry and Physics*, *19*(12), 7939–7954. https://doi.org/10.5194/acp-19-7939-2019

Fang, T., Guo, H., Zeng, L., Verma, V., Nenes, A., & Weber, R. J. (2017). Highly Acidic Ambient Particles, Soluble Metals, and Oxidative Potential: A Link between Sulfate and Aerosol Toxicity. *Environmental Science & Technology*, *51*(5), 2611–2620. https://doi.org/10.1021/acs.est.6b06151

Fanourgakis, G. S., Kanakidou, M., Nenes, A., Bauer, S. E., Bergman, T., Carslaw, K. S., Grini, A., Hamilton, D. S., Johnson, J. S., Karydis, V. A., Kirkevåg, A., Kodros, J. K., Lohmann, U., Luo, G., Makkonen, R., Matsui, H., Neubauer, D., Pierce, J. R., Schmale, J., … Yu, F. (2019). Evaluation of global simulations of aerosol particle and cloud condensation nuclei number, with implications for cloud droplet formation. *Atmospheric Chemistry and Physics*, *19*(13), 8591–8617. https://doi.org/10.5194/acp-19-8591-2019

Fountoukis, C., & Nenes, A. (2007). ISORROPIA II: a computationally efficient thermodynamic equilibrium model for K+–Ca2+–Mg2+–NH+4 –Na+–SO24−–NO−3 –Cl−–H2O aerosols. *Atmos. Chem. Phys.*, 21.

Galán Madruga, D., Fernández Patier, R., Sintes Puertas, M. A., Romero García, M. D., & Cristóbal López, A. (2018). Characterization and Local Emission Sources for Ammonia in an Urban Environment. *Bulletin of Environmental Contamination and Toxicology*, *100*(4), 593–599. https://doi.org/10.1007/s00128-018-2296-6

Guo, H., Liu, J., Froyd, K. D., Roberts, J. M., Veres, P. R., Hayes, P. L., Jimenez, J. L., Nenes, A., & Weber, R. J. (2017). Fine particle pH and gas–particle phase partitioning of inorganic species in Pasadena, California, during the 2010 CalNex campaign. *Atmospheric Chemistry and Physics*, *17*(9), 5703–5719. https://doi.org/10.5194/acp-17-5703-2017

Guo, H., Sullivan, A. P., Campuzano-Jost, P., Schroder, J. C., Lopez-Hilfiker, F. D., Dibb, J. E., Jimenez, J. L., Thornton, J. A., Brown, S. S., Nenes, A., & Weber, R. J. (2016). Fine particle pH and the partitioning of nitric acid during winter in the northeastern United States. *Journal of Geophysical Research: Atmospheres*, *121*(17). https://doi.org/10.1002/2016JD025311

Guo, H., Weber, R. J., & Nenes, A. (2017). High levels of ammonia do not raise fine particle pH sufficiently to yield nitrogen oxide-dominated sulfate production. *Scientific Reports*, *7*(1), 12109. https://doi.org/10.1038/s41598-017-11704-0

Guo, H., Xu, L., Bougiatioti, A., Cerully, K. M., Capps, S. L., Hite, J. R., Carlton, A. G., Lee, S. H., Bergin, M. H., Ng, N. L., Nenes, A., & Weber, R. J. (2015). Fine-particle water and pH in the southeastern United States. *Atmospheric Chemistry and Physics*, *15*(9), 5211–5228. https://doi.org/10.5194/acp-15-5211-2015

Kalkavouras, P., Bougiatioti, A., Kalivitis, N., Stavroulas, I., Tombrou, M., Nenes, A., & Mihalopoulos, N. (2019). Regional new particle formation as modulators of cloud condensation nuclei and cloud droplet number in the eastern Mediterranean. *Atmospheric Chemistry and Physics*, *19*(9), 6185–6203. https://doi.org/10.5194/acp-19-6185-2019

Kanakidou, M., Myriokefalitakis, S., & Tsigaridis, K. (2018). Aerosols in atmospheric chemistry and biogeochemical cycles of nutrients. *Environmental Research Letters*, *13*(6), 063004. https://doi.org/10.1088/1748-9326/aabcdb

Kaskaoutis, D. G., Grivas, G., Theodosi, C., Tsagkaraki, M., Paraskevopoulou, D., Stavroulas, I., Liakakou, E., Gkikas, A., Hatzianastassiou, N., Wu, C., Gerasopoulos, E., & Mihalopoulos, N. (2020). Carbonaceous Aerosols in Contrasting Atmospheric Environments in Greek Cities: Evaluation of the EC-tracer Methods for Secondary Organic Carbon Estimation. *Atmosphere*, *11*(2), 161. https://doi.org/10.3390/atmos11020161

Kerminen, V.-M., Hillamo, R., Teinilä, K., Pakkanen, T., Allegrini, I., & Sparapani, R. (2001). Ion balances of size-resolved tropospheric aerosol samples: Implications for the acidity and atmospheric processing of aerosols. *Atmospheric Environment*, *35*(31), 5255–5265. https://doi.org/10.1016/S1352-2310(01)00345-4

Koulouri, E., Saarikoski, S., Theodosi, C., Markaki, Z., Gerasopoulos, E., Kouvarakis, G., Mäkelä, T., Hillamo, R., & Mihalopoulos, N. (2008). Chemical composition and sources of fine and coarse aerosol particles in the Eastern Mediterranean. *Atmospheric Environment*, *42*(26), 6542–6550. https://doi.org/10.1016/j.atmosenv.2008.04.010

Kouvarakis, G., Mihalopoulos, N., Tselepides, A., & Stavrakakis, S. (2001). On the importance of atmospheric inputs of inorganic nitrogen species on the productivity of the Eastern Mediterranean Sea. *Global Biogeochemical Cycles*, *15*(4), 805–817. https://doi.org/10.1029/2001GB001399

Liu, M., Song, Y., Zhou, T., Xu, Z., Yan, C., Zheng, M., Wu, Z., Hu, M., Wu, Y., & Zhu, T. (2017). Fine particle pH during severe haze episodes in northern China: Fine Particle pH During Haze Episodes. *Geophysical Research Letters*, *44*(10), 5213–5221. https://doi.org/10.1002/2017GL073210

Meng, Z., Seinfeld, J. H., Saxena, P., & Kim, Y. P. (1995). Atmospheric Gas-Aerosol Equilibrium: IV. Thermodynamics of Carbonates. *Aerosol Science and Technology*, *23*(2), 131–154. https://doi.org/10.1080/02786829508965300

Meskhidze, N., Chameides, W. L., Nenes, A., & Chen, G. (2003). *Iron mobilization in mineral dust: Can anthropogenic SO2 emissions affect ocean productivity?* 5.

Mihalopoulos, N., Kerminen, V. M., Kanakidou, M., Berresheim, H., & Sciare, J. (2007). Formation of particulate sulfur species (sulfate and methanesulfonate) during summer over the Eastern Mediterranean: A modelling approach. *Atmospheric Environment*, *41*(32), 6860–6871. https://doi.org/10.1016/j.atmosenv.2007.04.039

Nair, A. A., & Yu, F. (2020). Quantification of Atmospheric Ammonia Concentrations: A Review of Its Measurement and Modeling. *Atmosphere*, *11*(10), 1092. https://doi.org/10.3390/atmos11101092

Nenes, A. (2003). Parameterization of cloud droplet formation in global climate models. *Journal of Geophysical Research*, *108*(D14), 4415. https://doi.org/10.1029/2002JD002911

Nenes, A., Krom, M. D., Mihalopoulos, N., Van Cappellen, P., Shi, Z., Bougiatioti, A., Zarmpas, P., & Herut, B. (2011a). Atmospheric acidification of mineral aerosols: A source of bioavailable phosphorus for the oceans. *Atmospheric Chemistry and Physics*, *11*(13), 6265–6272. https://doi.org/10.5194/acp-11-6265-2011

Nenes, A., Krom, M. D., Mihalopoulos, N., Van Cappellen, P., Shi, Z., Bougiatioti, A., Zarmpas, P., & Herut, B. (2011b). Atmospheric acidification of mineral aerosols: A source of bioavailable phosphorus for the oceans. *Atmospheric Chemistry and Physics*, *11*(13), 6265–6272. https://doi.org/10.5194/acp-11-6265-2011

Nenes, A., Pandis, S. N., & Pilinis, C. (1998). *ISORROPIA: A New Thermodynamic Equilibrium Model for Multiphase Multicomponent Inorganic Aerosols*. 30.

Nenes, A., Pandis, S. N., & Pilinis, C. (1999). Continued development and testing of a new thermodynamic aerosol module for urban and regional air quality models. *Atmospheric Environment*, *33*(10), 1553–1560. https://doi.org/10.1016/S1352-2310(98)00352-5

Nenes, A., Pandis, S. N., Weber, R. J., & Russell, A. (2020). Aerosol pH and liquid water content determine when particulate matter is sensitive to ammonia and nitrate availability. *Atmospheric Chemistry and Physics*, *20*(5), 3249–3258. https://doi.org/10.5194/acp-20-3249-2020

Nissen, K. M., Leckebusch, G. C., Pinto, J. G., Renggli, D., Ulbrich, S., & Ulbrich, U. (2010). Cyclones causing wind storms in the Mediterranean: Characteristics, trends and links to large-scale patterns. *Natural Hazards and Earth System Sciences*, *10*(7), 1379–1391. https://doi.org/10.5194/nhess-10-1379-2010

Pakkanen, T. A. (1996). Study of formation of coarse particle nitrate aerosol. *Atmospheric Environment*, *30*(14), 2475–2482. https://doi.org/10.1016/1352-2310(95)00492-0

Pandolfi, M., Amato, F., Reche, C., Alastuey, A., Otjes, R. P., Blom, M. J., & Querol, X. (2012). Summer ammonia measurements in a densely populated Mediterranean city. *Atmospheric Chemistry and Physics*, *12*(16), 7557–7575. https://doi.org/10.5194/acp-12-7557-2012

Perrino, C., Catrambone, M., Di Menno Di Bucchianico, A., & Allegrini, I. (2002). Gaseous ammonia in the urban area of Rome, Italy and its relationship with traffic emissions. *Atmospheric Environment*, *36*(34), 5385–5394. https://doi.org/10.1016/S1352-2310(02)00469-7

Pikridas, M., Bougiatioti, A., Hildebrandt, L., Engelhart, G. J., Kostenidou, E., Mohr, C., Prévôt, A. S. H., Kouvarakis, G., Zarmpas, P., Burkhart, J. F., Lee, B.-H., Psichoudaki, M., Mihalopoulos, N., Pilinis, C., Stohl, A., Baltensperger, U., Kulmala, M., & Pandis, S. N. (2010). The Finokalia Aerosol Measurement Experiment – 2008 (FAME-08): An overview. *Atmospheric Chemistry and Physics*, *10*(14), 6793–6806. https://doi.org/10.5194/acp-10-6793-2010

Pinder, R. W., Dennis, R. L., & Bhave, P. V. (2008). Observable indicators of the sensitivity of PM2.5 nitrate to emission reductions—Part I: Derivation of the adjusted gas ratio and applicability at regulatory-relevant time scales. *Atmospheric Environment*, *42*(6), 1275–1286. https://doi.org/10.1016/j.atmosenv.2007.10.039

Powley, H. R., Cappellen, P. V., & Krom, M. D. (2017). Nutrient Cycling in the Mediterranean Sea: The Key to Understanding How the Unique Marine Ecosystem Functions and Responds to Anthropogenic Pressures. In B. Fuerst-Bjelis (Ed.), *Mediterranean Identities—Environment, Society, Culture*. InTech. https://doi.org/10.5772/intechopen.70878

Psichoudaki, M., Nenes, A., Florou, K., Kaltsonoudis, C., & Pandis, S. N. (2018). Hygroscopic properties of atmospheric particles emitted during wintertime biomass burning episodes in Athens. *Atmospheric Environment*, *178*, 66–72. https://doi.org/10.1016/j.atmosenv.2018.01.004

Pye, H. O. T., Nenes, A., Alexander, B., Ault, A. P., Barth, M. C., Clegg, S. L., Collett, J. L., Fahey, K. M., Hennigan, C. J., Herrmann, H., Kanakidou, M., Kelly, J. T., Ku, I. T., Faye McNeill, V., Riemer, N., Schaefer, T., Shi, G., Tilgner, A., Walker, J. T., … Zuend, A. (2020). The acidity of atmospheric particles and clouds. *Atmospheric Chemistry and Physics*, *20*(8), 4809–4888. https://doi.org/10.5194/acp-20-4809-2020

Pye, H. O. T., Nenes, A., Alexander, B., Ault, A. P., Barth, M. C., Clegg, S. L., Collett Jr., J. L., Fahey, K. M., Hennigan, C. J., Herrmann, H., Kanakidou, M., Kelly, J. T., Ku, I.-T., McNeill, V. F., Riemer, N., Schaefer, T., Shi, G., Tilgner, A., Walker, J. T., … Zuend, A. (2020). The acidity of atmospheric particles and clouds. *Atmospheric Chemistry and Physics*, *20*(8), 4809–4888. https://doi.org/10.5194/acp-20-4809-2020

Quinn, P. K., Bates, T. S., Coffman, D., Onasch, T. B., Worsnop, D., Baynard, T., de Gouw, J. A., Goldan, P. D., Kuster, W. C., Williams, E., Roberts, J. M., Lerner, B., Stohl, A., Pettersson, A., & Lovejoy, E. R. (2006). Impacts of sources and aging on submicrometer aerosol properties in the marine boundary layer across the Gulf of Maine: IMPACTS OF SOURCES AND AGING ON AEROSOLS. *Journal of Geophysical Research: Atmospheres*, *111*(D23). https://doi.org/10.1029/2006JD007582

Rolph, G., Stein, A., & Stunder, B. (2017). Real-time Environmental Applications and Display sYstem: READY. *Environmental Modelling and Software*, *95*, 210–228. https://doi.org/10.1016/j.envsoft.2017.06.025

Seinfeld, J. H., & Pandis, S. N. (2006). *Atmospheric chemistry and physics: From air pollution to climate change* (2nd ed). J. Wiley.

Shi, G., Xu, J., Peng, X., Xiao, Z., Chen, K., Tian, Y., Guan, X., Feng, Y., Yu, H., Nenes, A., & Russell, A. G. (2017). pH of Aerosols in a Polluted Atmosphere: Source Contributions to Highly Acidic Aerosol. *Environmental Science & Technology*, *51*(8), 4289–4296. https://doi.org/10.1021/acs.est.6b05736

Sindosi, O. A., Bartzokas, A., Kotroni, V., & Lagouvardos, K. (2012). Verification of precipitation forecasts of MM5 model over Epirus, NW Greece, for various convective parameterization schemes. *Natural Hazards and Earth System Sciences*, *12*(5), 1393–1405. https://doi.org/10.5194/nhess-12-1393-2012

Song, S., Gao, M., Xu, W., Shao, J., Shi, G., Wang, S., Wang, Y., Sun, Y., & McElroy, M. B. (2018). *Fine particle pH for Beijing winter haze as inferred from different thermodynamic equilibrium models* [Preprint]. Aerosols/Atmospheric Modelling/Troposphere/Chemistry (chemical composition and reactions). https://doi.org/10.5194/acp-2018-6

Stein, A. F., Draxler, R. R., Rolph, G. D., Stunder, B. J. B., Cohen, M. D., & Ngan, F. (2015). Noaa's hysplit atmospheric transport and dispersion modeling system. *Bulletin of the American Meteorological Society*, *96*(12), 2059–2077. https://doi.org/10.1175/BAMS-D-14-00110.1

Stokes, R. H., & Robinson, R. A. (1966). Interactions in Aqueous Nonelectrolyte Solutions. I. Solute-Solvent Equilibria. *The Journal of Physical Chemistry*, *70*(7), 2126–2131. https://doi.org/10.1021/j100879a010

Sun, J., Qin, D., Mayewski, P. A., Dibb, J. E., Whitlow, S., Li, Z., & Yang, Q. (1998). Soluble species in aerosol and snow and their relationship at Glacier 1, Tien Shan, China. *Journal of Geophysical Research: Atmospheres*, *103*(D21), 28021–28028. https://doi.org/10.1029/98JD01802

Tao, Y., & Murphy, J. G. (2019). The sensitivity of PM2.5 acidity to meteorological parameters and chemical composition changes: 10-year records from six Canadian monitoring sites. *Atmospheric Chemistry and Physics*, *19*(14), 9309–9320. https://doi.org/10.5194/acp-19-9309-2019

Theodosi, C., Markaki, Z., & Mihalopoulos, N. (2008). Iron speciation, solubility and temporal variability in wet and dry deposition in the Eastern Mediterranean. *Marine Chemistry*, *120*(1–4), 100–107. https://doi.org/10.1016/j.marchem.2008.05.004

Trigo, I. F., Bigg, G. R., & Davies, T. D. (2002). Climatology of Cyclogenesis Mechanisms in the Mediterranean. *MONTHLY WEATHER REVIEW*, *130*, 21.

Tsiodra I., *Κατανομή αέριας και σωματιδιακής φάσης σε αερολύματα στην ανατολική Μεσόγειο*. Bachelor Thesis, Department of Chemistry, University of Crete, 2015, 59

Wexler, A. S. (2002). Atmospheric aerosol models for systems including the ions H^+, NH_4^+, Na^+, SO_4^{2-}, NO_3^-, Cl^-, Br^-, and H_2O. *Journal of Geophysical Research*, *107*(D14), 4207. https://doi.org/10.1029/2001JD000451

Young, A. H., Keene, W. C., Pszenny, A. A. P., Sander, R., Thornton, J. A., Riedel, T. P., & Maben, J. R. (2013). Phase partitioning of soluble trace gases with size-resolved aerosols in near-surface continental air over northern Colorado, USA, during winter: PHASE PARTITIONING DURING NACHTT. *Journal of Geophysical Research: Atmospheres*, *118*(16), 9414–9427. https://doi.org/10.1002/jgrd.50655

Zaveri, R. A., Easter, R. C., Fast, J. D., & Peters, L. K. (2008). Model for Simulating Aerosol Interactions and Chemistry (MOSAIC). *Journal of Geophysical Research*, *113*(D13), D13204. https://doi.org/10.1029/2007JD008782

Zhang, A., Wang, Y., Zhang, Y., Weber, R. J., Song, Y., Ke, Z., & Zou, Y. (2020). Modeling the global radiative effect of brown carbon: A potentially larger heating source in the tropical free troposphere than black carbon. *Atmospheric Chemistry and Physics*, *20*(4), 1901–1920. https://doi.org/10.5194/acp-20-1901-2020